THE PROCEEDINGS OF THE PHYSICAL SOCIETY

VOL. 58, PART 5 1 September 1946 No. 329

THE PERFORMANCE OF AIRCRAFT CAMERA LENSES

BY E. W. H. SELWYN AND J. L. TEARLE

Communication H.1072 from the Kodak Research Laboratories, Harrow

MS. received 2 *March* 1946

ABSTRACT. The estimation of the best combination of lens and film for aerial reconnaissance photography is not a simple problem, owing to the number of variables, such as focal length and aperture of the lens, the size and speed of the film, forward motion and speed of the aircraft which are involved. For quantitative considerations it is necessary to adopt a measure of the detail-revealing capacity of the negatives, and for this purpose the resolving power was chosen, since it was not only obviously related to the capacity of the negative to reveal detail, but also capable of justification as a possible means of estimating the performance of the lens in optical image formation. In order that the resolving power figures may correspond as closely as possible to practical performance, careful choice of test-object was necessary, for experiment showed that different test-objects gave different results. A test-object consisting of two rectangles separated by their width, with a difference in density of 0·2 between them and the background, was adopted. Apparatus with such test-objects at the focus of a collimator of long focal length was set up, and with it measurements were made of the photographic resolving power all over the field, and in a set of planes embracing the focus, for a representative collection of air camera lenses. The results showed that the photographic resolving power improved as the lenses were stopped down from their maximum apertures until very small apertures were reached, and that as a general rule the resolving power diminished towards the outer parts of the field. The variation with aperture was accounted for, in general terms, by theoretical considerations, and certain regularities in the change of resolving power with angular distance from the optical axis were also explained. A figure for the performance of any lens was obtained by averaging the resolving power over the field of the lens, having regard to the greater area covered at the larger angles. It was found that the performance of any of the lenses could be represented with very fair accuracy by the formula

$$R=\left[\frac{207}{fG}\right]^{\frac{1}{2}}\left[\frac{F.\,No.}{\tan^2\theta}\right]^{0\cdot3},$$

where R is the mean resolving power in lines per mm. over the field up to an angular distance θ from the axis, f is the focal length of the lens in inches, and *F. No.* its relative aperture. G is the granularity of the film in density-microns at a density of 1·0.

This formula has no substantial theoretical basis, although it can be accounted for to some extent. It has proved useful, for it assists in the choice of the focal length, aperture and angle of view most appropriate for any given purpose in aerial reconnaissance photography. It may also be used, at least until the progress of lens design renders it inaccurate in form, for estimating the merit of a given lens design by comparison of its performance with that given by the formula.

§ 1. INTRODUCTION

IN order to make clear the reason for examining the problem with which this paper deals, a brief sketch is given in this *Introduction* of the work on aerial photography of which it forms part.

Soon after the war began it seemed likely that photography from aircraft would be an important item in it. In spite of the considerable development of aerial photography in the war of 1914–1918, the problem of estimating what were the best possible results, and how they could be secured, still seemed to be largely unsolved, especially on the theoretical side. Consequently, very early in the war, the Kodak Research Laboratories took much interest in this problem in order to discover what sort of film was best for aerial photography. Preliminary discussions soon showed that it was one of some complexity. The main use of aerial photography was likely to be in reconnaissance, in which it is important to record the utmost possible detail. The other use, for map making, requires distortion of the image introduced both by the lens and by the deformation of the film base to be reduced to the minimum, and presumably some loss of definition would be tolerated if that were the necessary price to pay for absence of distortion. Aerial survey for map making, however, did not become an urgent problem till later in the war, and this paper is concerned with one broad aspect of the general problem of securing the best possible definition in aerial photographs.

The nature of the general problems may be gathered from the following considerations. It is necessary to give at least a certain minimum exposure if the negative is to be of value. Thus the time of exposure T, the focal ratio $F.No.$, the brightness of the subject B, and the speed of the film S must be in a very definite relation. This relation, in fact, is

$$S \propto (F.No.)^2/BT.$$

To see that this is so, it is only necessary to note that it constitutes the practical definition of S. For a given value of B, therefore, a wide variation in values of S, $F.No.$ and T is possible, which will, nevertheless, satisfy the condition that the exposure must be adequate. But out of the possible sets of values of S, $F.No.$ and T some will lead to sharper photographs than others, as may be seen in the following way. It is a matter of common experience that sharper photographs are obtained with slow films than with fast ones. But if the speed of the film is decreased then either T must be increased or $F.No.$ decreased, or both. An increase in T, however, necessarily causes an increase in the blurring of the photograph by the forward motion and vibration of the aircraft. Also it is a matter of common experience that a moderate reduction in the aperture of photographic objectives of normal construction improves the sharpness of the photographs taken with them, so that a decrease in $F.No.$ may be expected to diminish the sharpness. The increase in sharpness expected from the use of slow film is therefore offset, more or less, by the increase in time of exposure or aperture, or both. Hence, unless a remarkable exactness of balance occurs between the various effects involved, we must expect that some particular set of values of S, $F.No.$ and T will lead to the sharpest photographs.

The foregoing argument merely demonstrates that there is probably an optimum as regards sharpness. In order to understand how this optimum is determined it is necessary to know how the properties of the film affect the definition and how the optical properties of the lens are affected by a change in aperture.

A little consideration will also show that we must know more about the lens than the variation of its properties with aperture. On general grounds it is clear that the larger the image on the film can be made, even if the faults in the image given by the lens are magnified in proportion, the less serious will be the relative degradation of the image due to the film. We are thus led to expect that better results might be obtained with lenses of long focal length than with short. For a given size of film, however, the area of ground covered in a single photograph is less the longer the focal length of the lens. From an operational point of view it might be necessary to cover a large area of ground not only for estimating, for example, the damage suffered by a town from aerial bombardment, but also because it is not easy to get a given target into the centre of the picture under operational conditions. Thus it is also important to know whether the angle of view for which a lens is designed has any important effect on the definition.

Two considerable gaps in our knowledge thus existed. One was the way in which the film influences the definition, and the other the way in which the definition obtained with a lens of given design depends upon its aperture, focal length and the size of the film with which it is used which determines its operative angle of view. Until these gaps were filled it could not be asserted with certainty that the best was being achieved with available equipment, nor was it possible to indicate the most profitable directions in which improvement could be made. It might be suggested that this difficulty could be overcome, in empirical fashion, by making aerial photographs with every possible combination of lens and film. It is, however, neither easy nor inexpensive to make reliable tests in an aircraft, and the amount of experiment to arrive at an incontestable conclusion, when so many variables are involved, would be prohibitive.

To begin with, a purely theoretical attack was made. It was hoped that it might be possible so to relate the resolving power of a photographic lens, as observed visually, for preference, and the resolving power of the film, as found with a lens of extremely high resolving power, or with a test-object in contact with the film, that the resolving power of the combination of photographic lens and film could be estimated. The attempt proved abortive. Experiments carried out in the Kodak Research Laboratories, and a further more extensive series carried out by Mr. R. J. Hercock of the Ilford Laboratories, revealed no relation of the sort expected. Mr. Hercock, in fact, did discover an empirical relation which fitted his results, but the value of this for the desired use seemed doubtful. However, further theoretical examination of the problem, on similar lines to the original attempt, but this time bringing in the grain of the film explicitly as a factor disturbing the recognition of detail, suggested a relationship between the resolving power obtained in the negative and the quality of the image formed by the lens, the contrast, turbidity and granularity of the film, and the contrast of the object photographed, which was not in serious disagreement with any of the known facts. Previous to this work no satisfactory reason had been found, for instance, for the fact that photographic materials display a maximum in the curve of resolving power against exposure or density. The turbidity of the emulsion layer had been recognized as a feature reducing the contrast of the image formed in the layer, and it had been recognized that on development this contrast would be increased or decreased according to the slope of the (density: log. exposure) curve of the material, at the point of exposure. Thus the resolving power would be expected to increase with density and then to remain constant throughout the region where the slope of the (density: log. exposure) curve remains constant (the straight-line region of the characteristic curve). In fact, the resolving-power curve exhibits a maximum near the commencement of the linear region of the characteristic curve. This was accounted for by the continual increase of granularity with density, because an increase in granularity reduces the visibility of any given density difference in the developed image. Advantage was taken of the recognition of this property to construct an instrument for measuring granularity, which proved of great value later on in the work on aerial photography. An account of this instrument has already been published (Romer and Selwyn, 1943).

By means of this theory it was possible to account, qualitatively at least, for the very great differences frequently observed between the resolving powers obtained visually and photographically, for the fact that the resolving power in prints was not greatly affected by the contrast of the printing paper, and for the considerable increase of graininess of prints made from negatives taken under hazy atmospheric conditions compared with those taken under clear conditions. It was realised however, that more exact establishment of this theory would require much time. For the time being, therefore, the theory was used only as a guiding principle, and attention was concentrated on objectives of greater practical importance.

The initial attempts to estimate the effect of varying the aperture, angle of view and focal length were speculative and gave only a fragmentary idea of the nature of the variation. Although, therefore, they suggested the general direction in which the definition might be expected to vary, as the aperture, angle of view and focal length were changed, it was clear that many tests on lenses would be necessary before it could be said that the performance of camera objectives in aerial photography was understood. Some of the early arguments are used, in a form modified by later experience, in the body of this paper.

During the time these attempts at the problem had been in progress, numerous discussions had taken place with the staff of the Royal Aircraft Establishment and some degree of agreement had been reached on the type of work which could be carried out in the laboratory, in contrast with that which must necessarily be done in aircraft. At this stage, the Kodak Research Laboratories were placed under contract to the Ministry of Aircraft Production, with a fairly definite programme of investigations in view. Foremost among these investigations was the establishment of a technique of photographic testing of air camera lenses by which their performance in aerial photography could be estimated. It is with this problem and the results of systematic tests of all the lenses available that this paper is concerned. The results obtained enabled a test to be made of the belief, for which only slight and doubtful evidence was originally available, that the differences between lenses could be accounted for, for the most part, by differences in angle of view, aperture and focal length. In other words, given the focal length, aperture and angle of view, it should be possible to estimate with moderate accuracy the definition given by the lens. It will be seen that this was so for the lenses available for test. This general formula has not the validity of a law of nature ; it is a concise expression of the state to which lens design had arrived by about 1943, and no doubt departures from the general approximate rule which has been found will be more and more frequent in the future as the art of designing lenses progresses. Already some notable advances had been made in this direction.

The general formula connecting the resolving power with the aperture, angle of view, and focal length which was arrived at by this investigation would enable an estimate to be made of the best lens to be used under any given conditions, provided that the exposure time was sufficiently short to allow the effect of movement of the camera during flight to be neglected. But as soon as it was seen that the general formula in question was a fair representation of the performance of lenses on the ground, a laboratory investigation was begun on the effect of the forward motion of the aircraft upon the definition of negatives.* By adopting the general formula arrived at in the survey of lenses (with some limitations), using certain results obtained in subsidiary work concerning the variation of granularity with speed of films, and the information embodied in exposure tables worked out by the Royal Aircraft Establishment, it was found possible to express the definition obtained in aerial photographs as a function of all the "practical" variables entering into the problem, such as speed and height of aircraft, speed of film, aperture of lens (itself determined by the time of exposure and intensity of illumination of the ground), angle of view, and focal length of the lens. This formula is capable of use in so many different ways, according to the information required, that it has not been subjected yet to exhaustive practical test. One interesting feature of this particular work, however, was that it suggested that the best time of exposure, for anything approximating to normal conditions, was that already in use by the Royal Air Force. It is not certain whether this result should be regarded with most satisfaction by the laboratory workers or by those who arrived at the exposure by severely practical considerations.

In addition to the above work, several investigations of interest have also been carried out. These relate to the spread of light in the emulsion layer caused by the scattering from grain to grain, a check on the theory of resolving power of emulsions for the type of test-object used in the lens tests, and the nature of the correlation between speed and granularity of films for air photography. An investigation has also been made on the effect of obliquity of the incident light on the resolving power of an emulsion. Finally, the work on the interaction between the image given by the lens and the film, which leads to the observed resolving power, has been pursued to a state at which we can say with some confidence how the interaction comes about and what determines the resolving power in the negative.

§2. RESOLVING POWER AS A MEASURE OF PERFORMANCE

In the early stages of the work doubts were expressed whether measurements of resolving power could be used satisfactorily as a measure of performance. These doubts appear to have arisen, in the main, from acquaintance with the results of resolving-power tests using test-objects of high contrast. It is known, for instance, that the visual resolving power of a telescope, for objects of high contrast, may be a misleading guide to the state of correction of the lens. The same criticism can also apply to photographic tests, especially if, in addition to the contrast of the test-object being high, a fine-grain high-contrast photographic material is used. In such cases also the exposure is very important. This may be demonstrated by a modification of Jones's tone-reproduction diagram (1921). The curve A in figure 1 (*a*) represents the intensity distribution in the image of a point source of light, such as might be obtained from an imperfectly corrected lens. In figure 1 (*b*) this has been plotted on a logarithmic scale of intensity in the lower right-hand quadrant. By projection on to the characteristic curve of the photographic material (shown in the upper right-hand quadrant) the resultant density distribution may be obtained as shown in the upper left-hand quadrant. The full radius of the disk of light produced by the lens is 5 units, whereas under the particular conditions of exposure chosen for illustration, the full radius of the image is only 2 units. Such a possibility is not unknown in practice. Sharpness beyond expectations, based only on the state of correction of a lens, may be obtained on suitable material by careful attention to exposure.

---

* **This investigation is not described in this paper; it was carried out by Mr. J. M. Gregory, and will be published later.**

In order to explain how it is that resolving-power tests can be an adequate guide to performance in many cases, and in aerial photography in particular, it is convenient to use the theory of resolving power mentioned in § 1. That theory, to be stated precisely, requires that the test-object be in the particular form of long parallel lines across which the brightness varies as a sine-curve. The main effect of lack of sharpness is to decrease the contrast between light and dark parts of the image, in such a way that the smaller the scale of the image the greater is the reduction of contrast. If the contrast in certain details is above a certain minimum then those details will be seen, but if below, they will not. In more definite terms, if the detail is in the form of the above sine-curve test-object and the contrast is measured in suitable fashion, the curve of contrast against the logarithm of the reciprocal of the size of detail will follow a course such as that shown in figure 2. The appropriate measure of contrast is $\log P$, where $(1+P)/(1-P)$ is the ratio of maximum to minimum brightness in the image. The value of $\log P$ is approximately equal, for values of $\log P$ up to $\bar{1}\cdot 8$, to $\log\gamma + \log a + \log P_l + \log P_e$, where γ is the slope of the curve of density against log exposure for the photographic material, $(1+a)/(1-a)$ is the ratio of maximum to miminum brightness in the test-object, $\log P_l$ is a function of d (the separation between neighbouring pairs of dark lines in the image of the test-object) and is determined by the image-forming properties of the lens, and $\log P_e$ is a similar function of d which describes how the contrast is reduced by the scattering of light in the emulsion layer of the photographic material.

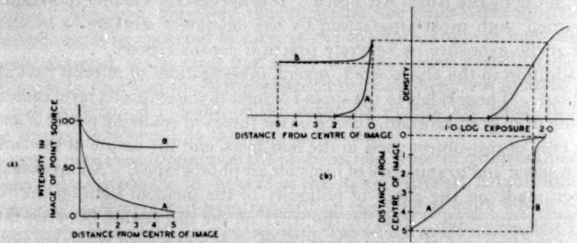

Figure 1.

(*a*) Schematic representation of intensity across image of point source as given by imperfect lens (Curve A). Curve B represents the intensity distribution when the point source is surrounded by a uniformly illuminated field.

(*b*) Tone-reproduction diagram showing derivation of density distribution in the developed photographic material.

If the aerial image is being viewed, P_e is unity and γ is unity, there being no photographic material involved, and the threshold contrast is represented by a straight line parallel to the axis of log $1/d$ at a value of log P of approximately $\bar{2}\cdot3$. The threshold for the photographic case is represented approximately by a straight line at a slope of 3/4,* the ordinate of which at $\log(1/d)=0$ is equal to $\log G^{\frac{1}{2}} - 2\cdot0$, where G is the granularity of the photographic material in density microns. The reason for the increase in the threshold contrast for smaller detail is that the granularity becomes relatively more obtrusive and disturbing to recognition of detail the finer the detail.

Where a log P curve intersects a threshold line, the contrast of the image is equal to the contrast threshold of the receptor (either the eye or the photographic material) and the value of $1/d$ at this point is equal to the resolving power. Thus in figure 2 the intersection of the log P_l curve with the threshold contrast line for the eye gives the visual resolving power of the lens; the intersection of the $\log\gamma + \log P_e$ curve with the threshold contrast line for the film gives the film resolving power, and the intersection of the $\log\gamma + \log P_e + \log P_l$ curve with the threshold contrast line for the film gives the resolving power of the lens and film together. For a set of test-objects of different contrast, the log P curves will consist of a set all of the same shape (namely that of the curve $\log P_l + \log P_e + \log\gamma$), but displaced from each other vertically by the differences in log a for the test-objects. If, therefore, we are prepared to make resolving-power tests on a number of test-objects of different contrast, we are able to reconstruct the curve of $\log P_l + \log P_e + \log\gamma$. If the observations are visual the reconstructed curve will be $\log P_l$; if the observations are photographic a knowledge of the γ-value and of the light-scattering properties of the photographic material will enable $\log P_l$ to be obtained from

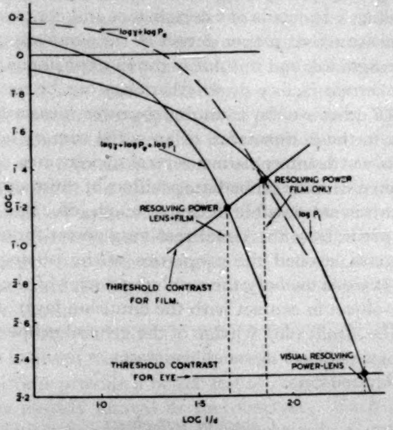

Figure 2. **Contrast in visual and photographic images, and thresholds of contrast plotted against reciprocal of size of image (logarithmic scales).**

*** These figures are derived from those given by Romer and Selwyn (1943) and apply therefore to Cobb test-objects. It is known, however, that approximately the same values apply for sine curve or other test-objects.**

$\log P_l + \log P_e + \log \gamma$. It is assumed also, of course, that the granularity of the film is known, otherwise the appropriate threshold line cannot be drawn. $\log P_l$ is determined only by the optical properties of the lens; it can be calculated from the light distribution in the image given by the lens of a point source.

Although the method of presentation may be unfamiliar, a set of measurements of resolving power for test-objects of different contrast is equivalent, therefore, to a description of the image-forming properties of the lens, and in that respect is not markedly inferior to any other description. Indeed, it is difficult to see what other measurable index of performance could be used: at any rate, no other has been suggested.

The diagram in figure 2 also indicates how far above the threshold contrast the actual contrast is, and to that extent is a measure of the visibility of objects which are greater in size than at the resolution limit. Now in aerial photography for reconnaissance, the quality of a lens is determined, very largely, by the smallest details visible. If details of a certain size and contrast can be recognized, larger details of the same contrast, or details of the same size and greater contrast, will certainly be recognized, and it is not of much importance whether they can be recognized with a certain facility or whether they can be recognized with a little greater facility. In other words, a resolving-power measurement is likely to be an adequate guide to the performance of an aerial camera lens. Before leaving this discussion it is worth interpolating several conclusions to be drawn from it, not directly connected with the immediate problem of estimating lens performance. It will be seen that it is not possible to derive much information about the photographic resolving power from the visual resolving power for a test-object of given contrast, or vice versa, even if the properties of the photographic material are known in detail. If we know only the resolving power of the film, measured, for instance, by a test-object in contact with the emulsion layer, the situation is even worse. Nevertheless, from a knowledge of the general properties of the curves of $\log P_l$ and $\log P_e$ against $\log(1/d)$ rough estimates or limits of resolving power can be obtained from limited data.

Choice of test-object

So far the discussion of the possibility of using a resolving-power measurement to assess the performance of lenses has been based, where exact quantitative statements are concerned, on the assumption that the test-object is of the sine-curve type. But, in fact, detail of such a character must be rare—the only example approximating to it which comes to mind is a corrugated iron roof upon which the sun is shining not too obliquely. The question therefore arises whether such a test-object can be used for testing the capacity of the lens to resolve details of other types, or whether we must seek other test-objects approximating more closely to those which arise in practice. In the latter case the above theory must be used only as an approximate indication of general trends. There is already some evidence in the literature that the value of resolving power obtained for a photographic material varies with the form of test-object employed. Ross (1924) found that a test-object consisting of a number of parallel lines separated by a distance equal to their width gave the same values of resolving power as a "double-star" test-object consisting of pairs of disks, but higher values than those given by a fan-shaped test-object. Sandvik (1927) investigated the variation of resolving power with the ratio of width of line to width of space, and found that the resolving power for a given photographic material increased uniformly with the logarithm of the line/space ratio. In 1928 he showed experimentally that the resolving power increases with the contrast of the test-object. The theory to explain these two results put forward by Frieser (1935, 1938) was based on the sine-curve test-object, and it was through his work that the simplification introduced by using a sine-curve test-object was first appreciated.

Some early experiments were made with a test-object (shown in figure 3) which is fairly typical of the parallel-line type. This was photographed by means of an 8-inch F/2·9 lens stopped down to F/8, using different films, at different exposure levels and different focus settings. A study of the negatives showed that the length of the lines of the test-object influenced the observer's estimate of the smallest group which could be resolved. For example, there was usually a gradual transition from groups which could be recognized clearly to groups which could not be recognized, so long as the resolution limit occurred at some group within a set of five of constant line length. When, however, the transition from resolved to unresolved groups occurred at a group near X in figure 3, where there is a sudden change in line length, it was found that the larger group on one side of X was clearly defined, whilst the smaller group on the other side of X showed no trace of line structure. The number of lines also influenced the result, for if only a small portion of the group at the resolution limit were exposed to view, the observer did not recognize it as resolved, but when more of the area was exposed to view the observer had no hesitation in deciding that the pattern was recognizable. The results obtained with the test-chart described by Sayce (1940), in which the lines are all of the same length but with the separation between them diminishing from end to end of the chart, are not likely, therefore, to bear any simple relation to those obtained with other charts.

Experiments were also carried out using letter charts of the type used by ophthalmic opticians, for the reason that the letters would presumably be unknown to the observer, and thus provide a better test of recognition than test objects the shape of which was already known to the observer. Such letter charts were, however, not very satisfactory, for they did not provide a very uniform scale of detail, and in any case the observer soon memorized the sequence of letters. There seemed little doubt from the somewhat scattered evidence that different resolving powers would be found with different test-objects, but this would be of no importance if the resolving powers yielded by different test-objects always bore the same ratio to each other. To check this point, comparisons were made between the parallel-line test-object shown in figure 3 and a test-object which was designed to eliminate the defects of the parallel-line type. This new object contained the minimum number of lines necessary for a determination of resolving power (namely, two) and in which the ratio line-length/line-width was constant at all sizes. Moreover, the length of line was no greater than was necessary to permit the recognition of the longer dimension, and therefore the direction, of the test-object. A test-object described by Cobb and Moss (1928), consisting of two bars of length three times their width, separated by a distance equal to their width, had hitherto been used for visual acuity measurements; its dimensions fitted the above desiderata sufficiently closely to suggest the name "Cobb test-object" for this type. The experiment was carried out with a composite chart consisting of groups of Cobb test-objects and groups of parallel line test-objects. Photographs were made at different settings of focus of an 8-inch F/2·9 " Pentac " lens, and the limit of resolution was assessed by a number of observers. The resolving-power limit as determined by the Cobb test-object was plotted against that determined by the parallel-line test-object, as in figure 4. Each point represents the mean estimate of a number of observers. (The departure of some of the points from the smooth curve is probably due to the fact that in the parallel line test-object the line frequencies of consecutive groups were in the ratio of 1·2 to 1, whereas in the Cobb test-object the ratio was 1·1 to 1.) It will be noted that although at the position of focus the two test-objects give substantially the same value of resolving power, there is an appreciable departure from equality on each side of the focus ; at positions inside the focus, the parallel-line test-object leads to higher values of resolving power than the Cobb test-object, whilst beyond the focus the reverse is true. The explanation for these results must be that the distributions of light in the image given by the lens are not the same on both sides of the focus position. The effect of this change must then be different in the image of the multi-line test-object from that in the image of the two-line test-object.

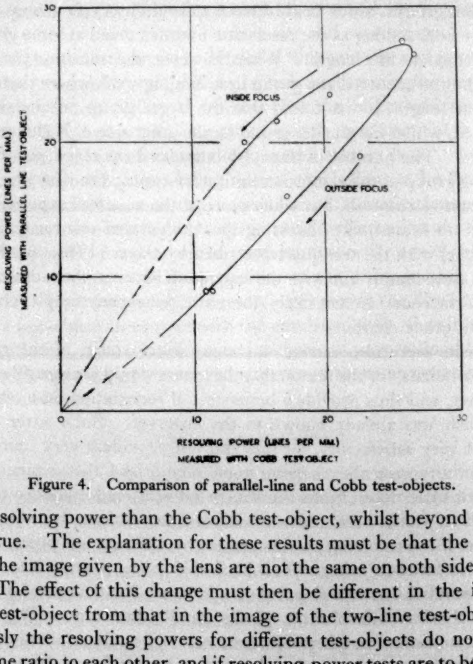

Figure 4. Comparison of parallel-line and Cobb test-objects.

Obviously the resolving powers for different test-objects do not, in general, bear the same ratio to each other, and if resolving-power tests are to be of value, the test-object must be chosen to simulate, as near as may be, the type of objects to be photographed. It was therefore decided to adopt the Cobb type of test-object, which is probably as nearly similar to the detail in air photographs as can be obtained in a simple geometrical pattern. Although no comparisons with other test-objects for accuracy have been made, it is possible that this type of test-object does not yield results of quite so high precision as others. By using a number of Cobb test-objects disposed at random, and plotting the number of a given size

PHYSICAL SOC. VOL. 58, PT. 5 (E. W. H. SELWYN AND J. L. TEARLE)

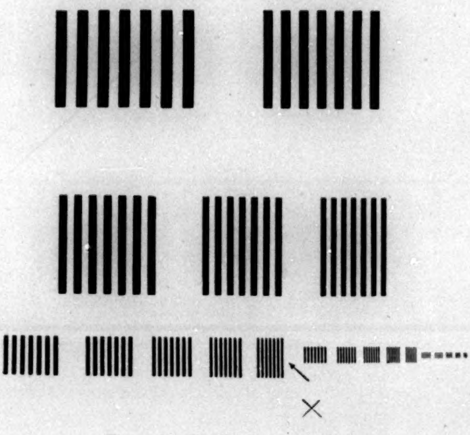

Figure 3. Parallel-line test-object.

To face page 502

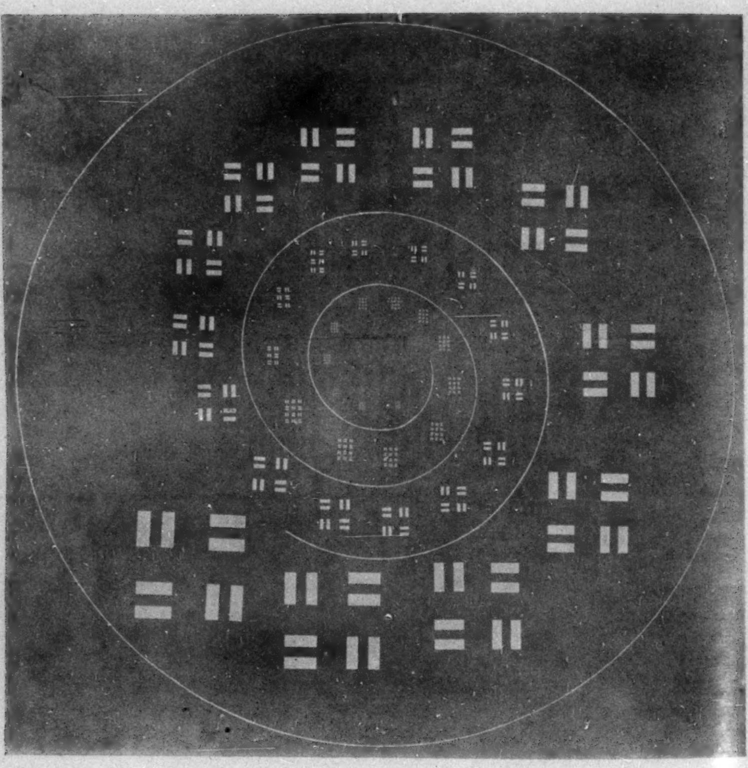

Figure 5. Form of test-object adopted for resolution tests.

recognized against the size an estimate may be made of the size at which half of each group are recognized, and the precision may be thereby somewhat improved (Romer and Selwyn, 1943). This method could not be applied to lens examination mainly because the complete test-object must be kept reasonably small. In the form used for the present work the test-chart consists of groups in a spiral arrangement, as shown in figure 5. Half the test-objects are vertical and half horizontal, so that measurements can be made along radial lines and along tangential lines. The definition of the lens used in preparing the test-chart and of the collimator used for the tests is likely to be worse for points off axis, so the smaller groups, the sharpness of which will be relatively more affected by poor definition in these two lenses, are placed near the centre.

Aerial photographs are different from ordinary photographs in that the atmosphere itself appears luminous and throws a veiling light over the surface of the earth, as a result of the scattering of the light by small suspended particles, Thus while an average subject photographed from the ground has a brightness range from the brightest part of the subject to the darkest of 160 : 1 (Jones, 1941), aerial photographs show that the ratio for subjects seen from moderate and high altitudes is only 10 : 1 or so. Detail can range in ratio of maximum to minimum brightness from 1 : 1 to 160 : 1 for photographs taken on the ground, and to 10 : 1 for aerial photographs. A rough mean for the detail in the terrestrial photograph may therefore be taken as $\sqrt{160}:1$, and for the aerial photograph as $\sqrt{10}:1$, say 3 : 1. Examination of details in aerial photographs larger than that just resolved, so as to avoid the reduction in contrast due to lack of sharpness, suggested that a much more nearly typical value of ratio of brightness was 1·6 : 1. In terms of the usual photographic units, therefore, the appropriate density difference in the test-object was estimated at 0·2 (i.e. log 1·6). Figure 5 has been reproduced to approximately this density. It is possible that for testing lenses for use in ordinary photography on the ground a somewhat higher contrast than this is desirable.

Suppose we now return to the example shown in figure 1, and consider what happens when the contrast is decreased. To decrease the contrast of a point source we must place around the point source an extended source of uniform brightness (as occurs for instance in astronomy where the stars are surrounded by the general illumination in the night sky). The image given by the lens then becomes as shown in curve B of figure 1 (*a*) and the photographic image as in curve B of figure 1 (*b*). It will be seen that when the contrast is low the photographic image of the point source extends to the full diameter of the optical image. Thus we may conclude that changes in the exposure are likely to affect the image less if the contrast is low and that the outer and weaker parts of the optical image are important when the contrast is low, but may be unimportant if the contrast is high. The latter point is, in fact, usually true whether the image is observed visually or photographically. Suppose that the images of a point source given by two lenses have intensity distributions as shown in figure 6 at A and B. A represents an image of moderate diameter, into which all the light from the lens comes to a focus. B represents a central bright image surrounded by a flare of 1/100 of the intensity, covering an area 100 times that of the bright core; the amount of light in the core is thus equal to the amount of light in the flare. The log P_t curves corresponding to these images are shown at A′ B′ of figure 6. The visual and photographic threshold lines are annotated " Visual High Contrast " and " Phot. High Contrast ". If the contrast of the point object is now reduced by surrounding it by a uniformly illuminated field, the log P_l curves A′ and B′ should be shifted downwards by an appropriate distance but, for convenience, the threshold lines have been shifted upwards by the same amount. They are annotated " Visual, Low Contrast" and " Phot. Low Contrast" respectively. In order not to complicate the argument, the effect of the spread of light in the emulsion layer is neglected. It will be seen that the resolving power when the contrast is high is determined very largely by the bright central core of the image which suffers from flare, but that as the contrast is decreased the flare becomes much more important. We shall be referring to this point later in connection with the effect of aperture on the resolving power.

Choice of photographic materials

It has already been mentioned that the prospects of simplifying the problem by using the theory of resolution were remote. The work therefore had to be proceeded with on an empirical basis, and for this reason the choice of photographic materials was governed by two practical considerations: firstly, it was required to know what standard of performance was obtained with existing equipment, and secondly, it was required to know how far this standard might be expected to rise, if the properties of the film could be improved, or if by some means the exposure time could be lengthened to permit the use of slower fine-grain materials. The first consideration naturally led to the choice of the existing Service type films, the Kodak versions of which were " Super-XX Panchromatic Aero Film " and " Panatomic X Aero Film ". The former is the faster of the two and has a lower resolving power. Partly in order that the effects of chromatic aberration of the lenses should remain the same in all the photographic tests, and also because panchromatic sensitization was not likely to be superseded by any other, such as infra-red, it was desirable that the film chosen to satisfy the second requirement should also be panchromatic. It should also have high resolving power and moderate speed. No existing high-resolution film has high speed, but the emulsion manufacturer is continually striving to increase resolving power whilst retaining a useful speed. Allowing for possible advances in this direction,

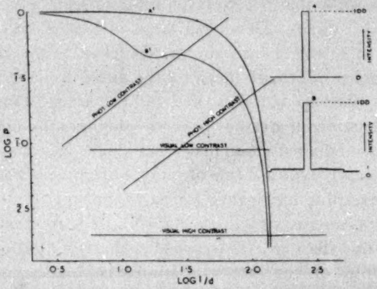

Figure 6. Effect of flare round image on log P_l curves, and effect of this on resolving power for high and low contrast test-objects.

and also in devices (for reducing vibration and compensating for the forward motion of the aircraft) which would permit of longer exposure times, it was decided to choose Kodak "Microfile" Panchromatic film. This has a resolving power about three times that of Super-XX, whilst its speed is about 1/80 that of the latter. If the speed of this film could be increased, and the exposure time increased, there was some possibility of it being brought into use.

Development conditions

Since the resolving power of the film is dependent on the contrast, not only of the test-object, but also of the emulsion, it was important that development conditions should be standardized. The Service type films were developed to give about the same contrast as obtained in the R.A.F. Photographic Reconnaissance Units, namely $\gamma^* = 1{\cdot}4$ for Super-XX and $\gamma = 1{\cdot}6$ for Panatomic-X, both films being developed in Kodak developer D.19b. Microfile film, in its normal use for microcopying documents, etc., is developed to a high contrast, but for pictorial photography a high contrast in the negative would lead to a density range too great to be printed on existing positive materials. Development was therefore standardized to make $\gamma = 1{\cdot}6$. Kodak developer DK.20 was used initially, but this was later replaced by Kodak developer D.76d, which was more conveniently available, and conditions were adjusted to produce the same negative characteristics as formerly.

Description of apparatus

The examination of lenses of focal lengths from 5 inches to 20 inches was carried out with the apparatus shown diagrammatically in figure 7. The test-object (B) was mounted at the focus of a collimator objective (A), and illuminated by light from a tungsten filament lamp. An opal diffusing screen (C) to ensure uniform illumination, and a minus-blue filter (as used in R.A.F. practice) were mounted between the source and the test-object. The test-object was exposed by means of a roller blind shutter (E) attached to the lamp-house (F) and a slide (D) carrying neutral filters, graded so that the brightness of the test-object could be altered in steps by a factor of $\sqrt{2}$, was fitted between the lamp-house and the shutter. The collimator objective was a Wray achromatic doublet of focal length 60 inches and aperture F/15, permitting lenses of aperture 4 inches to be tested.

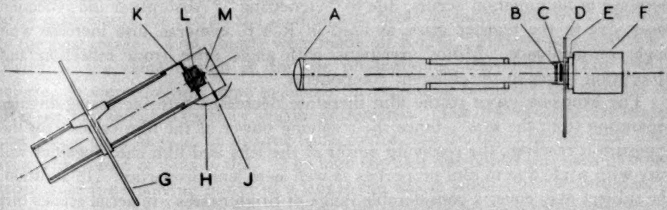

Figure 7. Arrangement of apparatus.

---

[*] In this connection γ is the slope of the straight portion of the characteristic curve of the material.

The camera incorporated a lens holder (K), capable of carrying lenses of external diameters up to 6 inches, and a film holder (G) sliding on rails, guided by two V-grooves and a knife-edge. The film (in strips 35 mm. wide) was held against a register glass of thickness 0·15 inch, in conformity with the standard register glass used in the smaller R.A.F. cameras. The length of the film holder was such that a total angle of view of 56° could be covered with a 20-inch lens. The camera could be rotated about a vertical axis M the position of which was adjusted to coincide with the front surface of the lens to be tested. This was to ensure that the lens did not move out of the beam of light from the collimator.

A larger collimator and camera was constructed later to accommodate lenses of focal lengths up to 50 inches. The collimator lens was a Cooke " Photo Visual " objective of focal length 134 inches and aperture 7 inches.

Both collimator objectives were well corrected, and their influence on the results obtained with different aircraft lenses was negligible. The lateral aberrations of a collimator objective of focal length F are reduced by a factor f/F in the image plane of a test lens of focal length f, and the longitudinal aberrations by a factor f^2/F^2. A number of 20-inch lenses, examined with the aid of both collimators in turn, showed the same values of resolving power, within the limits of experimental error.

§3. EXPERIMENTAL PROCEDURE

Exposure conditions

The illumination in the focal plane of a lens is not uniform, but decreases as the angular separation from the axis is increased. In a thin lens the effective aperture is reduced as the angle of incidence is increased, and the principal ray strikes the focal plane at a greater angle the greater the angle of incidence. Thus the intensity of illumination I at any angle is given by $I=I_0 \cos^4 \theta$, where I_0 is the intensity of illumination at the centre of the field. If the lens is of finite edge thickness, or, more particularly, consists of separated components, an additional decrease in illumination occurs, due to "vignetting". Absorption and reflection losses due to the register glass, as used in R.A.F. cameras, also increase with angle of incidence. Minor variations with angle arise from reflection and absorption losses in the different components.

The exposure given to the film therefore decreases with increasing angular separation from the axis. Since the resolving power of the film varies with the exposure it receives, the resolving power of the lens and film used together will vary with angle due to film properties as well as to lens properties. In addition, the subject may cover a considerable range of brightnesses: in aerial scenes this range is comparatively small, as stated above. In order to make a complete survey of the problem with regard to these practical considerations, it would be necessary to collect data on lens-film resolution for a number of different exposure levels. It was thought, however, that such a procedure would unnecessarily lengthen the programme of experimental work and complicate analysis of the data, and all variations in resolving power for a given lens-film combination were restricted to those due to the lens alone, by adopting one exposure only. The exposure chosen was that which would result in the maximum film resolution which occurs, for the most negative materials, when the density of the negative is about 1·0.

Measurements of the relative illumination at different positions in the field of each lens were made in order to discover how serious the variation was, and whether the technique of giving constant exposure to all parts of the film was justified.

Measurement of relative illumination in the focal plane

The relative illumination in the focal plane of each lens was measured by photographic photometry in the following way. Using an illuminated disk in the place of the test-object, exposures were made, of constant duration, at 0° and at 5° intervals on each side of the axis, up to the full angular extent of the test-lens, on a film of moderate contrast. This was repeated for different apertures of the lens, and the exposure level for each aperture was adjusted so that the densities obtained on development lay on the linear portion of the sensitometric curve of the material.* Sensitometric film-strips were developed together with the test-strips exposed by the lens, and the values of log exposure corresponding to the densities produced by the lens were read from the sensitometric curve thus obtained. Since we require to know only the relative values of the intensity at different points in the field, these log exposure values may be considered to be values of log intensity.

In order to allow for possible variations in the shutter speed, and the intensity of the light source, two exposures were made (by moving the film laterally inside the film-holder) at each position, and, therefore, at all except the axial position there were four exposures for each angle. It was found that there was little variation in the densities so obtained, and the values of log intensity were usually reproducible to within about $\pm 0{\cdot}02$. Greater precision than this could have been obtained by controlling lamp-voltage and shutter speed, but was considered unnecessary.

Measurement of visual resolving power

Although the research was to be primarily for the purpose of assessing the photographic performance of lenses, preliminary experiments had shown that some useful information might be gained if the resolving power of the aerial image were measured. The design of the apparatus did not permit visual measurements to be made easily for extra-axial images, and these measurements were confined to the axial image. Test-objects were made on Kodak "Maximum Resolution" Plates, to the same design as for the photographic test-object. The plates referred to were the only type available for recording faithfully the number of lines per mm. required for the visual measurements. Two test-objects were made, one having clear lines on an opaque background, and the other having clear lines on a background of density 0·2. The high contrast test-object was used in order to measure the resolving power of a lens in the way in which this measurement is usually carried out, and the low contrast test-object to provide measurements of resolving power approaching more closely those obtained photographically.

The test-objects were placed at the focus of the collimator objective, and a microscope was used to observe the image produced by the lens under test. The focus of the microscope was adjusted until the maximum number of groups of the test-object was resolved, and the number of the smallest resolvable group was recorded. The relative aperture of the microscope objective was always greater than that of the lens under test.

---

* It is not essential to the method that all the densities on the test negatives lie on the linear portion of the characteristic curve of the material, but this ensures the same degree of accuracy for all values.

Photographic resolution tests

After preliminary trials to ascertain what region of focus was to be explored, and to find the exposures necessary to give a density of about 1·0 at each position in the field, the film-holder was set and exposures were made on the axis and at 5° intervals up to the full angular extent of the lens, on both sides of the axis. This procedure was repeated at different settings of the film-holder, until seven planes, passing through the region of focus, had been explored. This series was then repeated at all apertures of interest, and for the other films.

Since most of the lenses were examined at about 5 apertures, this procedure resulted in about 100 negatives per lens, with 20 or more images on each negative. The amount of work involved in measuring the resolving power in the negatives, not to speak of the complexity of the problem of analysing the data, imposed limitations on the thoroughness with which the inspection could be carried out. It was therefore necessary to limit the measurements to one negative at each aperture, for each of the three films.

For this reason, from each set of 7 negatives, that one was chosen in which the best axial definition was obtained. The only other plane of "focus" of any significance would correspond to the negative in which the best average definition was obtained, having regard to the entire area of film which the lens was intended to cover. The selection of this plane would involve the inspection of all the images, however, and would not solve the problem. This method was used later in connection with the focusing of lenses in cameras. It is worth pointing out that in a lens afflicted with spherical aberration both the plane in which the best axial definition occurs and the optimum focal-plane shift away from the lens as the aperture is reduced. Thus in setting cameras to give the best performance at different apertures without re-focusing, it is necessary to compromise on a focal setting which will be the optimum with respect both to the range of apertures and to the angle of view to be covered. Having chosen the negative, the number of the smallest group of the test-object recognizable at each angle was recorded and converted into resolving power in lines per mm., applying a correction discussed below. The resolving powers for radial and tangential lines were recorded separately.

In outline the method is similar to that adopted by Gardner and Case (1937) at the National Bureau of Standards, but there are several points of divergence between the two methods. The National Bureau of Standards apparatus has a number of fixed collimators accurately positioned so that measurements of distortion may be made. A high contrast test-object is used in which the number of lines and the ratio of length to separation is not the same for all line frequencies. The photographic material used is the Eastman "Type VB Spectrographic" plate, which has the same order of resolving power as "Microfile" film. The problem in hand at the National Bureau of Standards is to calibrate lenses in terms of the optimum focal length having regard both to resolution and distortion, and is, therefore, different from the problem with which this paper is concerned.

Measurement of resolving power in negatives

In determining the limit of resolution from the negative, the conditions of viewing were first standardized. The illumination of the field of the microscope was kept fairly constant from negative to negative, and the degree of magnification was kept constant for a given photographic material within the obvious limits that the magnification should not be so small that the size of test pattern is near the limit of the acuity of the eye, nor so large that the obscuring power of the graininess obliterates the image. It was found that a convenient magnification was 20 for the Service type films, and this had to be increased to 75 when observing good images on "Microfile" film. Since all the negatives were of approximately the same density, the conditions of illumination were kept constant, once a satisfactory level of illumination had been found. It is an advantage of the low contrast test-object that glare is absent when viewing the negative. The "spurious" resolution effect referred to by Gardner and Case (1937) has not been observed by the authors with the low contrast Cobb test-object. This effect, which is observable with multi-line high contrast test-objects, is that lines of a particular size appear to be resolved, although closer inspection reveals more lines than appear in the original test-object. With the Cobb test-object one should observe a strong line in the middle and possibly weaker lines on the outside if this effect occurred, but in fact, when the contrast of the test-object is low, the effect cannot occur.

The measurement of resolving power is to some extent subjective and is liable to errors which may appear large by physical standards. It is usually necessary for the observer to set himself some criterion of resolution, with the result that some observers judge as resolved a pattern which other observers would consider inadequately defined. These differences occur largely amongst inexperienced observers, and it has been found that when a number of workers have gained experience the agreement between them is good. The resolving-power determinations were carried out in the present work by one observer, who adopted the criterion that a group of a given size was resolved if the Cobb element appeared to consist of two separate patches, each *quasi* rectangular in form, and if the direction in which the "lines" were oriented agreed with that on the original test-object. It is sometimes found that the pattern appears to consist of two lines pointing in a direction at right angles to that in the original test-object. This is due to fortuitous "clumps" of grain.

L. C. Martin and C. A. Padgham* have investigated the precision of photographic resolution measurements under conditions similar to those described in this paper, and their results agree with estimates made by the present authors which suggest a standard deviation of about 10% for repeated measurements on the same negative. It was found, in addition, that the percentage precision of measurement was the same for both high and low contrast test-objects.

In converting the number of the smallest groups which can be resolved into resolving power in lines/mm., a correction must be applied for the increase in magnification for extra-axial images. In practice the resolving power was calculated from the dimensions of the test-object rather than by measurements on the negative. If $1/R_0$ is the separation between lines in the object, F the focal length of the collimator, f the focal length of the test lens, and θ the angular separation from the axis at which the image falls, then the line frequency R in the negative is given by

$$R_R = (R_0 F \cos\theta)/f$$

and

$$R_T = (R_0 F \cos^2\theta)/f,$$

where the suffixes R and T indicate radial and tangential lines respectively.

---

* Private communication.

As a result of this distortion of the test-object the length of radial lines becomes greater than 3 times the width of line whilst the length of tangential lines becomes less than 3 times the width of line by a factor $\cos\theta$. This change of shape is, however, small enough to be of little importance.

§4. EXPERIMENTAL RESULTS

The lenses examined in this survey were mainly of British manufacture, although a few American and German objectives were included. The focal lengths ranged from 5 to 49 inches and their maximum apertures from F/2·9 to F/7. The types of construction included wide and narrow angle, triplet and telephoto types but in spite of this variety there was sufficient similarity in their performance to enable results to be calculated as typical of the majority for presentation below.

Variation of resolving power with aperture

In figure 8 resolving power is plotted against ***F. No.***, both on logarithmic scales, for six of the lenses tested. The results are quite typical. The measurements refer to the axis only, but include visual measurements with high and low contrast test-objects, as well as photographic measurements on the three films with low contrast test-objects. The broken line indicates the value of resolving power calculated from the formula $1/\lambda(F.No.)$, λ being taken as $0{\cdot}55\,\mu$. This is a customary value to adopt for a perfectly corrected lens (Conrady, 1929). Strictly, it refers to visual observation of two close point-sources seen against a non-luminous background. It will be seen that except at the highest apertures the observed resolving powers for high contrast Cobb test-objects approximate to those given by the formula, being usually some 10% lower. The greater departures at the higher apertures must be due to uncorrected aberrations. With low contrast test-objects the visual resolving powers are inevitably less than for high contrast test-objects, but the deviations from the formula at large apertures are also so considerable that the curves of resolving power against ***F. No.*** display a definite maximum. The photographic resolving powers are much lower than the visual, and diminish in the order Microfile, Panatomic-X, Super-XX. They also display maxima in the curves of resolving power against ***F. No.*** and the maxima tend, though perhaps not in strongly marked fashion, to larger values of ***F. No.*** in the order Microfile, Panatomic-X, Super-XX.

It is not difficult to account for these results in approximate fashion. To do this we shall use the theory already mentioned, which, although strictly applicable only to sine-curve test-objects, may be expected to give a qualitative account of the results to be expected from other types of test-object. It is first necessary to make some estimate of the curves of $\log P_t$ against $\log(1/d)$ for different apertures, and for this purpose it is convenient to note that if the lens were perfectly corrected (and if the light from the test-object were monochromatic—though this does not make an important difference) the curves for $\log P_t$ for different apertures would be all of the same shape but separated from each other in the $\log(1/d)$ direction by an amount equal to the logarithm of the ratio of successive F-numbers. A set of such curves is shown by the light lines of figure 9.

When the path differences introduced by imperfect correction are less than half a wave-length, the diameter of the central nucleus in the image of a point source is no greater than when correction is perfect. There is, however, some

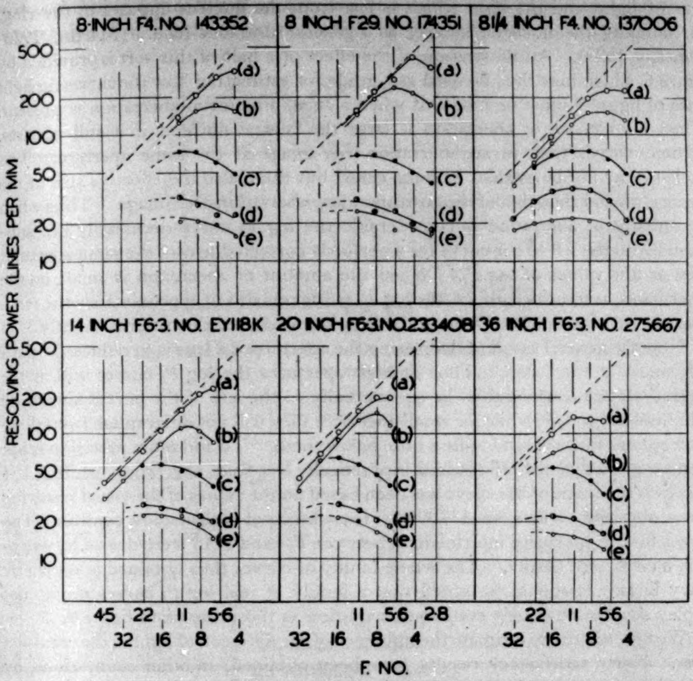

Figure 8. Typical curves showing variation of visual and photographic resolving power with aperture (for axial region only).

(*a*) Visual, (*b*) Visual, (*c*) Microfile Film, (*d*) Panatomic X film, (*e*) Super XX film. Curve (*a*) refers to high contrast test-object, and curves (*b*) to (*e*) to low contrast test-object.

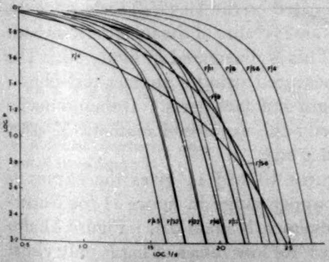

Figure 9. Log P_l curves for perfectly and imperfectly corrected lens at different apertures. Thin lines are curves for perfectly corrected lens and thick lines for imperfectly corrected.

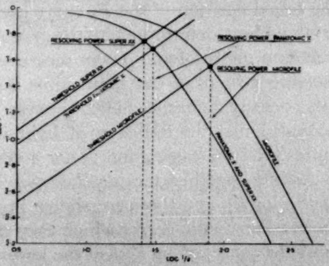

Figure 10. Estimation of log P_e curves from resolving power of films.

loss of light, and the light which is lost from the nucleus appears in the rings surrounding the nucleus, usually as a general luminous halo. (Martin, 1926; Conrady, 1929). An illustration of the effect of a halo of this sort is provided by figure 6, which may thus be used as a guide for estimating how the curves in light lines of figure 9 must be modified when a small amount of aberration is present. When the amount of aberration is large the central nucleus, if it still persists, becomes larger than in an aberration-free image at the same aperture. The nucleus may not be evident in some cases, but there also the effective size of the image is greater than that of the corresponding aberration-free image. Thus when the amount of aberration is considerable the log P_l curve necessarily lies substantially to the left of the curve for a perfectly corrected lens of the same aperture, even at low values of log P_l. When the amount of aberration is small, on the other hand, as indicated above, the log P_l curve remains of approximately the same shape as that for a perfectly corrected lens, but is shifted downwards slightly.

Now the general result of decreasing the aperture of a lens is to reduce the path differences at the focus. Thus at high apertures the log P_l curves will, if the aberrations are considerable, lie substantially to the left of the curves shown by light lines in figure 9, while for small apertures they will not differ much from these latter curves, but will tend to lie a little below them. To add more precision it has been assumed that at F/45 the lens is practically free from aberration, while at F/4 a guess at the shape of the curve has been based on the values of the visual resolving power obtained on lens No. 137006 for test-objects of high and low contrast. The curves for the apertures intermediate between F/4 and F/45 were drawn by eye to form a consistent family. The whole family of curves thus obtained is shown by heavy lines. It should be noted that a family of real log P_l curves might not display such an obviously systematic variation as those shown in figure 9.

We now require to estimate the influence of the diffusion of light in the emulsion layer. Fairly satisfactory results have been obtained, in other connections, by assuming that the intensity of illumination in the emulsion decreases exponentially with the distance from a long, narrow, brightly illuminated strip of the emulsion. If this is true, then the curve of log P_e against log $(1/d)$ has a definite shape which is the same for all photographic materials but which lies towards higher values of log $(1/d)$ the less the diffusion of light in the emulsion layer. The actual position of the P_e curve can be located on the log $(1/d)$ scale, once the threshold line (determined by the granularity and γ-value of the material) has been fixed, and the resolving power measured. This is illustrated in figure 10. The resolving powers of the three films were measured using a contact test-object, with a density difference of 0·2 between the light and dark parts. It should not be concluded that the diffusion of light is exactly the same in Panatomic-X as in Super-XX—the calculation is not a very exact one.

Adding together the log P curves of figures 10 and 11 gives the curves of log P_l + log P_e, and these are shown in their upper range in figure 11 for Super-XX and Panatomic-X, for which they are conveniently identical. Figure 11 also shows the curves of log P_l over the lower range: for low values of log P only visual resolution is possible, and it is not necessary to include the log P_l + log P_e curves. The resolving power at any aperture may be read from these curves. When plotted, the variation of resolving power with aperture is as shown in figure 12, which also includes values for Microfile film. The qualitative resemblance to the curves shown in figure 9 will be obvious, and in the main phenomena shown by photographic lenses at the centre of the field may be regarded as accounted for. It should be particularly noted that the results of the tests are inconsistent with any assumption except that at full aperture important amounts of aberration exist at the centre of the field.

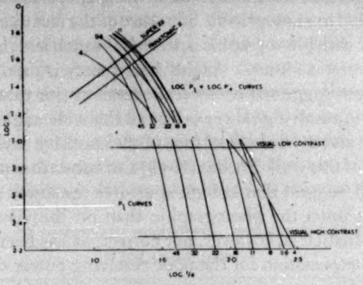

Figure 11. Log P_l and log $P_l+\log P_e$ curves and threshold curves for imperfect lens shown in figure 9.

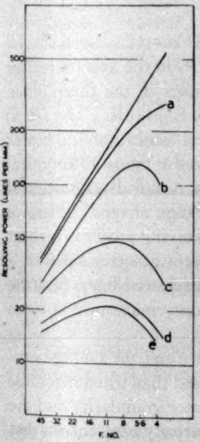

Figure 12. Resolving powers at different apertures, estimated from figure 11.

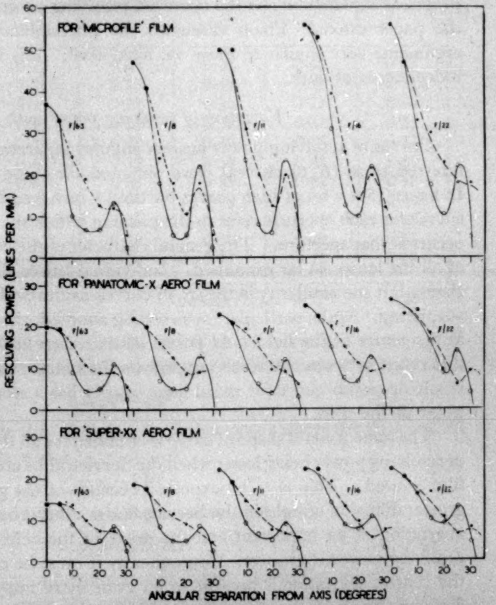

Figure 13. Typical [resolving power, angular separation from axis] curves. Full curves: radial lines. Dotted curves: tangential lines.

Although there is no published evidence that the variation of photographic resolving power with aperture had been investigated, either theoretically or experimentally, before the work described in this paper was commenced, there has been some discussion in photographic literature of the fact that the resolving power of a lens when used with photographic materials is much less than the figure usually accepted as the theoretical limit. As the discrepancy is particularly great at high apertures, it has been suggested on several occasions (for example, Zeigler, 1936) that the reduction in resolving power is due to the wide angle of the cone of light incident on the film and the finite thickness of the emulsion layer . In a paper seen late in the progress of this work Roeder (1941) also subscribes to this view, although he does, in addition, suggest that at high apertures the lower contrast of the image has a greater effect upon the photographic than on the visual resolving power. The proposed explanation is, however, not correct, as has been shown by Gregory (1946). A similar explanation for the poor resolving power observed off-axis has also been shown by Gregory to be incorrect. Pinoir (1944) also discusses the above points, and shows that there is serious quantitative disagreement between the proposed explanation and the observed resolving power. It is interesting that in the paper quoted, Pinoir discusses the phenomenon of resolving power by arguments very similar to those we have used. His work was, of course, quite independent of ours.

Variation of resolving power with angle

Curves of resolving power against angular separation from the axis (hereafter referred to as (R, θ) curves) were obtained for these lenses in the three films. In figure 13 is a set of such curves for the 14-inch lens No. EY 118K. The (R, θ) curves for each aperture refer to the plane in which the best axial resolving power occurs at that aperture. The general character of the curves in figure 15 is typical of all the lenses so far examined. Individual lenses show minor divergencies of shape, but the similarity in the (R, θ) curves over a wide range of types of lens is surprising. At the particular focus setting adopted, the resolving power is highest at the centre of the field. At points off-axis there is, except at special points, a difference between the resolving powers for radial and tangential lines, and the resolving-power curve for radial lines usually has a secondary maximum at some point in the filed.

The same general shape of curve is obtained for all three films, the average level of resolving power being lower when the Service films are used than when Microfile film is used. This is to be expected because of the greater granularity and the greater diffusion of light in the Service films. But it has already been shown that aberration of an important amount exists in the centre of the field, where the resolving power is greatest. Consequently it must be concluded that, away from the centre, aberration is present to an even more important degree. Stopping down the lens is for that reason more effective in improving photographic resolution at points off-axis than on-axis, as may be seen from figure 13. Some curious changes, such as in the curves for Microfile film, where the minimum at F/8 is lower than at F/6·3 but increases as the aperture is decreased below F/8, are almost certainly due to the re-focusing at each aperture.

One curious feature of the (R, θ) curves for radial lines deserves some mention. It was found that the secondary maximum and the minimum in the (R, θ) curves occurred at more or less constant positions in the field. Table 1 gives the tangents of the angles corresponding to these positions, and also the tangents of the semi-angle of view, defined as the angle at which the resolving power falls to zero. It will be seen that, with few exceptions, the maximum occurs at about 0·8 of the linear field and the minimum at about 0·5 of the linear field.

In most photographic objectives, the field curvature is such that the sagittal and tangential surfaces depart from the Gaussian image plane, and then re-cross it at some point towards the edge of the field. It is to be expected, therefore, that if the shape of the (R, θ) curve is determined by field curvature, the resolving power should first decrease as the angular separation from the axis is increased from zero, and then increase as the image surface swings back to re-cross the "focal plane".

Table 1. Positions of secondary maximum, minimum and zero in (R, θ) curves for radial lines

Lens		$\tan\theta$			Ratio (1) : (3)	Ratio (2) : (3)
		At max. (1)	At min. (2)	At zero (3)		
30-inch	156449	0·18	0·09	0·29	0·62	0·31
20-inch	73051	0·36	0·25	0·49	0·73	0·51
20-inch	154107	0·27	0·18	0·36	0·75	0·50
20-inch	233408	0·47	0·32	0·58	0·81	0·55
14-inch	227628	0·38	0·28	0·49	0·78	0·57
14-inch	EY118K	0·47	0·32	0·58	0·81	0·55
10½-inch	263403	0·47	0·28	0·58	0·81	0·48
8¼-inch	137006	0·58	0·36	0·73	0·79	0·49
8-inch	230863	0·47	0·28	0·58	0·81	0·48
8-inch	174351	0·47	0·32	0·58	0·79	0·55
5-inch	143352	0·58	0·36	0·75	0·77	0·48
				Means......	0·77	0·50

Suppose that the surface upon which radial lines are imaged (the sagittal surface) is generated by the rotation about the x-axis of the curve

$$x = \alpha y^2 - \beta y^4. \qquad \text{......(1)}$$

The secondary maximum in the (R, θ) curve will then occur where the above curve crosses the focal plane, that is at

$$y_2 = (\alpha/\beta)^{\frac{1}{2}}, \qquad \text{......(2)}$$

and the secondary minimum where x is a maximum, that is at

$$y_1 = (\alpha/2\beta)^{\frac{1}{2}}. \qquad \text{......(3)}$$

The "edge" of the field cannot be determined easily. However, there is a fairly close limit to the "edge" since the curve of x falls away from the focal plane extremely rapidly after crossing it. It may be assumed that worse definition is tolerated at the "edge" of the field than at the secondary minimum in the (R, θ) curve. That is to say, a greater value of x may be tolerated at the "edge" of the field than at y_1, and the limit of the field may be determined by making x at the "edge" $-\eta$ times as great as at y_1, where η is greater than unity. Thus

$$\eta\alpha^2/4\beta = \alpha y_3^2 - \beta y_3^4,$$

whence
$$y_3=\left[\frac{\alpha\{1+(1+\eta)^{\frac{1}{2}}\}}{2\beta}\right]^{\frac{1}{2}}.$$

Thus the ratio y_2/y_3, which corresponds with the ratio (1) : (3) of table 1, is given by

$$y_2/y_3=\left[\frac{2}{1+(1+\eta)^{\frac{1}{2}}}\right]^{\frac{1}{2}}.$$

and the ratio y_1/y_3, which corresponds with the ratio (2) : (3) of table 1, is given by

$$y_1/y_3=\left[\frac{1}{1+(1+\eta)^{\frac{1}{2}}}\right]^{\frac{1}{2}}.$$

The first ratio is equal to 0·75 and the second to 0·53 when η is equal to 6, which is probably not an unreasonable value.

The ratio y_2/y_1 is independent of any assumption as to the value of η, and is equal to $\sqrt{2}$. The experimental value, as determined by the ratio of the η values for the secondary maximum and the minimum, is 1·56, i.e. within 10% of the calculated value. Considering that no special efforts were taken to ascertain the precise positions of these features, the agreement is close enough to give some support for the assumption that for these lenses the sagittal field curvature is of the form described by equation (1). It may be observed that the *relative* positions of the minimum, secondary maximum, and zero in the (R, θ) curves are independent of the coefficients α and β. Equation (1) represents the third and fifth order field-curvature for an infinitely narrow pencil of rays. The positions of the secondary maximum and minimum do not change when the aperture is varied, however, and it may be inferred that the above discussion is equally valid for lenses of high aperture.

In the published field-curves for a number of lenses (for example, Hay and von Rohr, 1932) the tangential field-curves display the characteristics of equation (1) as often as do the sagittal field-curves, and yet the (R, θ) curves for tangential lines rarely exhibit the secondary maximum. The reason for this may be that the aberrations of aperture, which do not apparently affect the validity of the above discussion for radial lines, are more serious in their effect on the resolving power for tangential lines. Such defects as coma and transverse chromatic aberrations, as well as the effects of vignetting, might be expected to exert a greater influence on the resolution of tangential lines than of radial lines.

It has already been mentioned that the drop in resolving power away from the axis cannot be explained away as a result of the obliquity of the light. Washer (1945) has recently shown that even if a lens is completely free from aberrations the resolving power will be less for points off-axis than on-axis, owing to the smaller angular aperture of the cone of light reaching the image. The effect is, however, too small to be of any importance in real objectives of the type tested, and in any case cannot be put forward to account for the present results since reducing the aperture improves the definition.

Variation of illumination across field

Typical curves of log relative illumination plotted against angular separation from the axis are shown in figure 14. In most cases the measurements were made up to angles much greater than the lenses were intended to cover. The decrease in illumination from centre to corners of the film size for which the lenses were designed was in most cases fairly small. The resolving power of most photographic materials increases rapidly as the exposure is increased from zero, and reaches a maximum value when the mean density on the film is about 1·0. At greater exposures the resolving power falls slowly. If the exposure at the centre of the field is such as to give a density of 1·0, at other points in the field the film will have a lower effective resolving power if no compensation is introduced. In practice the variation of film-resolving power may be reduced to a minimum by arranging that the optimum exposure is reached at some intermediate zone of the film.

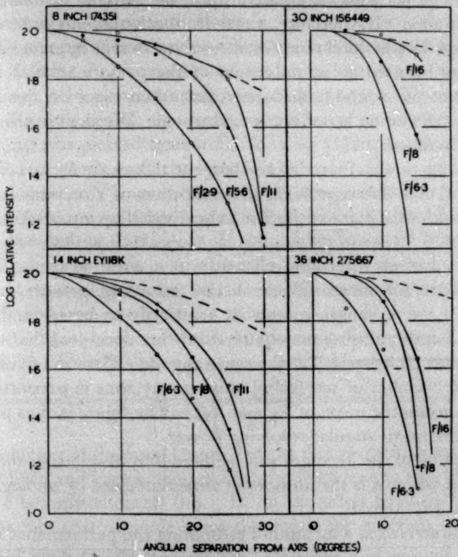

Figure 14. Decrease of intensity towards corners of field. Broken curve represents $I=I_0 \cos^4 \theta$.

From a curve of film-resolving power against log exposure, the effective film-resolving power at the corners of the field was calculated for the standard R.A.F. film sizes, and it was found that in only a few lenses was the vignetting serious enough to introduce any appreciable change in the effective film-resolving power. Moreover, since at the corners of the field the definition is determined by the lens rather than the film, the resolving power of the lens-film combination is very insensitive to changes in film characteristics.

Although vignetting tends to reduce the effective film-resolving power, it may have a beneficial use in removing some of the aberrant light from outer zones of the lens at the higher obliquities. Examples of this effect were encountered in studying the results of the present work.

§ 5. ANALYSIS OF RESULTS

An exact but simple comparison between the performances of different lenses is almost impossible. Not only is the problem complicated by differences in focal length, aperture, angle of view, and the differences in resolving power for radial and tangential lines, but the variation of resolving power with angle from the axis is different for different lenses. If, however, we are prepared to forego detailed comparison, and to take a more general view, the problem is not so difficult. The interpreter of an aerial reconnaissance photograph requires to be able to recognize details of objects on the ground. In practice this means, at present standards of performance, that the finer the detail resolved the better the photograph. The value of a photograph is also dependent upon the number of details visible in it, that is upon its area. If, therefore, a system of calculation can be devised which will give a figure for the total number of resolved details in an aerial photograph, that figure may be used as an indication of the performance of the camera in question. Some considerable discussion has taken place on this point and the best system of calculation is not yet agreed upon. We shall in this account keep to the original method.

If the resolving powers for radial and tangential lines are R_R and R_T respectively, we can imagine that this represents the resolution of a rectangular unit of area $1/R_R R_T$. Consider the plane of the film to be divided up into a series of concentric zones by means of circles of radii r_0, $r_0\sqrt{2}$, $r_0\sqrt{3}$, etc., so that each zone has area πr_0^2. The number of resolvable elements in a zone is evidently $\pi r_0^2 \bar{R}_R \bar{R}_T$, if $\bar{R}_R$ and $\bar{R}_T$ are the mean values of the resolving powers over the zone. The values of r_0 were chosen somewhat arbitrarily to be 10 mm. for a lens of 5 inches focal length and proportionately for other focal lengths, so that corresponding zones for all lenses fall at the same angular separation from the axis. It follows that the number of resolvable units in any zone is proportional to $(Rf)^2$, where R is the geometric mean of $\bar{R}_R$ and $\bar{R}_T$. The figure is thus proportional to the square of the mean angular resolving power.

The calculation of the averages was facilitated by re-plotting the (R, θ) curves as (R, n) curves, where n is the number of zones enclosed by an angle θ to the axis and is equal to $161{\cdot}3 \tan^2 \theta$.

Having thus arrived at a method of estimating the performance of a lens, on a given film, we are now in a position to examine whether there is any general rule connecting the performance of a lens with its aperture, focal length, angle of view and type of film with which it is used.

There were indications of such a general rule before the full data were obtained. For instance Hay and von Rohr (1932) give figures for spherical aberration, coma and field curvatures for a large number of lens specifications, taken from patents. These are all for a standard focal length of 100 mm. The curves given for spherical aberration extend to a value of aperture which is presumably the full aperture at which the lens is intended to work, and the curves for curvature of field extend to an angle which is presumably the angle covered by the lens. When these values are plotted one against the other and a mean curve is drawn through them it is found that there is an approximately constant ratio between the *F. No.* and the square of the angle of view. This is a natural consequence of the difficulty of reducing aberrations to tolerable values at high apertures and wide angles. On the assumption, therefore, that all these lenses were intended to give approximately the same level of performance, it may be concluded that the relation between the average number of resolvable units per zone, $\bar{N}$, the ***F*. *No*.**, the number of zones, n_∞, which the lens covers before the resolving power falls to zero, and the focal length, f, will be approximately of the form

$$\frac{F.\,No.}{n_\infty} = \phi(\bar{N}, f),$$

since

$$\theta_\infty^2 \doteqdot \tan^2\theta_\infty = n_\infty/161\cdot 3.$$

In an attempt to determine the nature of ϕ, a three-dimensional model was constructed, in which the average number of resolvable units per zone (obtained on Super-XX film) was plotted against ($F.\,No./n_\infty$) and f. This model confirmed that ($F.\,No./n_\infty$) was an appropriate argument in the functional relation, and furthermore, showed that the ***F*. *No*.** need not be restricted to the maximum aperture. The same relation held, approximately, for all apertures. To test whether this was also true if n was varied, the average number of resolvable units per zone up to the nth zone was plotted against $F.\,No./n$ for different apertures. With one or two exceptions, a single curve was obtained for each lens ; in the exceptional cases, different values of $\bar{N}$ were obtained for the same value of $F.\,No./n$, according to whether the ***F*. *No*.** were high or low. In general, however, the agreement was good enough to warrant further consideration, and on re-plotting the curves on double-logarithmic paper, the points were found to approximate to a straight line for each lens. At this stage the data for the other films were included and a number of graphs, such as that shown in figure 15, were obtained.

Assuming that the points for different apertures lie in the same straight line, the average number of resolvable units per zone ($\bar{N}$) may be expressed in the form

$$\bar{N} = A\left[\frac{F.\,No.}{n}\right]^b, \qquad \ldots\ldots(4)$$

where A is a function of the focal length and the film properties and b is the slope of the straight lines and varies, though slightly, from lens to lens and film to film. The value of b is approximately 0·6. If, on the other hand, it is necessary to account for the fact that in some cases the points for different apertures lie on different straight lines, equation (4) must be written

$$\bar{N} = A\frac{(F.\,No.)^b}{n^c}. \qquad \ldots\ldots(5)$$

For the sake of simplicity, we shall adopt the form in equation (4), for we can thus set $F.\,No./n = 1$ and find a single value of A for each lens-film combination. This value of A was found to be directly proportional to focal-length, in the following manner :—

for “ Super-XX ” film $A = 3kf$,
for “ Panatomic-X ” film $A = 4kf$,
for “ Microfile ” film $A = 15kf$.

The factor multiplying the focal length contains a constant k the value of which depends upon the units in which the resolving power is measured and on the size of the zones into which the film is divided.

The following considerations may help to explain why $\bar{N}$ is proportional to f. Suppose we have two series of lenses of the same ***F. No.*** but of different focal lengths, such that in one series there are no aberrations whatever, and the other series is of lenses all of the same design, but made to different scales, so as to have different focal lengths, and with considerable amounts of aberration. For the lenses without aberrations the resolving power in lines/mm. will be the same for all focal lengths, because the image size is independent of the focal length. The angular resolving power will therefore be proportional to the focal length and $\bar{N}$ will be proportional to the square of the focal length. When the lenses have considerable amounts of aberration, the size of the image is proportional to the focal length, so that the angular resolving-power, and $\bar{N}$ also, will be independent of focal length. In fact, even in this case, $\bar{N}$ will increase a little with focal length because the diffusion of light in the emulsion layer will be of less importance when the optical image is large, and also because the threshold of resolution is lower for large images than for small. Now the path-length errors are proportional to the focal length, and, therefore, however well or ill the lens may be designed,

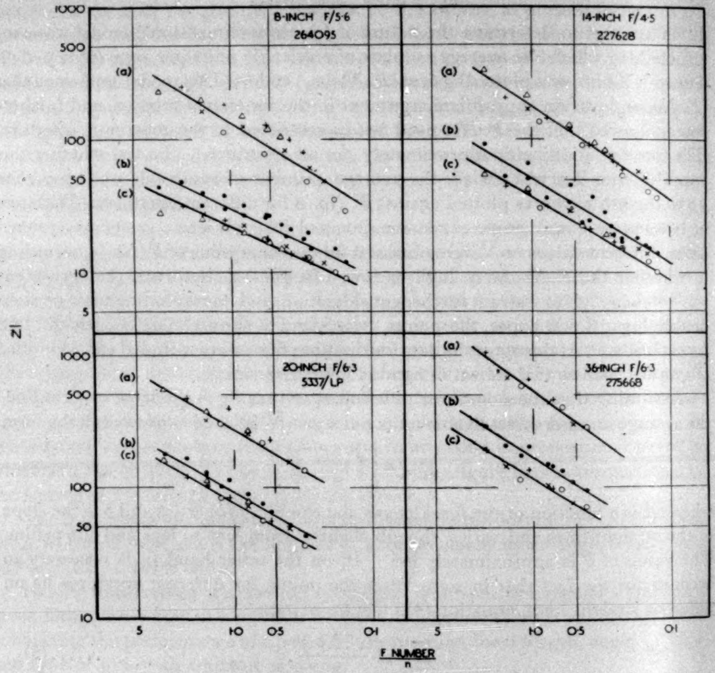

Figure 15. Variation of $\bar{N}$ with *F. No.*/*n*.
(*a*) Microfilm film, (*b*) Panatomic-X film, (*c*) Super-XX film.

there is some short focal length at which the lens is nearly perfect and some long focal length at which the correction is bad. In other words, for short focal lengths $\bar{N}$ will vary as f^2 and for long focal lengths will be constant, or nearly so. For moderate focal lengths, therefore, it is not unreasonable to find $\bar{N}$ varying approximately as f. What is perhaps more surprising is that the proportionality between $\bar{N}$ and f is not seriously disturbed by changes in aperture. Figure 16, which is illustrative only, will perhaps make the argument clear.

The general level of the resolving power varies according to the film used for taking the photographs. Two quantities have arisen during the theoretical discussions to which these differences of level might be attributed. They are the granularity and the diffusion of light in the emulsion layer. The dimensions of granularity are [Density: Length] and the dimension appropriate to the diffusion of light is [Length], since it may be conveniently measured by the distance in which the light flux in the emulsion layer coming from a long illuminated narrow strip drops by the ratio e. Either quantity, therefore, will satisfy the dimensional requirements of the formula. But in fact the diffusion of light is not likely to be of any importance. It will be seen from figure 2 that log P_e does not drop much below 0 for values of $1/d$ less than 20. Values as high as this are observed only on the axis. As soon as any appreciable angle is covered, the resolving power drops considerably below 20 lines/mm. and the diffusion of light in the emulsion layer is an unimportant item in the degradation of the image.

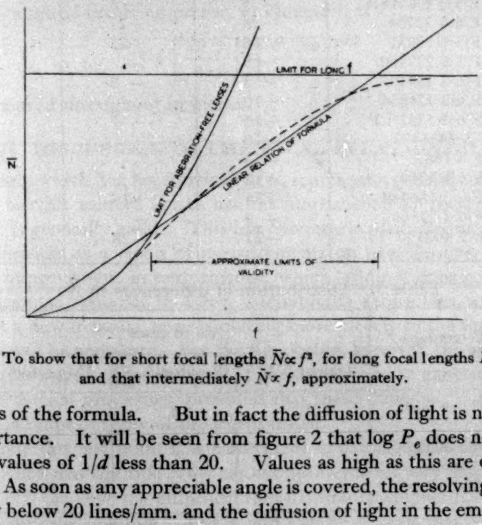

Figure 16. To show that for short focal lengths $\bar{N} \propto f^2$, for long focal lengths $\bar{N}$ is constant, and that intermediately $\bar{N} \propto f$, approximately.

The granularity values, measured by the method described by Romer and Selwyn (1943), at a density of 1·0 are 1·6, 1·2, and 0·3 density-microns for Super-XX Aero, Panatomic-X Aero and Microfile films respectively. The reciprocals of these figures are in the ratio 3 : 4 : 16, from which it may be concluded that the complete formula is

$$\bar{N}=\frac{Kf}{G}\left[\frac{F.\,No.}{n}\right]^{b}, \qquad \ldots\ldots(6)$$

in which b has the approximate values of 0·55, 0·6 and 0·75 for Super-XX Aero, Panatomic-X Aero and Microfile films respectively. Substituting these values in (6) and comparing the calculated value of $\overline{N}$ with the experimental values, K is found to be approximately $5{\cdot}5 \times 10^4$. In table 2 the departure of the performance of individual lenses from that of the "average" lens as given by (6) is shown, and in table 3 the frequency with which these differences occur is shown.

Table 2. Mean percentage differences of experimental values of $\overline{N}$ from those given by equation (6)

Film / Lens	Super-XX ($b=0{\cdot}55$)	Panatomic-X ($b=0{\cdot}6$)	Microfile ($b=0{\cdot}75$)
5-inch F/4 143352	−21	−10	− 3
8-inch F/4 230863	−14	−13	+ 9
8-inch F/2·9 174351	−12	− 8	− 2
8-inch F/5·6 264095	−15	− 6	+ 7
8¼-inch F/4 137006	− 7	+21	+30
10½-inch F/6 263403	+ 4	+ 3	− 2
14-inch F/4·5 227628	−24	−24	−24
14-inch F/6·3 EY118K	− 5	− 8	−12
14-inch F/5·6 72754	+25	+27	+19
20-inch F/5·6 73051	+16	+23	+15
20-inch F/5·6 277490	−19	..	..
20-inch F/6·3 154107	− 3	− 8	−20
20-inch F/6·3 174856	+10	..	+50
20-inch F/6·3 5337/LP	+10	− 1	−16
50 cm. F/5 2451477	−10	..	− 1
24-inch F/6 7887	− 3	..	− 5
24-inch F/6 EA504	− 2	..	−32
30-inch F/6·3 156449	+34	+19	+69
36-inch F/6·3 275667	− 9	− 1	−14
49-inch F/7 402490	−23	−28	−39

Table 3. Distribution of differences in $\overline{N}$.

Percentage difference	No. of cases		
	(Super-XX)	(Panatomic-X)	(Microfile)
10% or less	10	8	7
11%–20%	5	2	6
20% or more	5	5	6

The standard deviation for repeated measurements of the resolving power of the same image on the same negative is of the order of 10%, but in view of the large number of readings made for a given lens, at different angles to the axis, and since all the readings were made by the same observer, the averaged values of resolving power are probably reliable to within much less than 10%. (It should be noted that since $\overline{N}$ is proportional to the *square* of the angular resolving power, the differences in terms of angular resolving power are approximately half of the values listed in table 2.) The differences shown in table 2 may therefore be regarded as real differences, and due to differences in performance between different lens types.

A single value of *b* may be adopted without serious change in the reliability of the empirical relation. Thus, eliminating the parameters introduced originally,

$$\bar{N} = 5{\cdot}5 \times 10^4 \times \frac{f}{G}\left[\frac{F.No.}{n}\right]^{0{\cdot}6} \quad \text{resolvable units per zone}$$

$$= 2{\cdot}6 \times 10^3 \times \frac{f}{G}\left[\frac{F.No.}{\tan^2\theta}\right]^{0{\cdot}6} \quad \text{since } n = 161{\cdot}3\tan^2\theta$$

$$\text{or} \quad \frac{2{\cdot}6}{4\pi} \times \frac{10^3}{f^2}\ \frac{f}{G}\left[\frac{F.No.}{\tan^2\theta}\right]^{0{\cdot}6} \quad \text{resolvable units per sq. mm. on the film}$$

$$= \frac{207}{fG}\left[\frac{F.No.}{\tan^2\theta}\right]^{0{\cdot}6}.$$

The mean resolving power on the film is thus

$$\bar{R} = \left[\frac{207}{fG}\right]^{\frac{1}{2}}\left[\frac{F.No.}{\tan^2\theta}\right]^{0{\cdot}3} \text{ lines per mm.}$$

and the mean angular resolving power, in radians^{-1}, is

$$25{\cdot}4\left[\frac{207f}{G}\right]^{\frac{1}{2}}\left[\frac{F.No.}{\tan^2\theta}\right]^{0{\cdot}3}, \qquad \ldots\ldots(7)$$

since *f* is measured throughout in inches.

§6. DISCUSSION OF EMPIRICAL RELATIONSHIP

The formula which has been arrived at to represent a general view of the performance of aircraft camera lenses has no fundamental or theoretical basis to ensure that it is generally valid. This has been made plain during the latter part of this investigation, as a result of measurements on new designs. These have shown some improvement in performance, which, while it does not so far make the above formulae seriously in error, undoubtedly shows that with continued improvement a new formula, approximating more closely to the theoretical limit of perfection, will be necessary. For the time being, however, the above formulae are a satisfactory statement of the level of performance to be expected from a lens of given dimensional properties, provided that these dimensional properties are not outside the range of those of the lenses tested.

To illustrate this last point it is convenient to use again the argument of §5. It will be obvious that the rule $\bar{N} \propto f$ cannot be obeyed for very short focal lengths for which $\bar{N} \propto f^2$,so that the empirical formula predicts higher resolving powers than are theoretically possible. And it will also be obvious that $\bar{N} \propto f$ cannot be true beyond focal lengths at which the lens may be regarded as badly corrected.

The correction of aberrations is better in the centre of the field than towards its outer parts, with the result that the diffusion of light in the emulsion layer is relatively more serious in the centre of the field than elsewhere. Thus the importance of the diffusion of light in the film is dependent upon the angle of view. In the formula the influence of diffusion does not appear explicitly, but may be involved implicitly in the term *G*, since there is an approximate connection between *G* and the diffusion. But the influence of granularity also varies over the field of the lens, as a result of its relatively greater obscuring effect for fine detail than for large. To represent the influence of granularity by a single term unconnected with the angle of view is, therefore, theoretically incorrect. It is more than probable that the different values of b found for the three materials arise because of this effect. Unfortunately the data are quite inadequate for investigating this question more fully, and any attempt at more precise formulation of the experimental data than is represented by equation (5) would be somewhat artificial.

There are a few minor limitations to the generality of the results. The average resolving power was computed for circular films, since the analysis would have been rather complex if rectangular films had been considered. In addition, in the collimator method of examining lenses, only a small fraction of the total field of the lens is illuminated, and the effect of light scattered by the lens is less than under practical conditions. Another departure from strictly practical conditions was that the brightness of the test-object was increased for extra-axial exposures to compensate for the decrease in illumination due to vignetting, etc.

In spite of the foregoing discussion, it is somewhat surprising, in view of the known differences in construction of the lenses under examination, that their performances may be defined, as well as they are, solely by the dimensional properties of focal length, aperture and angle of view. The empirical formula implies the existence of a standard of performance, and this can only mean that the designer endeavours to reduce the aberrations to a level which experience has taught him will lead to a satisfactory result. Another designer may aim for a different type of correction, but the extent of the correction upon which he decides will probably be such as to lead to a photographic performance approximately equal to that accepted by the first designer. This is not to say that the empirical expression is inflexible; the lenses upon which it was based were designed during and after the 1914–18 war and up to the early years of the second war, and all that is claimed is that the formula represents the standard prevailing up to about 1943, when this work was completed. Indeed, since that time advances have been made which have raised the performance of individual lenses to such an extent that a repetition of the present research with a wide enough range of the latest products of the British optical industry would result, if not in a change in the form of the relationship, then certainly in a change in the constants. For the time being, however, the formula is useful, not only for its original purpose, but also as a standard of reference by which the merit of a given lens for air photography may be estimated by comparing its performance with that calculated from the formula, and for estimating the effect of moderate changes in the focal length, aperture and angle of view of a lens of given basic design.

§7. ACKNOWLEDGMENTS

One of us is indebted to the Ministry of Aircraft Production for permission to submit part of this work to the University of London as a Ph.D. thesis, and both of us are indebted to the Ministry for permission to publish in the present form.

In addition, the authors wish to acknowledge their indebtedness to the many discussions they have had, not only with colleagues, but with those who have collaborated in a large programme of work of which this research is but part.

REFERENCES

Cobb, P. W. and Moss, F. K., 1928. *J. Franklin Inst.*, **205**, 831.
Conrady, A. E., 1929. *Applied Optics and Optical Design* (Oxford).
Frieser, H., 1935. *IX Congrès Internat. de Phot.*, Paris, 207.
Frieser, H., 1938. *Z. wiss. Phot.*, **37**, 19.
Gardner, I. C., and Case, F. A., 1937. *J. Res. Nat. Bur. Stand., Wash.*, **18**, 449.
Gregory, J. M., 1946. *Proc. Phys. Soc.* (in course of preparation).
Hay, A., and von Rohr, M., 1932. *Handb. wiss. und angew. Phot.*, Band 1, " Das Phot. Objektiv " (Vienna : Julius Springer).
Jones, L. A., 1921. *J. Opt. Soc. Amer.*, **5**, 232.
Jones, L. A. and Condit, H. R., 1941. *J. Opt. Soc. Amer.*, **31**, 651.
Martin, L. C., 1926. *Trans. Opt. Soc., London*, **27**, 249.
Pinoir, R., 1944. *Sci. Industr. Photogr.* (2), **15**, 257.
Roeder, H., 1941. *Phot. Industr.*, **39**, 385, 401, 418, 432, 439.
Romer, W. and Selwyn, E. W. H., 1943. *Phot. J.*, **75**, 571.
Ross, F. E., 1924. *The Physics of the Developed Photographic Image*. Eastman Kodak Monograph, No. 5.
Sandvik, O., 1927. *J. Opt. Soc. Amer.*, **14**, 169 ; 1928. *Ibid.*, **16**, 244.
Sayce, L. A., 1940. *Phot. J.*, **80**, 454.
Washer, F. E., 1945. *J. Res. Nat. Bur. Stand., Wash.*, **34**, 175.
Zeigler, H. W., 1936. *Amer. Phot.*, **30**, 553.

THE DETERMINATION OF DISSOCIATION ENERGIES BY THE BIRGE-SPONER EXTRAPOLATION

By A. G. GAYDON,
Warren Research Fellow of the Royal Society, Imperial College, London

MS. received 28 *March* 1946

ABSTRACT. A critical examination is made of the Birge-Sponer method of determining dissociation energies of diatomic molecules. Dissociation energies of certain classes of molecules as determined by linear extrapolation are compared with values determined independently. For the ground states of ordinary molecules the linear extrapolation tends to give too high results, often by around 20%. For molecules in which ionic binding is important the extrapolation often comes too low, sometimes much too low. For the molecules in which one atom has a $^1S_0$ ground state the linear extrapolation is much too high. The method appears to work satisfactorily for ionized molecules. Excited states of molecules cannot, in general, be relied on to give good extrapolations. These empirical observations are discussed in terms of the potential-energy curves and the binding forces in the molecules at large inter-nuclear distances.

§1. INTRODUCTION

The method of determining the dissociation energies of diatomic molecules by extrapolation of the vibrational energy levels to their convergence limit was first put forward by Birge and Sponer (1926). Since then some other methods have been used as well to ascertain the dissociation energies of certain molecules, but for the large majority of diatomic molecules we are still dependent on the Birge-Sponer extrapolation.

When data are available for a large number of vibrational levels, the graphical extrapolation, made by plotting the vibrational energy intervals $\Delta G(v+\frac{1}{2})$ against the vibrational quantum number v, or sometimes against the vibrational energy term $G(v)$, may be expected to lead to a fairly reliable result. In the majority of cases, however, only a few levels are known and the interval between these decreases approximately linearly, and it is then customary to make a *linear extrapolation.* It has been generally realized that there is a tendency for this linear extrapolation to come too high. Birge (1929) discussed the form of the curve of $\Delta G(v+\frac{1}{2})$ against v for a few molecules and showed that its shape and curvature changed rather unexpectedly in some cases ; the sudden inflections, which he believed he had established for the excited states of O_2 and some of the halogens, have not, however, received much support from later, more precise, spectroscopic observations. Rydberg (1931) suggested that an alternative form of extrapolation, in which $[\Delta G(v+\frac{1}{2})]^2$ is plotted against v, might be better in some cases ; and since this method usually gives a lower value of the dissociation energy than that obtained by linear extrapolation, it has sometimes been used. Nevertheless, the linear extrapolation is still in most general use and forms the basis for most of the values of dissociation energies now in the literature.

For a fair number of molecules accurate values of the dissociation energy have been obtained by other methods, such as by observation of band structure up to the convergence limit at which continuous absorption begins (O_2 and the halogens), of atomic fluorescence (halides of alkali-metals, Tl, etc.), of predissociation (HgH, N_2, CO, SO, etc.), or by thermochemical methods (alkali-metal halides, etc.) or by combinations of these methods (HCl, HBr, HI, NO). These methods have been reviewed in the author's recent book (Gaydon, 1946) and the values for the dissociation energies have been listed. It is the purpose of this paper to make a systematic comparison between these accurate values of dissociation energies with those obtained by linear extrapolation, with a view to making better use of the linearly extrapolated values for the many molecules for which this is the only method available.

In their original paper Birge and Sponer pointed out that their method of extrapolating was only justified if the vibrational energy levels converged to a limit at a finite value of the vibrational quantum number v. Kratzer (1924) showed that if the force between the nuclei at very large internuclear distance, r, is expressed as a power series in $(1/r)$, then, if the dominant term at large r is $1/r^2$ or $1/r^3$, there will be an infinite number of vibrational energy levels, so that the curve of $\Delta G(v+\frac{1}{2})$ against v would approach the v axis asymptotically. If, however, the dominant term in the expression for the force is $1/r^4$ or higher power of $(1/r)$, then the maximum value of v will be finite. For non-polar molecules the force at large internuclear distance varies as a high power of $(1/r)$ and the extrapolation is therefore permissible. For polar molecules dissociating to ions, however, the force must vary as $1/r^2$ at large distances and the extrapolation should not be made by the method of Birge and Sponer. It is clear that the rate of convergence of the vibrational levels near the limit will depend on the form of the law of force at large distances and we may, therefore, expect the curve of $\Delta G(v+\frac{1}{2})$ against v to show a different trend for classes of molecules with different forms of binding. It therefore appears best to treat separately certain general classes of molecules.

§ 2. EXTRAPOLATION FOR THE GROUND STATES OF NEUTRAL MOLECULES WITH NON-IONIC BONDING

First, we shall compare the accurately determined dissociation energy D_0 and the linearly extrapolated value D_{lin} for the ground electronic states of those neutral molecules for which ionic binding forces are not unduly important. The values of the dissociation energies are taken from the author's book, where full references may be found. For N_2, NO, CO and CN the values have been discussed by Gaydon and Penney (1945) and differ from those in the older literature (e.g. Herzberg, 1939). For SO and S_2, values higher than those given by Herzberg have been adopted.

It is possible to make the linear extrapolation either graphically from the first part of the curve of $\Delta G(v+\frac{1}{2})$ against v or analytically. The latter method is more usual and has been adopted here.

If the energies of the vibrational levels are expressed as a power series

$$G(v) = \omega_e(v+\tfrac{1}{2}) - x_e\omega_e(v+\tfrac{1}{2})^2 + \ldots, \qquad \ldots\ldots(1)$$

where v takes integral values 0, 1, 2, ..., it can be shown that, neglecting higher terms, the energy interval from the lowest level, $v=0$, to the limit, which is the required dissociation energy, is

$$D_{lin} = \frac{\omega_e^2}{4x_e\omega_e} - \tfrac{1}{2}\omega_e. \qquad \ldots\ldots(2)$$

It is often given as $D_{lin} = \omega_0^2/4x_e\omega_e$ where $\omega_0 = \omega_e - x_e\omega_e$; for all practical purposes this is satisfactory, but it may be pointed out that it is not strictly correct as it differs from (2) by $\frac{1}{4}x_e\omega_e$.

The values of D_{lin} have been calculated with the aid of equation (2) from collected values of ω_e and $x_e\omega_e$ given by Herzberg (1939); for ClF the value is from a more recent paper by Wahrhaftig (1942). Table 1 shows the values of D_0, D_{lin}, and the ratio D_0/D_{lin}.

Table 1. Values of D_0, D_{lin} (in ev.) and D_0/D_{lin} for the ground states of molecules with non-ionic bonding

Molecule	D_0	D_{lin}	D_0/D_{lin}	Molecule	D_0	D_{lin}	D_0/D_{lin}
H_2	4·478	4·55	0·99	O_2	5·084	$6{\cdot}3_0$	0·81
KH	1·86	2·02	0·92	SO	5·148	6·3	0·82
AgH	2·3	2·7	0·85	S_2	4·4	5·7	0·77
OH	4·4	5·3	0·83	Se_2	2·8	4·5	0·62
				TeO	2·725	$5{\cdot}7_6$	0·48
HCl	4·431	5·15	0·86				
HBr	3·60	4·78	0·75	N_2	9·764	11·8	0·83
HI	2·75	4·0	0·69	P_2	5·033	$6{\cdot}6_6$	0·76
				As_2	3·94	5·1	0·77
Li_2	1·12	1·46	0·77	Bi_2	1·72	2·27	0·76
Na_2	0·77	1·07	0·71				
K_2	0·51	0·74	0·69	ClF	2·616	1·93	1·35
				Cl_2	2·476	2·44	1·02
CO	11·11	11·2	0·99	ICl	2·153	3·08	0·70
NO	6·49	7·6	0·85	Br_2	1·971	3·02	0·65
CN	7·6	9·9	0·77	IBr	1·818	2·85	0·64
				I_2	1·542	2·37	0·65

The table includes practically all the non-ionic molecules for which adequate data for D_0 and $x_e\omega_e$ are available. The exceptions are certain molecules containing elements of Group II of the Periodic Table, which have $^1S_0$ ground states and which, for reasons given presently, are best considered separately. It will be noted that OH, HCl, HBr and HI are included in table 1 ; ionic forces probably contribute to a certain extent to the bonding in these molecules, but since the electron affinity of the non-metal is in each case small (around 3 to 4 ev.) compared with the ionization potential of hydrogen (13·5 ev.), these molecules will dissociate to neutral atoms and the force between the atoms at large distances is unlikely to be appreciably affected by ionic forces.

It will be seen from table 1 that there is a general tendency for the true dissociation energy to lie below the linearly extrapolated value. The average value of D_0/D_{lin} is 0·79, and for thirteen of the 28 molecules the values lie between 0·75 and 0·85, with six above 0·85 and nine below 0·75. Thus we see that for this class of molecules the most probable value of the dissociation energy is about 20% below that given by the linear extrapolation. Clearly the scatter in the values of D_0/D_{lin} is rather great, but apart from the general tendency for D_{lin} to be too high it is possible to distinguish at least one systematic effect. D_0/D_{lin} tends to be highest for molecules composed of light elements and lowest when heavy elements are involved. This effect is well shown both by the group containing the halogen molecules and by that consisting of molecules built from Group VI elements. It is not easy to express this effect in quantitative form, but it would seem that one might do worse than to adopt a dissociation energy 10% below the linearly extrapolated value for hydrides and molecules composed of light elements, while for molecules containing a very heavy element a value only 70% of that given by linear extrapolation seems reasonable.

It may be pointed out that if the experimental data are not of high accuracy there may be a tendency for the next term, $y_e\omega_e(v+\frac{1}{2})^3$, in the series expansion for $G(v)$ (equation (1)), to be masked by the experimental error. Since this term is usually negative, the result will be to obtain a slightly higher value of the apparent $x_e\omega_e$ than the true one, thus bringing D_{lin} down slightly.

§ 3. MOLECULES CONTAINING AN ATOM WITH $^1S_0$ GROUND STATE

The form of the graphical Birge-Sponer extrapolation or the accuracy of the linear extrapolation must clearly be related to the potential-energy curve for the molecular state, especially its shape at fairly large internuclear distances. Now an atom with a closed shell or closed sub-shell of electrons, i.e. an atom in a $^1S_0$ state, has no resultant electric or magnetic moment and is, therefore, likely to exert a smaller force on another atom at a distance than is an atom with a resultant moment. This is borne out by the fact that the rare gases do not, with the exception of some excited states for He_2, form molecules at all. For the elements of Group II of the Periodic Table, however, although their ground states are $^1S_0$, many stable diatomic molecules are known. In these cases the binding forces are believed to be mainly due to excited states of the atom, although as a result of interaction between the various potential-energy curves and the rule that curves of the same species may not cross, the ground states of these diatomic molecules do probably correlate with ground atomic states. Clearly, the form of the extrapolation is likely to be affected by the fact that the binding is largely due to excited states, and that at large internuclear distances the force between the atoms is likely to be abnormally small. It thus seems desirable to treat molecules of this type separately.

Although a large number of diatomic molecules formed from elements of Group II are known, for relatively few of them is it possible to compare D_0 and D_{lin}; apart from the scarcity of accurate values of the dissociation energy, for many of these molecules, especially the halides, the band systems are not strongly degraded, so that the values of $x_e\omega_e$ derived from the analyses of band heads are far from accurate. The data are most complete for the hydrides; for many of these predissociation has been observed, which sets at any rate an upper limit for D_0. The values are given in table 2.

Table 2. D_0, D_{lin} (in ev.) and D_0/D_{lin} for hydrides of Group II elements

Molecule	D_0	D_{lin}	D_0/D_{lin}
ZnH	0·84	1·35	0·62
CdH	0·678	1·29	0·53
HgH	0·372	0·64	0·58
BeH	$\sim$2·3	3·6	$\sim$0·64
CaH	$\leqslant$ 1·70	2·6	$\leqslant$ 0·65
SrH	$\leqslant$ 1·66	2·6	$\leqslant$ 0·64
BaH	$\leqslant$ 1·82	2·6	$\leqslant$ 0·69

Thus for these hydrides the true value of the dissociation energy is much less than the linearly extrapolated value, often being only about 60% of that value. The unusually rapid rate of convergence of the vibrational levels for these molecules is shown by the high values of $x_e\omega_e$ and the strong negative curvature of the graphs of $\Delta G(v+\frac{1}{2})$ against v in many cases. For molecules other than hydrides the evidence is scanty. For CaCl predissociation shows that $D_0 \leqslant 2{\cdot}76$, while a poor linear extrapolation gives 5·1 ev., so that $D_0/D_{lin} \leqslant 0{\cdot}54$. For HgCl recent measurements (Wieland, 1941) give a linear extrapolation to 1·6 ev., and a good graphical extrapolation to 1·13, the ratio of which is 0·70. While the data are clearly inadequate for sweeping generalizations, we may reasonably suspect that molecular states correlated to an atom in a $^1S_0$ state tend to give an abnormally high linear Birge-Sponer extrapolation. The alkaline-earth metals mostly have low ionization potentials, and many of their compounds, especially their halides, may show partially ionic bonding which may confuse the relation between their true dissociation energies and the linearly extrapolated values.

§4. MOLECULES WITH PARTIALLY IONIC BONDING

For molecules composed of a metal with low ionization potential and a non-metal with high electron affinity the bonding force tends to be largely of an ionic nature. For all molecules except CsF the ionization potential of the metal exceeds the electron affinity of the non-metal, and the ground states are believed to dissociate to neutral atoms. Nevertheless, since the ionic forces in some of these cases are believed to be relatively important, it is probable that the potential energy curve will assume a different form from that for molecules in which ionic bonding is unimportant. Thus, it seems likely that the relation between the true value of the dissociation energy and the linearly extrapolated value may be abnormal. In making the comparison we are again handicapped by lack of data. The most ionic molecules are the halides of the alkali metals. Good values of the dissociation energy are available for most of them, thermochemical values agreeing closely with those obtained by observation of atomic fluorescence. These molecules do not, unfortunately, readily give discrete band spectra from which values of ω_e and $x_e\omega_e$ can be obtained ; for some of them, however, Beutler and Levi (1934) have succeeded in observing some rather diffuse bands from which approximate values of ω_e and $x_e\omega_e$ have been derived. The only other molecules of this type for which data are satisfactory are TlCl, TlBr, and GaI ; the measurements are most precise in the case of TlCl, for which the dissociation energy has been derived both thermochemically and by atomic fluorescence, while the values of ω_e and $x_e\omega_e$ have been obtained by Howell and Coulson (1938) from origin measurements.

The values of D_0, D_{lin}, D_0/D_{lin}, and also the difference between the metallic ionization potential (I) and the electron affinity ($E.A.$) of the non-metal are shown in table 3. It will be seen that for most of the molecules listed the true dissociation energy is much *higher* than that obtained by linear extrapolation ; this is particularly true for the halides of potassium, for which the values of $x_e\omega_e$ are likely to be more accurate than for the halides of Na and Li. There is some doubt about the values of D_0 for GaCl, GaBr, InCl, InBr and InI, but here again it is quite likely that the true dissociation energy is much higher than the linearly extrapolated value. For HF, although the ionization potential of hydrogen exceeds the electron affinity of fluorine by over 9 ev., it is believed that ionic bonding is fairly important; if we accept Herzberg's (1939) value for D_0 we obtain $D_0/D_{lin} = 1{\cdot}07$; a rather lower value of D_0 appears probable to the author, but it seems fairly certain that the ratio is not less than 1.

Table 3. Ground states of molecules with predominantly ionic bonding

Molecule	D_0	D_{lin}	D_0/D_{lin}	$I-E.A.$
LiI	3·6	4·2	0·86	1·6
NaCl	4·24	4·4	0·96	1·4
NaBr	3·83	$2{\cdot}6_6$	1·43	1·5
NaI	3·11	3·4	0·91	2·1
KCl	4·40	2·7	1·63	0·6
KBr	3·93	2·2	1·78	0·7
KI	3·31	2·0	1·65	1·1
TlCl	3·80	2·1	1·81	2·3
TlBr	3·2	2·9*	1·10	2·5
GaI	2·85	2·9	0·98	2·8

* From Howell and Coulson (1941).

Thus we see that values for the dissociation energies of molecules with partially ionic bonding which have been derived from a linear Birge-Sponer extrapolation should be treated with caution. In some cases such values may be too low, instead of, as is usually thought to be the case, on the high side. It is not always easy to say definitely which molecules are subject to appreciable ionic binding forces; the rough rule, suggested by Mulliken, that ionic bonding is likely to be predominant when the metallic ionization potential exceeds the electron affinity of the non-metal by less than 3 ev., is helpful, but there are cases when such forces are still important even when the ionization potential is a good deal higher than the electron affinity, as in HF.

§ 5. THE EXTRAPOLATION FOR EXCITED STATES

So far we have considered the extrapolation only for the ground states of molecules. For these, the perturbations of the potential-energy curve by those of other states are likely to cause only a general deepening of the potential minimum without any violent alteration in its general form. (The special cases where the ground state correlates with an atom is a $^1S_0$ state, and where the perturbations are due to ionic terms, have been discussed already.) For excited electronic states, however, mutual interactions are more likely to cause perturbations which will modify the shape of the potential curves in an irregular way, and deviations from a smooth Birge-Sponer extrapolation of the vibrational energy levels may be expected to be more frequent.

It should be especially noted that interaction from ionic terms is likely to be more frequent and more severe for excited states. Thus, for the halides of Al, Ga, In, and Tl, the dissociation limit to ions (e.g. to $Al^+ + Cl^-$, etc.) lies below the limit going to a normal halogen atom and a metal atom in its lowest excited state* (e.g. to $Al(^2S) + Cl(^2P)$). Many of the excited states of molecules formed from one strongly electro-positive and one strongly electro-negative atom are influenced by ionic forces, and may even dissociate to ions; in this case the Birge-Sponer extrapolation would take quite a different form, and it would be quite incorrect to assume a linear convergence of the vibrational levels, of which there would in this case be an infinite number.

There are a fair number of examples of abnormalities for excited states. The most obvious group calling for comment is that of the upper states of the main systems of the alkali-metal hydrides. For all these the spacing of the vibrational energy levels at first increases so that $x_e\omega_e$ has a fairly large negative value; instead of converging, the levels diverge. The unusual form of the potential curves for these states has been attributed by Mulliken (1936) to interaction with the potential curve arising from ionic products. Although a linear extrapolation is clearly impossible, the curve of $\Delta G(v+\frac{1}{2})$ against v appears to be smooth, rising to a flat maximum and then falling fairly sharply, so that a graphical extrapolation to the dissociation limit is not necessarily ruled out; a good value can be obtained in this way for KH, and the method can also be used for NaH. For some of the excited states of the alkali-metal molecules (K_2, Li_2, etc.) a similar, but less marked, effect is observed. The vibrational energy levels at first show a slow rate of convergence which slowly increases, but at high vibrational quantum numbers the rate of convergence increases sharply and the graphical extrapolation appears to indicate a dissociation energy for these states of only about half that given by linear extrapolation.

The most extreme anomaly is for the excited state of AgH. From the analysis by Bengtsson and Olsson (1931) it appears that the vibrational levels at first show rapid and increasing convergence, but the curve of $\Delta G(v+\frac{1}{2})$ against v flattens out abruptly at higher v, and the rate of convergence must be practically zero for a number of levels before increasing again (see Herzberg, 1939; Gaydon, 1946).

---

* By lowest excited state is meant the lowest main term other than the ground one, ignoring multiplet splitting; for Al, etc., the ground state is ^2P and the lowest excited state ^2S.

It has been shown (Herzberg and Mundie, 1940) from the form of the limiting curve of dissociation, as obtained from predissociations, that the excited $^1\Pi$ states of AlH and BH possess potential maxima. Mulliken (1937) has shown that some of the potential curves of the excited states of the silver halides, and probably the copper halides, possess quite marked maxima. In these cases even a graphical Birge-Sponer extrapolation would be of no avail, as it would lead to the energy of the potential maximum instead of to the dissociation limit. The author is inclined to think that the potential curves of the excited states of many other halides, including probably those of Al, B, Ga and In, may possess similar maxima.

Although it is clear that there are many instances in which the extrapolation (especially the linear form) is likely to fail when applied to excited molecular states, there are still many for which it seems to work satisfactorily. As examples may be quoted the upper states of the main systems of O_2, P_2 and the various halogen molecules; it is true that at one time Birge (1929) pointed out certain irregularities in the curves of $\Delta G(v+\frac{1}{2})$ against v for some of these, but these irregularities have been largely smoothed away by later experimental work, and were in any case not of a magnitude seriously to affect the accuracy of the extrapolation. Many of the lower excited states of N_2 and CO give satisfactory extrapolations to the expected limits when the author's (Gaydon and Penney, 1945; Gaydon, 1946) latest values for the dissociation energy are used.

In general it seems that where a reasonable extrapolation from ground state data is available it is to be preferred to one for an excited state, but for molecules with atomic (non-ionic) binding, especially homonuclear molecules and molecules formed from non-metallic elements, extrapolations from the lower excited states are permissible. For metallic halides, and probably hydrides and oxides as well, it is unsafe to place reliance on extrapolations for excited states.

§ 6. THE EXTRAPOLATION FOR IONIZED MOLECULES

So far we have considered the extrapolations for neutral molecules which dissociate to two neutral atoms. For singly ionized molecules, however, dissociation will take place to one neutral atom and one charged atom. The force between a charged and a neutral atom at large distances is likely to be much greater than that between two neutral atoms. Thus the potential-energy curve at large internuclear distances is likely to take a rather different form for ionized molecules, and it would seem best to make a separate comparison of the true and linearly extrapolated values of the dissociation energy for this type of molecule. The few available values are collected in table 4.

Table 4. Ionized molecules

Molecule	D_0	D_{lin}	D_0/D_{lin}
H_2^+	2·649	2·50	1·06
HCl^+	4·5	4·0	1·12
O_2^+	6·48	6·48	1·00
N_2^+	8·73	9·2	0·95
CO^+	8·2	9·8	0·84

For O_2^+ the value of D_0 is derived from a good graphical extrapolation for the excited state; it is probably of quite high accuracy, but does, of course, assume a normal trend for the extrapolation. The values for N_2^+ and CO^+ are derived from the values of $D(N_2)$ and $D(CO)$ given by Gaydon and Penney (1945) combined with the ionization potentials of N_2 and CO; for CO the value 14·1 ev. for $I(CO)$ has been used, but it is just possible that the value is 14·55 ev.

From the values collected in table 4 there appears to be little evidence for any systematic deviation from the linear value. It would therefore seem that ionized molecules are rather more suitable for making a linear extrapolation than neutral molecules, for which the true value, as we have seen, tends to be around 20% below that of the linear extrapolation. However, all the molecules included in table 4 are relatively light. For BeH^+, MgH^+ and CdH^+ accurate values of D_0 are not available, but the rate of convergence of the ground state vibrational energy levels does increase slightly with v, and the linear extrapolation is probably a little high. Most probably the linear extrapolation is fairly good for light ionized molecules and a little high for the heavier ones, although not to the same extent as for the corresponding neutral molecules.

§ 7. THE RELATION BETWEEN THE FORM OF THE EXTRAPOLATION AND THE POTENTIAL-ENERGY CURVE

Clearly, the rate of convergence of the vibrational energy levels must be related to the shape of the potential-energy curve for the particular molecular state. Now for the lower vibrational levels the rate of convergence is frequently nearly a linear function of the vibrational quantum number, and we have been chiefly concerned with the linear extrapolation. One of the simplest functions for representing the potential-energy curve of a diatomic molecule is that due to Morse, which is of the form

$$U = D_e(1 - e^{-\beta(r-r_e)})^2.$$

One of the main virtues of this function is that when inserted in the wave equation it leads to a series of vibrational energy levels which do converge linearly. Thus it seems desirable to make use of this simple function as a basis for comparing the form of the potential curve and departures from linear convergence of levels.

For normal molecules, in which ionic binding forces are unimportant, the lower vibrational levels usually show a very nearly linear rate of convergence, but, as we have seen, extrapolation of this convergence leads to a dissociation energy of the order 20% too high. We may take the ground state of O_2 as a typical example. For this, some 21 vibrational levels are known up to over 3·4 ev., and over this range the rate of convergence is nearly linear, showing only a slight sign of an increased rate at the highest observed values of v. Figure 1 shows a curve (dashed line) obtained from a Morse function (which uses the values of D_e, ω_e and r_e, which are derived from the three spectroscopic constants D_0, ω_e and B_e) and a curve (full line) plotted from a modified function proposed by Hulburt and Hirschfelder (1941) which uses the five spectroscopic constants D_0, ω_e, $x_e\omega_e$, B_e and α_e; the five-constant function can be relied upon in this case to come very close to the true potential curve. It will be seen from figure 1 that at $r > r_e$ the true potential curve lies above that given by the Morse function. The true curve tends to approach the dissociation limit more rapidly than the Morse curve, and this more rapid approach to the limit is associated with a less rapid rate of convergence of the lower vibrational levels and an increasing rate of convergence of the higher ones.

For molecules dissociating to atoms of which one is in a $^1S_0$ state, the vibrational

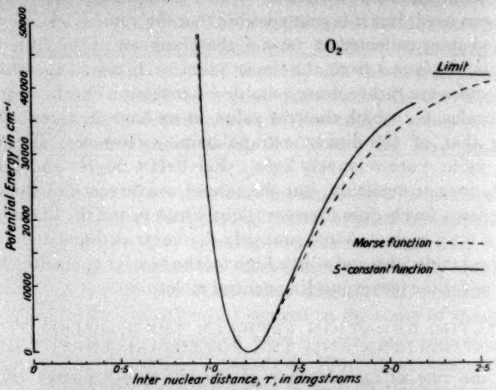

Figure 1. Potential-energy curves for the ground state O_2.

levels converge with unusual rapidity; even for the lower levels there is usually a marked departure from a linear rate of convergence, and the linear extrapolation, for which there is really little justification, comes much too high. Clearly, in these cases the potential curves must depart considerably from the Morse form.

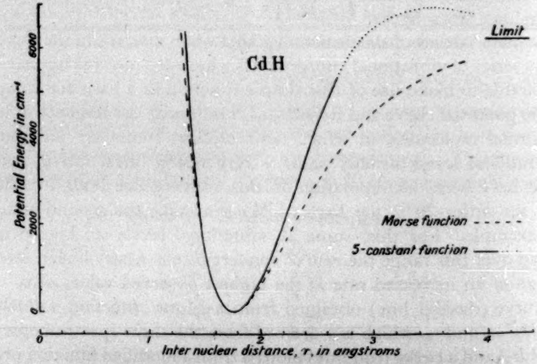

Figure 2. Potential curves for the ground state of CdH.

Owing to this big difference it is not easy to plot the potential curve, even when experimental data are adequate, as for many of the alkaline-earth hydrides. Figure 2 shows the potential curve for the ground state of CdH drawn to a Morse function (dashed line) and also a curve drawn to a five-constant Hulburt-

Hirschfelder function (full line, with upper part dotted). This latter curve probably approaches the true curve quite well around the minimum, but may be subject to appreciable error as r increases, and the potential maximum to which it leads should not be taken seriously. However, it serves to show that the strong departure from a linear rate of convergence of the vibrational levels is again associated with a much more rapid rise of the potential curve towards the dissociation limit than that given by the Morse function.

The differences between the actual potential curve and the Morse form so far considered have been in the region where r is greater than r_e but is still not very large ($\sim 2r_e$); this is probably the region of most importance for the extrapolation, and here the tendency is for the rate of convergence to be initially less than that given by the Morse function, but to increase and exceed it at high v, and for the true potential-energy curve to lie above that of the Morse function. At larger internuclear distances there may be a tendency for the reverse effect. The Morse function corresponds to an exponential falling off of the potential energy at very large r. The actual potential energy at very large distances is, however, likely, on account of interaction of two atoms, to fall off much less rapidly than that given by the exponential law. The weak van der Waals forces between atoms are known (see, for example, Margenau and Watson, 1936) to fall off as $1/r^7$, corresponding to a potential energy varying as $1/r^6$. There may be other forces, which vary as a still lower power of $(1/r)$: thus the resonance interaction between like atoms in different states gives a force proportional to $1/r^4$; polarization forces also are likely to be important in many cases, and these will again give a potential energy which, at large distances, falls off less rapidly than it would if it obeyed the exponential law. The force between two atoms in P states may vary as $1/r^6$. Thus the true potential curve should cross the Morse curve somewhere at large internuclear distances and then approach the dissociation limit less rapidly. It would not, therefore, be surprising if towards the limit the rate of convergence of the vibrational levels were to decrease slightly.

There are not many examples for which we have adequate data on the vibrational levels very near to the dissociation limit, but there is some evidence to support this conclusion. For the upper state of O_2 and for the ground state of H_2 Birge (1929) assumed an inflection in the curve of $\Delta G(v+\frac{1}{2})$ against v at high v, but later experimental work has not provided much support for any marked change, although a slight trend towards a slower rate of convergence may exist. For the upper states of the alkali metals (K_2, Li_2) there is no evidence for a decreased rate of convergence—indeed, the reverse is true. For the upper states of the halogens and mixed halogen molecules, however, there is definite evidence of a decrease in the rate of convergence of the vibrational levels as the limit is approached. This occurs for the upper states of the main systems of all the halogen molecules for which data exist.

The effect is well illustrated by ICl; the curve of $\Delta G(v+\frac{1}{2})$ against v for the upper state is shown in figure 3, in which data are from Darbyshire (1932). The graph at first shows negative curvature corresponding to a slow but steady increase in the rate of convergence of the levels; between about $v=20$ and $v=25$ the graph shows an inflection and the "toe" turns up so that the rate of convergence (i.e. the slope) decreases to a value below that at $v=0$. This tendency for a more positive curvature to the graph in the region of the "toe" would tend, if it occurred for other molecules, to bring the dissociation energy a little higher than that which would be obtained by a graphical Birge-Sponer extrapolation using only points before the "toe" was reached. The effect must, however, be very small. The laws of force which we have discussed will only apply at large values of r where the potential energy is already small, and the effect on the dissociation energy will be almost negligible. Even in the case of ICl, which is one of the most extreme examples, the "toe" represents only about 0·04 ev., and the difference in dissociation energy obtained by using the true curve and by using an extrapolation from before the inflection (i.e. from around $v=20$) would amount to only about 0·02 ev. There is little reason to think that this effect is important for any neutral molecule.

As we have already pointed out, ionized molecules dissociate to one charged atom and one neutral atom. The force between these atoms at large distances is likely to be that between a charge and an induced dipole, which is proportional to $1/r^4$. It is, therefore, especially likely that for ionized molecules the curve of $\Delta G(v+\frac{1}{2})$ against v will show an inflection towards a slightly higher limit. There are no available data to check this supposition, but the fact that for the lighter ionized molecules the linear extrapolation does not show any systematic tendency to be too high may be connected with the existence of "toes" to the curves. If this is so, the dissociation energy of O_2^+, which depends on a good graphical extrapolation for the excited state, may be a little higher than is generally assumed, although any considerable change would lead to a discrepancy between the spectroscopic and the electron-impact values for the ionization potential of O_2.

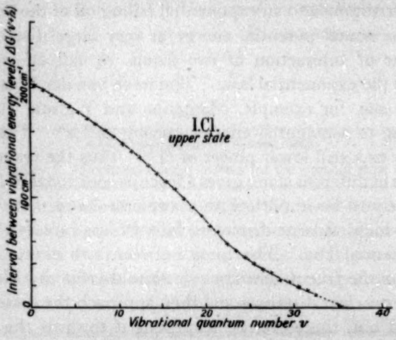

Figure 3. Graph of $\Delta G(v+\frac{1}{2})$ against v for the upper state of ICl.

For molecules in which ionic bonding is important there is no case in which the data are adequate for the drawing of an accurate potential curve. In many cases, however, the low value of the linear extrapolation seems likely to be associated with the fact that the true potential curve lies below the Morse function curve in the region where r is a little greater than r_e.

§ 8. SUMMARY

Although the remarks contained here may appear to be a severe criticism of the Birge-Sponer extrapolation, they should really lead to an increase in its usefulness by giving a fuller understanding of the limitations of the method and the likely deviations from the value given by linear extrapolation.

Where data are adequate for a good graphical extrapolation for a ground state, the result should be satisfactory. Where, for a non-ionic molecule, the lower levels appear to converge linearly, the true dissociation energy tends to be around 80 % of that given by linear extrapolation, being perhaps a little nearer this extrapolated value for light molecules and rather lower for heavy molecules. When dissociation leads to an atom in a $^1S_0$ state the levels do not usually converge linearly; the true dissociation energy is then often not much over half the linearly extrapolated value. Extrapolations for excited states should be treated with caution, especially when ionic forces are likely to be important; satisfactory values may be obtained for the lower excited states of molecules composed of non-metals, especially if a graphical method is used.

For molecules with largely ionic bonding the linear Birge-Sponer extrapolation does not appear satisfactory; in a number of examples it gives a value which is too low. For ionized molecules there appears little evidence to suggest any failure of the linear extrapolation.

For most types of molecule the above considerations should assist in the estimation of the dissociation energy, taking the linearly extrapolated value as a basis, and should also help in the assessment of the reliability of the value.

There are two groups of molecules for which data are still inadequate to give much guidance. For metallic oxides there will usually be some tendency towards ionic bonding. The electron affinity of atomic oxygen is not quite certain, but definitely exceeds 2 eV. and may be nearer 3; the ionic bonding forces are probably not very important, provided the metallic ionization potential exceeds about 7 eV., and the linear extrapolation can then be expected to be a little too high, as usual; for the oxides of the more electropositive metals any figure based on linear extrapolation should be taken as only provisional. The halides of the elements of Group II are another unsolved problem, as we have the complexities due both to ionic bonding and also to the presence of an atom with $^1S_0$ ground state; in many of them, too, the value of $x_e\omega_e$ derived from head measurements may be inaccurate owing to the systems being weakly degraded. The evidence for CaCl and CaF suggests that the linear extrapolation may be appreciably too high, as in the hydrides of Group II elements, but this may not always be so.

ACKNOWLEDGMENTS

In conclusion I wish to express my thanks to Dr. M. Blackman for helpful discussion on the interaction of atoms at large distances and to Sir Alfred Egerton for his interest in this work.

REFERENCES

Bengtsson, E. and Olsson, E., 1931. *Z. Phys.*, **72**, 163.
Beutler, H. and Levi, H., 1934. *Z. Phys. Chem.*, B, **24**, 263.
Birge, R. T., 1929. *Trans. Faraday Soc.*, **25**, 707.
Birge, R. T. and Sponer, H., 1926. *Phys. Rev.*, **28**, 259.
Darbyshire, O., 1932. *Phys. Rev.*, **40**, 366.
Gaydon, A. G., 1946. *Dissociation Energies* (London: Chapman and Hall) (in press).
Gaydon, A. G. and Penney, W. G., 1945. *Proc. Roy. Soc.*, A., **183**, 374.

Herzberg, G., 1939. *Molecular Spectra and Molecular Structure* (New York: Prentice-Hall).
Herzberg, G. and Mundie, L. G., 1940. *J. Chem. Phys.*, **8**, 263.
Howell, H. G. and Coulson, N., 1938. *Proc. Roy. Soc.*, A., **166**, 238.
Howell, H. G. and Coulson, N., 1941. *Proc. Phys. Soc.*, **53**, 706.
Hulburt, H. M. and Hirschfelder, J. O., 1941. *J. Chem. Phys.*, **9**, 61.
Kratzer, A., 1924. *Z. Phys.*, **26**, 40.
Margenau, H. and Watson, W. W., 1936. *Rev. Mod. Phys.*, **8**, 22.
Mulliken, R. S., 1936. *Phys. Rev.*, **50**, 1017 and 1028.
Mulliken, R. S., 1937. *Phys. Rev.*, **51**, 310.
Rydberg, R., 1931. *Z. Phys.*, **73**, 376.
Wahrhaftig, A. L., 1942. *J. Chem. Phys.*, **10**, 248.
Wieland, K., 1941. *Helv. Phys. Acta*, **14**, 420.

ULTRA-VIOLET ABSORPTION BAND-SYSTEMS OF SiS, SiSe AND SiTe

By E. E. VAGO and R. F. BARROW,
Physical Chemistry Laboratory, University of Oxford

MS. received 15 *April* 1946

ABSTRACT. A new ultra-violet band-system, E–X, of each of the molecules SiS, SiSe and SiTe has been observed in absorption at 800–1000° C., and vibrational analyses have been done. The D–X systems, already known in emission, have also been photographed in absorption. These observations have extended the D–X systems of SiSe and of SiTe and have led to somewhat improved values of the vibrational constants. The results are summarized in the following table :—

Molecule	State	ν_e	ω_e	$x_e\omega_e$	$y_e\omega_e$	D_e
SiS	E	42322·1	402·3	−1·74	−0·025	1·2 ev.
	D $^1\Pi$	35028·8	512·0	−2·38	−0·045	2·3
	X $^1\Sigma$	0	749·5	−2·56	—	6·6
SiSe	E	38505·9	308·8	−1·95	−0·032	1·3
	D	32450·3	399·8	−1·93	—	2·0
	X ($^1\Sigma$)	0	580·0	−1·78	—	6·0
SiTe	E	33991	242	(−3·63)	(+0·13)	(1·4)
	D	28661·8	338·6	−1·70	—	2·0
	X ($^1\Sigma$)	0	481·2	−1·30	—	5·6

§ 1. INTRODUCTION

SiS, SiSe and SiTe each give rise to one band-system (D–X) in the near ultra-violet region, which appears readily in emission in positive-column discharges. For several reasons, including the fact that two near ultra-violet absorption systems of GeS (which is isosteric with SiSe) were known, we thought it likely that the absorption spectra of the silicon compounds would contain systems lying at shorter wave-lengths than the D–X systems already known. This has proved so : SiS, SiSe and SiTe each show banded absorption in the ultra-violet region, and the bands of each molecule may be assigned to two systems D–X and E–X.

The D–X system of SiS was originally developed rather well in emission, and the absorption measurements have added nothing to the vibrational analysis of Barrow and Jevons (1938). Development of the D–X systems of SiSe and of SiTe in emission was, however, somewhat incomplete (Barrow, 1939), and the absorption work has supplemented the original vibrational analyses and has led to improved values of the constants.

Vibrational analyses of the three new E–X systems have been carried out, and a preliminary account of the work has been published (Vago and Barrow, 1946). The detailed results are given and discussed in the present paper.

§ 2. EXPERIMENTAL METHODS AND RESULTS

The absorption spectra were studied at temperatures in the range 800–1000° C. by methods already described (Barrow and Vago, 1944). An account of the preparation of SiS has been given elsewhere (Barrow and Jevons, 1938). SiSe and SiTe were made via the magnesium compounds. A mixture of finely-divided Mg and Se or Te was heated gently, using silica as a diluent to moderate the violence of the reaction. The products were mainly MgSe or MgTe mixed with silica: they were heated *in vacuo* at 1100° C. for about three hours to form the silicon compounds. These were found to sublime only very slowly, and since the other components of the reaction mixture were not volatile, the crude products were used without purification. SiSe and SiTe proved objectionable substances, as, like SiS, they hydrolyze rapidly in moist air.

A hydrogen tube was used as source of continuous radiation. The spectra were photographed in (i) a Hilger medium quartz prism instrument (E. 498), (ii) a first order of a concave grating spectrograph with a linear dispersion of about 7·4 A./mm., and (iii) in a large quartz Littrow spectrograph with a dispersion of about 2·4 A./mm. at 2500 A. Ilford Ordinary, Process and Q. 1 plates were used: they were developed in Process developer to secure maximum contrast.

The absorption spectra of all three molecules showed two distinct band-systems, but, whereas not much difficulty was experienced in getting good spectrograms of the three D–X systems and of the E–X system of SiS, strong contrast was never obtained on plates of the E–X system of SiSe; and the E–X system of SiTe was even harder to photograph. These difficulties seemed to be due to the intrinsic weakness of the systems: they could probably have been overcome by the use of longer columns of vapour, but in fact the spectrograms of the new systems of SiSe and SiTe proved adequate for their vibrational analyses. A reproduction of the E–X system of SiS is given in plate 1: the other E–X systems are generally similar in appearance.

The measurements of the E–X systems are set out in the Delandres schemes in tables 1–3. Additional or amended measurements of band-heads of the D–X systems of SiSe and SiTe are given in table 4: these confirm the original v', v'' assignments. There can be few doubts about the correctness of the analyses given for the E–X systems, since the ground-state differences are also known from the D–X systems. Unfortunately, however, the distribution of intensities in the E–X systems and the populations in the initial levels (determined by the Boltzmann law) combine to make the $v'=0$ progressions very difficult to observe. Indeed, we failed to measure any band-heads of this progression on the first plates of the SiS system, and they were only found on later plates of more contrast of the absorption at somewhat higher temperatures. It is therefore possible, but, we think, unlikely, that we have failed to observe $v'=0$ progressions in the E–X systems of SiSe and SiTe.

Table 1. Measurements of band-heads of the E←X system of SiS

Italic numerals denote wave-lengths in air (I.A.);
Large Roman, wave-numbers *in vacuo* (cm.^{-1});
Small Roman, wave-number differences.

v′	v″→0		1		2		3
15	47664 *2097·35*						
	326						
14	47337·9 *2111·80*						
	336·9						
13	47001·0 *2126·94*						
	343·3						
12	46657·7 *2142·59*						
	349·4						
11	46308·3 *2158·76*						
	355·5						
10	45952·8 *2175·46*						
	360·6						
9	45592·2 *2192·67*						
	365·2						
8	45227·0 *2210·38*						
	369·4						
7	44857·6 *2228·58*	744·5	44113·1 *2266·20*				
	374·8		375·6				
6	44482·8 *2247·36*	745·3	43737·5 *2285·66*	740·2	42997·3 *2325·01*		
	378·7		376·3		375·5		
5	44104·1 *2266·66*	742·9	43361·2 *2305·50*	739·4	42621·8 *2345·50*		
	384·6		384·2		385·0		
4	43719·5 *2286·60*	742·5	42977·0 *2326·11*	740·2	42236·8 *2366·88*	735·9	41500·9 *2408·85*
	384·8		386·8		387·2		385·8
3	43334·7 *2306·91*	744·5	42590·2 *2347·24*	740·6	41849·6 *2388·78*	734·5	41115·1 *2431·46*
			391·4		390·8		391·6
2			42198·8 *2369·01*	740·0	41458·8 *2411·30*	735·3	40723·5 *2454·84*
			394·4		394·7		393
1			41804·4 *2391·36*	740·3	41064·1 *2434·48*	733	40331 *2478·7*
					395		399
0					40669 *2458·1*	737	39932 *2503·5*

Table 2. Measurements of band-heads of the E←X system of SiSe

* The 3,0 and 5,1 bands are coincident.

$v' \downarrow$ $v'' \rightarrow$	0		1		2		3		4
8	40698·0 *2456·38*								
	276·8								
7	40421·2 *2473·20*								
	284·8								
6	40136·4 *2490·75*								
	287·7								
5	39848·7 *2508·74*	575·2	39273·5* *2545·48*	570·7	38702·8 *2583·02*				
	286·1		285·6		287·5				
4	39562·6 *2526·88*	574·7	38987·9 *2564·13*	572·6	38415·3 *2602·35*	568·2	37847·1 *2641·42*	568·1	37279·0 *2681·68*
	289·1		290·8		290·9		290·8		
3	39273·5* *2545·48*	576·4	38697·1 *2583·40*	572·7	38124·4 *2622·21*	568·1	37556·3 *2661·88*		
	295·5		297·7		298·7		295·6		
2	38978·0 *2564·78*	578·6	38399·4 *2603·43*	573·7	37825·7 *2642·92*	565·0	37260·7 *2683·00*		
			301·4		299·0		302·0		
1	—		38098·0 *2624·03*	571·3	37526·7 *2663·98*	568·0	36958·7 *2704·92*		
			305·3		305·3		305·9		
0	—		37792·7 *2645·23*	571·3	37221·4 *2685·83*	568·6	36652·8 *2727·50*	556·5	36096·3 *2769·55*

Table 3. Measurements of band-heads of the E←X system of SiTe

$v' \downarrow$ $v'' \rightarrow$	0		1		2		3		4
6	35210·1 *2839·26*	478·0	34732·1 *2878·34*						
	218·2		218·2						
5	34991·9 *2856·97*	478·0	34513·9 *2896·54*						
	219·5		218·2						
4	34772·4 *2875·00*	476·7	34295·7 *2914·97*						
	219·7		221·0						
3	34552·7 *2893·28*	478·0	34074·7 *2933·87*						
	222·5		220·2						
2	34330·2 *2912·04*	475·7	33854·5 *2952·96*	475·1	33379·4 *2994·99*				
			225·5		226·8				
1	—		33629·0 *2972·76*	476·4	33152·6 *3015·48*	472·5	32680·1 *3059·08*	470·0	32210·0 *3103·73*
			233·2		234·1		236·9		
0	—		33395·8 *2993·52*	477·3	32918·5 *3036·92*	475·3	32443·2 *3081·42*		

The electronic and vibrational constants for the three known states of these molecules are collected together in table 5. The new data on the D–X and E–X systems of SiSe and of SiTe have led to slight changes in the values of the constants for the D and X states of these molecules. The ground-state constants for SiS determined from the extensive D–X systems were found to be in good agreement with the figures found from the analysis of the E–X system. The E-state data for SiS and SiSe call for no particular remark. The expression given for the vibrational energy in the E state of SiTe is, however, inherently rather unlikely, as it includes unexpectedly large anharmonic and cubic terms. Errors in these terms might be attributed to unsuspected perturbations, or to the incorrect location of some of the band-heads (the Te isotope effect might be partly responsible). However, the expression given represents satisfactorily the experimental measurements, and at the worst the value of ω_e is not likely to be much in error.

Table 4. Additional or amended measurements of band-heads of the D–X systems of SiSe and SiTe

SiSe v', v''	SiSe ν	SiTe v', v''	SiTe ν
8,0	35431·6 cm.$^{-1}$	7,0	30867·8 cm.$^{-1}$
7,0	055·1	8,1	700·1
8,1	34854·0	6,0	549·3
6,0	679·1	7,1	385·0*
7,1	476·0	5,0	232·3*
5,0	302·2*	6,1	070·8*
6,1	101·1*	4,0	29910·4*
5,1	33727·1	5,1	752·4
4,1	346·1	3,0	586·3*
		4,1	431·6
		2,0	257·4*
		3,1	106·9

* Band-head also measured in emission.

Table 5. Summary of electronic and vibrational constants

Molecule	State	ν_e	ω_e	$x_e\omega_e$	$y_e\omega_e$	κ_e
SiS	E	42322·1	402·3	−1·74	−0·025	1·42 × 10^5
	D	35028·8	512·0	−2·38	−0·045	2·31
	X	0	749·5	−2·56	—	4·94
SiSe	E	38505·9	308·8	−1·95	−0·032	1·16
	D	32450·3	399·8	−1·93	—	1·96
	X	0	580·0	−1·78	—	4·11
SiTe	E	33991	242	(−3·63)	(+0·13)	0·79
	D	28661·8	338·6	−1·70	—	1·55
	X	0	481·2	−1·30	—	3·13

Note.—The units are cm.$^{-1}$ (*in vacuo*), except for κ_e, the force constant, which is given in dynes/cm. The signs of the vibrational constants are those applicable when the vibrational energy levels are represented by

$$[\omega_e(v+\tfrac{1}{2})+x_e\omega_e(v+\tfrac{1}{2})^2+y_e\omega_e(v+\tfrac{1}{2})^3+\ldots].$$

§ 3. DISCUSSION

It was largely the existence of two absorption systems of GeS which led us to look for second absorption systems of the present molecules: in particular, the expectation was that SiSe, being isosteric with GeS (48 electrons), would be spectroscopically rather similar. How close the constants are for these compounds may be judged from the following figures:—

	GeS		SiSe	
State	ν_e	κ_e	ν_e	κ_e
E	4·82 ev.	$1{\cdot}27\times10^5$	4·77	$1{\cdot}16\times10^5$ dyne/cm.
D	4·08	1·85	4·02	1·96
X	0	4·36	0	4·11

The isosteric group SiTe, GeSe and SnS show analogous behaviour in regard to their electronic and vibrational constants. The rotational constants of such groups of molecules may also be expected to lie rather close together.

Lacking rotational analyses, we can only speculate about the molecular types of the E states of these molecules. One possibility—and it is no more than that—may, however, be suggested. The lowest known excited states of SiO and of SiS are $^1\Pi$, and the presumption is therefore strong that these states (and probably the similar states of SiSe and SiTe) correspond to the lowest excited singlet state of CO, A $^1\Pi$. Now, although the bond in unexcited CO is much stronger than, for example, that in unexcited SiS, it might perhaps be expected that the *relative* change in bond strength in going from the unexcited $^1\Sigma$ level to the $^1\Pi$ level should be similar for the two molecules. To test this possibility we set the force constants for the ground states at 100, and calculate those for the excited states as percentages of the ground-state force constants. The figures are given in table 6.

Table 6. Force constants, relative to those for the ground states

CO		SiO		SiS		SiSe		SiTe	
A $^1\Pi$	48·8	$^1\Pi$	47·0	D $^1\Pi$	46·8	D	47·7	D	49·5
$a'\,^3\Sigma$	29·7		—	E	28·8	E	28·2	E	25
$a\,^3\Pi$	64·3		—		—		—		—
X $^1\Sigma^+$	100	$^1\Sigma$	100	X $^1\Sigma$	100	X	100	X	100

It appears that for the three molecules CO, SiO and SiS the force constant for the $^1\Pi$ level is about 48% of that in the ground state: the values for the D levels of SiSe and SiTe suspected to be $^1\Pi$ are also close to 48%. The figures for the E levels are much lower and agree fairly well with that for the $a'\,^3\Sigma$ state of CO. This measure of agreement may be quite fortuitous—it is noteworthy that the $a'\,^3\Sigma$ level lies somewhat *below* the A $^1\Pi$ level in CO, whereas the E states for the silicon compounds lie a little *above* the corresponding D states; but for what it is worth it suggests that the E states of SiS, SiSe and SiTe are of the type $^3\Sigma$, analogous to the $a'\,^3\Sigma$ state of CO.

The energies of dissociation of the silicon compounds are of interest. We have, it is true, no very precise information, but only figures derived from long extrapolations of the vibrational levels: nevertheless some tentative conclusions can be reached. Let us consider SiS (see also Barrow and Jevons, 1938). The energy of dissociation for the ground state, D_X, calculated by the Birge-Sponer extrapolation, is 6·72 ev. The values for the D and E states, calculated in the same way, but including the cubic terms, are 1·75 and 1·36, giving $(\nu_e+D)_D=6{\cdot}09$ and $(\nu_e+D)_E=6{\cdot}61$. Now it may be presumed that the ground state of SiS is formed from Si and S atoms in their ground states, ^3P. It is also most probable that the D $^1\Pi$ state dissociates into two ^3P atoms, since the next combination of atomic states that could give a singlet molecular state is, by the Wigner-Witmer rules, $^1D+{}^1D$, which lies at about 2 ev. above $^3P+{}^3P$. If the combination $^1D+{}^1D$ were involved, we should have, using $D_X=6{\cdot}7$, $(\nu_e+D)_D=8{\cdot}7$ or $D_D=4{\cdot}4$, which seems hopelessly out of agreement with the extrapolated value of 1·75. Thus it is most likely that the D $^1\Pi$ state of SiS also dissociates into Si(^3P) + S(^3P).

The evidence about the E state is much less conclusive. It may be a triplet state, in which case it could arise either from $^3P+{}^3P$ or from $^3P+{}^1D$ atomic states. However, the figure for $(\nu_e+D)_{\mathrm{E}}$, 6·6 ev. is close to the mean of $(\nu_e+D)_{\mathrm{D}}$ and D_{X}, 6·4, so that the dissociation SiS(E)→Si(^3P) + S(^3P) is feasible, and the data for SiSe (which molecule may be presumed to behave similarly to SiS) suggest that this is the most reasonable hypothesis.

The extrapolated values of D for SiO, SiS, SiSe and SiTe are given in table 7.

Table 7. Energies of dissociation (ev.)

Molecule: SiO SiS

State	$D_{\text{extrapolated}}$	ν_e+D	D_{mean}	$D_{\text{extrapolated}}$	ν_e+D	D_{mean}
E	—	—	(1·7)	1·36	6·61	1·22
D	—	—	2·95	1·75	6·09	2·13
X	8·26	8·26	8·26	6·72	6·72	6·47
					6·47	

Molecule: SiSe SiTe

State	$D_{\text{extrapolated}}$	ν_e+D	D_{mean}	$D_{\text{extrapolated}}$	ν_e+D	D_{mean}
E	0·89	5·67	1·27	—	—	1·37
D	2·57	6·59	2·02	2·09	5·64	2·03
X	5·86	5·86	6·04	5·52	5·52	5·58
		6·04			5·58	

On the basis of the arguments outlined above, we have assumed that each of the X, D and E states of all these molecules gives a pair of unexcited atoms on dissociation, and have then determined mean values of D_{X}. These mean values have been used to calculate the improved values of D_{D} and D_{E} given in the columns "D_{mean}". For the SiO(D) and SiTe(E) states, large cubic terms make extrapolation impossible: the figure given for SiO(E) comes from a rough prediction of that level (see below). There may be considerable errors in these figures, but they probably indicate correctly the general trends. Comparison with the force constants given in table 5 tends to show—reasonably enough—that in a given state the most tightly-bound molecule in the equilibrium position often requires also the greatest amount of energy to dissociate it into isolated atoms. Similarly, for any single molecule, the X state is more stable in both senses than the D state, which is in turn more stable than the E state.

Finally, it would seem to be fairly safe to predict the existence of an E–X system of SiO at shorter wave-lengths than the $^1\Pi-{}^1\Sigma$ system. Crude extrapolation puts the E level at about 6·6 ev. above the ground state, so that the 0,0 band of this system should lie at about 1850 A. The vibration frequency in the E state should be about 670 cm.$^{-1}$ and the energy of dissociation *ca.* 1–2 ev.

REFERENCES

Barrow, R. F. and Jevons, W., 1938. *Proc. Roy. Soc.*, A, **169**, 60.
Barrow, R. F., 1939. *Proc. Phys. Soc.*, **51**, 267.
Barrow, R. F., and Vago, E. E., 1944. *Proc. Phys. Soc.*, **56**, 79.
Vago, E. E. and Barrow, R. F., 1946. *Nature, Lond.*, **157**, 77.

PHYSICAL SOC. VOL. 58, PT. 5 (E. E. VAGO AND R. F. BARROW)

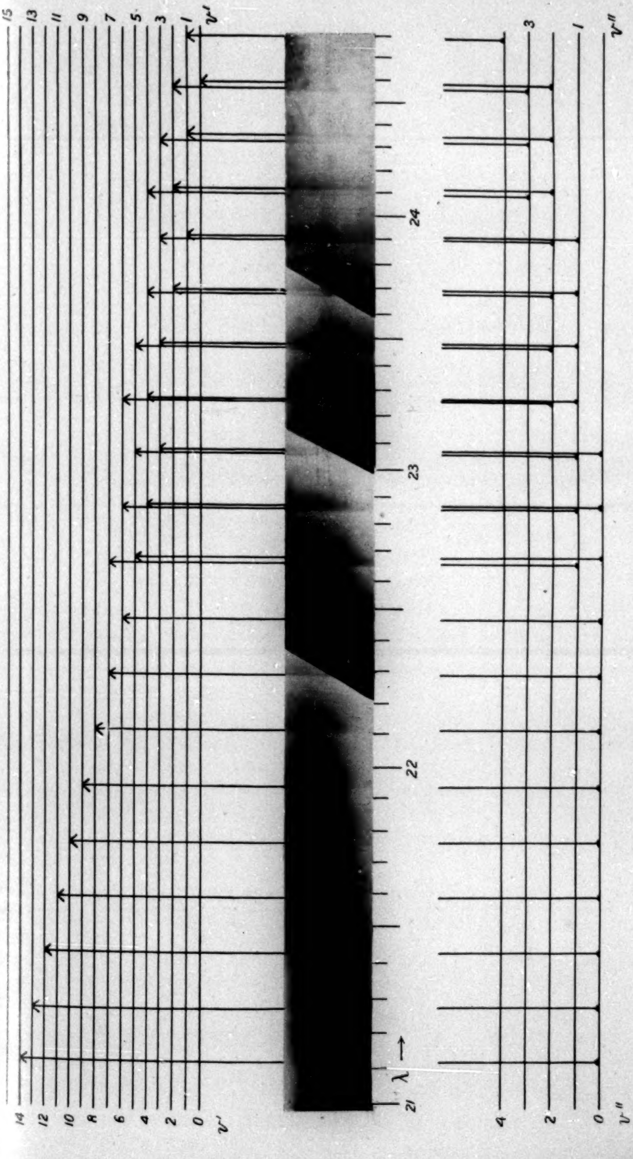

Bands of the E ← X system of SiS in absorption (medium quartz prism spectrograph).

THE ALGEBRAIC ANALYSIS OF THE HIGHER-ORDER ABERRATIONS OF OPTICAL SYSTEMS

TANGENTIAL ABERRATIONS OF A SYSTEM OF COAXIAL SPHERICAL REFRACTING SURFACES

By H. A. BUCHDAHL,
Ministry of Munitions Annexe 9/101;
Physics Department, University of Tasmania

MS. received 16 *November* 1945

ABSTRACT. The behaviour of an optical system is known if the position of the point of intersection of an arbitrary ray passing through the system with any chosen plane of reference can be determined. In the present paper tangential aberrations of any order are defined in terms of the distance of this point from an ideal image point, using elementary methods only. It is shown how these aberrations may be computed in practice without the use of any trigonometrical traces.

As a practical example, the computations necessary for the determination of the complete primary and secondary aberrations and of the tertiary spherical aberration are given in detail for the case of a Cooke Triplet. The information so obtained is compared with that yielded by strict trigonometrical tracing, illustrating the good agreement between them and the simplicity of the computations involved.

---

§1. INDEX OF SYMBOLS

The following list gives most of the symbols employed in the text. Each number in brackets refers to the paragraph in which the symbol first occurs.

Symbol	*Meaning of symbol*
a_ν	coefficient of $y^{3-\nu}u^{\nu}$ in the expansion of v'. (11)
a (suffix)	extreme ray of pencil. (3)
α	a quantity linearly related to y and u. (4)
A	$\sum_{\nu=1}^{3} a_\nu p_1^{3-\nu}$. (12)
A_n	$\frac{1}{n!}\cdot\frac{d^nA}{dp_1^n}$. (13)
b_ν	coefficient of $y^{5-\nu}u^{\nu}$ in the expansion of v'. (11)
b (suffix)	extreme ray of pencil. (3)
B	$\sum_{\nu=1}^{5} b_\nu p_1^{5-\nu}$. (12)
B_n	$\frac{1}{n!}\cdot\frac{d^nB}{dp_1^n}$. (13)
c	Nir. (4)
c^*	Nur. (14)
C'	coma. (13)
γ_ν	terms of Γ_1 and Γ_2. (8)
Γ_ν	terms of the expansion of $\Delta\Lambda^*$. (5)
d	distance of diaphragm from preceding surface. (10)
d'	distance between successive surfaces. (15)

D	$\sum_{\nu=1}^{f} \Delta\Lambda_\nu$. (4)
D^*	$\sum_{\nu=1}^{f} \Delta\Lambda^*_\nu$. (5)
δ_0	$x-y+1$. (7)
δ_ν	coefficient of $z^{2\nu+1}$ in the expansion of Δ. (7)
$\delta y_j, \delta u_j$	increments in y, u in the equations giving $\sin U_j$, etc. (5)
$\delta y'_j, \delta u'_j$	increments in y, u in the equation giving $\sin U'_j$, etc. (5)
$\delta y^*_j, \ldots$	increments in $y, \ldots$ in the equations giving $\tan U_j, \ldots$ etc. (14)
Δ	$\Delta(\sin U + \sin I)$. (4)
ΔX_j	$X'_j - X_j$. (1)
$\Delta^* X_j$	$X_{j+1} - X'_j$. (1)
e	radius of aperture of diaphragm. (10)
f (suffix)	final surface. (5)
f'	posterior focal length. (10)
F′	paraxial focus (point conjugate to axial point of object). (3)
$g_n(x)$	coefficient of t^n in the expansion of $\sqrt{(1-t)(1-xt)}$. (6)
G_ν	terms of the expansion of Δ. (5)
h	height of object. (11)
h'	paraxial image height. (3)
H'	$(l'_{0f} - L'_f) \tan U'_f$. (3)
i	paraxial angle of incidence. (1)
I	angle of incidence. (1)
θ	c_q/c_p. (9)
k	N/N'. (7)
l	paraxial axial intersection length. (1)
L	axial intersection length. (1)
λ	invariant of Lagrange type. (4)
Λ	$N(l-L)u \sin U$. (4)
Λ^*	$N(l-L)u \tan U$. (5)
N	refractive index. (1)
p (suffix)	quantities refering to the ray (1,0). (4)
p_ν	coefficients in the expansion of y of principal rays. (10)
q (suffix)	quantities referring to the ray (0,1). (4)
r	radius of surface. (1)
R, R′	arbitrary conjugate rays. (3)
R_0	associated ray of R. (4)
t_ν	coefficient of $u'_{pf} y^{3-\nu} u^\nu$ in the expansion of $\tan U'_f$. (13)
t_n	current symbol in computing scheme. (15)
u	paraxial inclination of ray to axis. (1)
u	$\equiv u_1$. (5)
U	inclination of ray to axis. (1)
v'	$H' - h'$. (3)
w	semi-aperture of incident pencil of parallel rays. (13)
x	$(L-r)/r$. (7)
y	kx. (7)
y	lu. (1)

y	$\equiv y_1$. (5)
z	$\sin U$. (7)
0 (suffix)	quantities referring to focal paraxial ray. (5)
$'$	denotes any quantity behind surface corresponding to the "undashed" quantity before it. (1)
(α, β)	a paraxial ray determined by $y_1=\alpha$, $u_1=\beta$. (4)
$[\alpha, \beta]$	a ray determined by $L_1 \sin U_1=\alpha$, $\sin U_1=\beta$. (4)

The quantities L, U, I, N, r, d' are the same as those used by Conrady (1929), so that the equations determining the passage of a ray through a surface are:

$$r \sin I=(L-r)\sin U, \qquad \ldots\ldots(1.1)$$

$$\Delta(N \sin I)=0, \qquad \ldots\ldots(1.2)$$

$$\Delta(U+I)=0, \qquad \ldots\ldots(1.3)$$

$$r \sin I'=(L'-r)\sin U', \qquad \ldots\ldots(1.4)$$

$$\Delta^* L=-d', \qquad \ldots\ldots(1.5)$$

and similar paraxial equations, i.e.

$$ri=(l-r)u, \qquad \ldots\ldots(1.6)$$

$$\Delta(Ni)=0, \qquad \ldots\ldots(1.7)$$

$$\Delta(u+i)=0, \qquad \ldots\ldots(1.8)$$

$$ri'=(l'-r)u', \qquad \ldots\ldots(1.9)$$

$$\Delta^* l=-d'. \qquad \ldots\ldots(1.10)$$

It should be noted that H' is positive if the point of intersection of R′ with the plane of reference lies *below* the axis of the system. The phrase "correct to the nth order", as applied to any expression, is understood to mean that any errors involved in it are of at least the $(n+1)$th order.

§ 2. INTRODUCTION

It has been stated occasionally (Conrady, 1929, chap. 6; Hardy and Perrin, 1932, chap. 6) that the algebraic determination of the aberrations of lens systems other than the primary involves computations of such magnitude as to make such analysis useless from a practical point of view. Thus Conrady (p. 255) states: "... due consideration of the disturbing effects ... leads to the vast complication of the problem of determining the true secondary aberrations which up to the present has rendered the complete evaluation of the latter a task of almost hopeless complexity". Confining ourselves to the monochromatic tangential aberrations of a system of coaxial spherical refracting surfaces we shall show in the present paper (after suitably defining the "aberration of order n" of an arbitrary ray passing through the system) that the computation of the secondary aberrations represents relatively little labour in this case (see § 15, table 1); and that even the computation of the tertiary aberrations would not in practice be a task of insuperable magnitude. The methods used are essentially elementary in character; being entirely algebraic, the computations require no trigonometrical tracing, and are peculiarly adapted to the use of calculating machines. The simplicity of the method rests partly upon the choice of suitable variables, and partly upon a procedure which avoids the necessity for the explicit derivation of any summation theorems.

§3. DEFINITION OF THE ABERRATIONS

(*a*) Let an arbitrary ray R passing through the system from a given object point be defined by the values of $L \sin U$ and $\sin U$ at the first surface (see §4 (*b*)). A paraxial ray from the axial point of the object (the latter being perpendicular to the axis) intersects the axis in the conjugate point F′ in the image space. The plane through F′ perpendicular to the axis (i.e. the paraxial focal plane) is intersected by the emerging ray R′, conjugate to R, at a perpendicular distance H' below the axis. If the system were perfect, all possible rays R′ from the given object point would have to pass through the ideal image point lying in the paraxial focal plane and a certain distance h' below F′, where h' is proportional to the height of the object. Let

$$v' = H' - h'. \qquad \ldots\ldots(3.1)$$

v' may simply be called the *aberration of the ray R*, v' being regarded as a function of the pair of variables $L_1 \sin U_1$ and $\sin U_1$. (Regarding the height of the object as variable, these two variables are independent.) Now clearly, if the sign of U_1 be reversed, the signs of $\sin U_1$, $L_1 \sin U_1$, and of v' are all reversed. Accordingly v' may be expanded in a series of homogeneous polynomials of the third, fifth,...., $(2n+1)$th degree $(n=1, 2, 3, \ldots)$ in the independent variables $L_1 \sin U_1$, $\sin U_1$. We define the *aberration of order n* to be the polynomial of *degree* $(2n+1)$ in this expansion. Accordingly the primary aberrations involve four independent coefficients, the secondary six, and so on. Hence the determination of the aberrations up to and including the nth order requires the evaluation of $\sum_{\nu=1}^{n} (2\nu+2) = n(n+3)$ independent coefficients.

It may be useful slightly to extend the definition of v'. Instead of considering the intersection of R′ with the paraxial focal plane we may consider the intersection, H', with some arbitrary plane of reference (which is, of course, perpendicular to the axis). Then H' may also be expressed as a series of homogeneous polynomials of degree $(2n+1)$, $(n=0, 1, 2, \ldots)$. We define v' in this case as H' minus the polynomial of the first degree. Our previous definition is contained in this as a special case.

(*b*) The four primary coefficients are, of course, intimately related to the primary aberrations of von Seidel. The actual relationships between them may be established by defining the spherical aberration, distortion, tangential coma and curvature of field purely geometrically and then expressing these in terms of v'. At the same time these definitions may, if desired, be retained for practical purposes on proceeding to higher orders. Accordingly we take as a measure of the

(i) *spherical aberration* the distance below the axis at which a ray from the axial point of the object strikes the paraxial focal plane;

(ii) *distortion* the value of v' corresponding to principal rays, i.e. rays passing through the centre of the diaphragm.

If the extreme rays of a pencil of rays be distinguished by the letters a and b respectively (the extreme rays being determined by the rim of the diaphragm), then

(iii) *coma* is measured by the length of the line drawn from the intersection of the a and b rays to the principal ray, parallel to the focal plane; whilst the

(iv) ***curvature of field*** is the perpendicular distance from the intersection of the a and b rays to the focal plane.

In the course of the evaluation of v' to the nth order, the direction of the ray in the image space is in any case determined to the $(n-1)$th order, so that all the data necessary for the calculations (i) to (iv) are available. By far the most important of these in practice is the coma, partly because of its connection with the question of unevenness of illumination in the image, and partly because it is not so easily found by inspection of the values of v' corresponding to different rays of a pencil (see § 5).

It should be observed that in the definition of v', as well as its computation, the position of the diaphragm is not involved. The variation of the aberrations with shift of diaphragm may therefore be investigated *after* the main computations have been carried out.

§ 4. ASSOCIATED RAYS

(*a*) With any given ray $\mathrm{R}\equiv[L_1 \sin U_1, \sin U_1]$ we may associate a paraxial ray $\mathrm{R}_0\equiv(L_1 \sin U_1, \sin U_1)$, i.e. a paraxial ray the nominal initial data of which are the same as the actual data of R. We shall say that R and R_0 are *associated rays*. (The particular choice of the data determining R_0 is dictated by the equations of § 4 (*b*)).

Let α be any quantity connected with the paraxial ray R_0 which is linearly related to y_1 and u_1. Let A be a quantity connected with the associated ray R which reduces to α in the (paraxial) limit. Then clearly the difference $A-\alpha$ will be small, and it is easily seen that it must be of at least the third degree in y_1, u_1. (A is not thus uniquely determined; for instance, taking $\alpha\equiv u$, A might represent U, or $\sin U$, etc.)

Now one of the main difficulties of higher-order theory is the fact that we cannot simply replace any particular A by the corresponding α of the associated ray, as is done in primary theory, since such a procedure would make all but the primary terms meaningless. Accordingly it is desirable to find, if possible, expressions for the differences of the type $A-\alpha$, as explained above, for subsequent use, at the same time choosing the most convenient explicit form of A corresponding to the particular α.

In the following we define a ***surface invariant*** to be any quantity X_j obeying the equation

$$X_j'-X_j=\Delta X_j\equiv 0. \qquad (j=1,2\ldots,f) \qquad \ldots\ldots(4.1)$$

X_j shall be called a ***transfer invariant*** if

$$X_{j+1}-X_j'=\Delta^* X_j\equiv 0; \qquad (j=1,2\ldots,f-1) \qquad \ldots\ldots(4.2)$$

whilst if X_j satisfies both (4.1) and (4.2) simultaneously it shall be called a (true) ***optical invariant***, for which evidently

$$X_i=X_j=X_k', \text{ for all } i, j, k. \qquad \ldots\ldots(4.3)$$

Moreover, it will be convenient to use the term ***quasi-invariant*** for any quantity which reduces to an optical invariant in the (paraxial) limit.

Now if we consider two ***arbitrary*** paraxial rays, say $(\bar{y}_1, \bar{u}_1)$ and (y_1, u_1), then the expression

$$\lambda=N(l-\bar{l})u\bar{u} \qquad \ldots\ldots(4.4)$$

is an optical invariant. For $\Delta^*\lambda_j=0$, obviously; and, at any surface,

$$\Delta\lambda=\Delta N\{(l-r)-(\bar{l}-r)\}u\bar{u}=\Delta Nr(i\bar{u}-\bar{i}u), \text{ by (1.6).} \qquad \text{......(4.5)}$$

$\therefore$ since $\Delta Nri=\Delta c=0$,

$$\Delta\lambda=c\Delta\left(\bar{u}-\bar{i}\frac{u}{i}\right)=c\Delta\left(\bar{u}+\bar{i}-\frac{i+u}{i}\bar{i}\right)=0, \qquad \text{......(4.6)}$$

since $\Delta(u+i)=\Delta(\bar{i}/i)=0$, by (1.7), (1.8).

Now let Λ be a quasi-invariant which reduces to λ in the limit. Then the fact that the expression

$$D=\sum_{\nu=1}^{f}\Delta\Lambda_\nu \qquad \text{......(4.7)}$$

does not vanish identically is implicitly connected with what may be called the imperfection of the optical system. A heuristic examination of such quasi-invariants may therefore be expected to yield a method whereby the desired differences, $A-\alpha$ (of which the difference $\Lambda-\lambda$ is itself merely a characteristic example), and thus the aberrations of the system, can be determined with reasonable ease.

(*b*) The equation (1.1) suggests the following explicit form of Λ:

$$\Lambda=N(l-L)u\sin U, \qquad \text{......(4.8)}$$

where (y_1, u_1) and $[L_1\sin U_1, \sin U_1]$ are *arbitrary* rays. Then at any surface

$$\Delta\Lambda=c\Delta(\sin U+\sin I)=Ni\Delta(L\sin U), \qquad \text{......(4.9)}$$

since

$$\begin{aligned}\Delta\Lambda&=\Delta N\{(l-r)-(L-r)\}u\sin U\\&=\Delta Nr(i\sin U-u\sin I), \text{ by (1.1), (1.6)}\\&=c\Delta\left(\sin U-\frac{u}{i}\sin I\right), \text{ by (1.7)}\\&=c\Delta\left(\sin U+\sin I-\frac{u+i}{i}\sin I\right),\end{aligned}$$

which is (4.9), since $\Delta(u+i)=\Delta(\sin I/i)=0$.

The great importance of equation (4.9) lies in its simplicity, in the sense that $\Delta\Lambda$ is split up into two factors, one of which depends upon y_1 and u_1 only, whilst the other factor is independent of these. Since the expression $\Delta(\sin I+\sin U)$ recurs frequently below, we shall simply write Δ for it, whenever confusion is not likely thereby to arise. Thus

$$\Delta\Lambda=c\Delta. \qquad \text{......(4.10)}$$

Equation (4.10) suggests that the adopted expression for Λ, (4.8), is the most convenient for our purpose.

Since, by definition, α depends linearly upon y_1 and u_1, we may write

$$\alpha_j=\alpha_{pj}y_1+\alpha_{qj}u_1, \qquad \text{......(4.11)}$$

where the α_{pj}, α_{qj} are constants of the system. These constants are easily obtained in any given case. It is only necessary to trace the two (*paraxial*) rays (1,0) and (0,1) through the system. Then the actual value of α_j in the former is α_{pj}, whilst the value of α_j in the latter is α_{qj}.

We have, by (4.10), since $\Delta^*\Lambda_\nu = 0$,

$$N_j(l_j - L_j)u_j \sin U_j = N_1(l_1 - L_1)u_1 \sin U_1 + \sum_{\nu=1}^{j-1} c_\nu \Delta_\nu,$$

or

$$N_j y_j \sin U_j - N_j u_j L_j \sin U_j = N_1 y_1 \sin U_1 - N_1 u_1 L_1 \sin U_1 + \sum_{\nu=1}^{j-1} c_\nu \Delta_\nu. \qquad \ldots\ldots(4.12)$$

Hence, since y_1 and u_1 are independent variables, (4.12) splits up, by virtue of (4.11), into the two equations

$$\left.\begin{aligned} N_j y_{pj} \sin U_j - N_j u_{pj} L_j \sin U_j &= N_1 \sin U_1 + \sum_{\nu=1}^{j-1} c_{p\nu} \Delta_\nu, \\ N_j y_{qj} \sin U_j - N_j u_{qj} L_j \sin U_j &= -N_1 L_1 \sin U_1 + \sum_{\nu=1}^{j-1} c_{q\nu} \Delta_\nu. \end{aligned}\right\} \qquad \ldots\ldots(4.13)$$

These equations may be solved for $L_j \sin U_j$ and $\sin U_j$. Remembering that

$$\begin{vmatrix} y_{pj} & u_{pj} \\ y_{qj} & u_{qj} \end{vmatrix} = \frac{N_1}{N}, \qquad \ldots\ldots(4.14)$$

which follows at once by considering the optical invariant (4.4) for the special case of the two rays (1,0) and (0,1), we obtain the simple result

$$\sin U_j = u_{pj} L_1 \sin U_1 + u_{qj} \sin U_1 + \sum_{\nu=1}^{j-1} \frac{1}{N_1}(c_{p\nu} u_{qj} - c_{q\nu} u_{pj})\Delta_\nu, \qquad \ldots\ldots(4.15)$$

and analogous equations for $L_j \sin U_j$, $\sin I_j$, $\sin I_j'$, the only change being that u_{pj} is replaced by y_{pj}, i_{pj}, i'_{pj} respectively, and similarly for u_{qj}. Equation (4.15) may be rewritten more simply in terms of the associated ray of $[L_1 \sin U_1, \sin U_1]$, i.e.

$$\sin U_j = u_j + \sum_{\nu=1}^{j-1} \frac{1}{N_1}(c_{p\nu} u_{qj} - c_{q\nu} u_{pj})\Delta_\nu, \qquad \ldots\ldots(4.16)$$

and analogous equations for $L_j \sin U_j$, $\sin I_j$, $\sin I_j'$. Notice that the equations for $\sin U_j'$ and $L_j' \sin U_j'$ are similar, except that the summations are extended from $\nu = 1$ to $\nu = j$ instead of to $j-1$.

We have thus found the desired equations giving the differences between corresponding quantities of associated rays.

§5. PRINCIPLES OF THE PRESENT METHOD

(*a*) Writing $\Lambda^* = \Lambda \sec U$ we have, since $\Delta^*\Lambda^* = 0$,

$$\Lambda_f^{*\prime} = \Lambda_1^* + \sum_{\nu=1}^{f} \Delta\Lambda_\nu^*. \qquad \ldots\ldots(5.1)$$

Adopting the restricted definition of v' from § 3 it follows, on taking the paraxial ray contained in Λ^* to pass through the axial point of the object, that

$$\Lambda_f^{*\prime} = N' u_{0f}'(l_{0f}' - L') \tan U_f' = N_f' u_{0f}' H' \qquad \ldots\ldots(5.2)$$

and

$$\Lambda_1^* = N_1 u_{01} H_1 = N_1 u_{01} h = N_f' u_{0f}' h', \qquad \ldots\ldots(5.3)$$

where h is the height of the object, so that

$$N_f' u_{0f}' v' = \sum_{\nu=1}^{f} \Delta\Lambda_\nu^* = D^*, \text{ say.} \qquad \ldots\ldots(5.4)$$

(We have distinguished quantities referring to this particular paraxial ray by the suffix 0, and we shall refer to it in future as the "focal paraxial ray".) Accordingly we may take the "contribution by the jth surface to the final aberration" to be $\Delta\Lambda_j^*/N_j'u_{0j}'$.

Now suppose (dropping the suffixes referring to the particular surface) $\Delta\Lambda^*$ to be expanded in ascending powers of $\sin U$ (see § 8), say

$$\Delta\Lambda^* = \Gamma_1 + \Gamma_2 + \Gamma_3 + \ldots, \tag{5.5}$$

where Γ_n is the term in $\sin^{2n+1} U$. Γ_n may be rewritten by absorbing $\sin^{2n+1} U$ in the factor that multiplies it. We have then Γ_n in the form of the sum of a number of terms each of which consists of the product of $2n+1$ sines of one or more of the angles U, I, I', as well as of certain quantities referring to the focal paraxial ray. Replacing the sines formally by the corresponding quantities of the associated ray, the latter being regarded as functions of y_1 and u_1, we are led to the series

$$\Gamma_1(y,u) + \Gamma_2(y,u) + \Gamma_3(y,u) + \ldots, \qquad \ldots\ldots(5.6)$$

where $\Gamma_n(y,u)$ is a homogeneous polynomial of degree $2n+1$ in y, u. (We have simply written y, u for y_1, u_1, respectively, and shall do so below whenever this procedure is not likely to cause confusion.)

Now clearly the errors committed in this process cause $\Gamma_2, \Gamma_3, \ldots$ to lose their definite meaning for our purpose since the terms neglected in Γ_1 are of the fifth and higher degree, i.e. of the same (and higher) degree as Γ_2, and so on. However, returning to equation (4.16), we see that it may be written

$$\sin U_j = u_{pj}\left(y - \frac{1}{N_1}\sum_{\nu=1}^{j-1} c_{q\nu}\Delta_\nu\right) + u_{qj}\left(u + \frac{1}{N_1}\sum_{\nu=1}^{j-1} c_{p\nu}\Delta_\nu\right). \qquad \ldots\ldots(5.7)$$

Hence, putting

$$\left.\begin{aligned} \delta y_j &= -\frac{1}{N_1}\sum_{\nu=1}^{j-1} c_{q\nu}\Delta_\nu, \\ \delta u_j &= +\frac{1}{N_1}\sum_{\nu=1}^{j-1} c_{p\nu}\Delta_\nu \end{aligned}\right\} \qquad \ldots\ldots(5.8)$$

and $\delta y_j'$, $\delta u_j'$ similarly with the summations extended from $\nu = 1$ to j instead of $j-1$, we have

$$A_j = \alpha_{pj}(y + \delta y_j) + \alpha_{qj}(u + \delta u_j), \qquad \ldots\ldots(5.9)$$

where A stands for *any one* of the quantities $L \sin U$, $\sin U$, $\sin I$, $\sin I'$, and each α corresponds to the particular A. When A stands for $L' \sin U'$ or $\sin U'$, δy and δu must be replaced by $\delta y'$ and $\delta u'$ respectively in (5.9).

The important feature of (5.9) is that the value of any of the quantities which A represents is given by an equation closely analogous to the paraxial linear equation (4.11), i.e. by giving y and u on the right-hand side of the latter the *same* increments δy and δu, *irrespective* of which of the four alternative expressions A happens to represent. Hence, assuming δy_j and δu_j to be expressed as functions of y and u correct to the $(n-1)$th order (see below), we need only substitute $y + \delta y_j$ and $u + \delta u_j$ for y and u respectively in (5.6), rejecting all terms of degree greater than $2n+1$, in order to make that series represent $\Delta\Lambda_j^*$ exactly to the nth order. The terms of the resulting series may then be grouped together so as to give rise to a series of homogeneous polynomials in y, u of degree

3, 5, ... $2n+1$. Then the polynomial of degree $2m+1$ is the contribution (except for the constant factor $1/N'u'_{0j}$) by the jth surface to the aberration of order m.

(*b*) We have yet to show how the δy_j and δu_j are to be determined as functions of y and u. The simplest way of doing this, both in theory and in practice, is by means of a step-by-step method, following closely the procedure outlined above. For this purpose we imagine Δ to be expanded (at any surface) in a series exactly analogous to (5.5) (see § 7), i.e.

$$\Delta = G_1 + G_2 + G_3 + \dots, \qquad \dots\dots(5.10)$$

which again leads to a derived series, similar to (5.6), i.e.

$$G_1(y,u) + G_2(y,u) + G_3(y,u) + \dots. \qquad \dots\dots(5.11)$$

Rejecting all but G_1, δy_j and δu_j may be calculated correct to the first order (i.e. 3rd degree) by means of (5.8); thus

$$\left.\begin{aligned} \delta y_j &= -\frac{1}{N_1}\sum_{\nu=1}^{j-1} c_{q\nu} G_{1\nu}(y,u), \\ \delta u_j &= +\frac{1}{N_1}\sum_{\nu=1}^{j-1} c_{p\nu} G_{1\nu}(y,u). \end{aligned}\right\} \qquad \dots\dots(5.12)$$

Hence from (5.11) we can write down, using the expressions (5.12) at every surface, the terms

$$G_{1j}(y+\delta y_j, u+\delta u_j) + G_{2j}(y,u), \qquad \dots\dots(5.13)$$

rejecting all terms of degree higher than the fifth. (5.13) is then the expansion of Δ_j correct to the second order. This allows us immediately to calculate δy_j and δu_j correct to the second order by substituting in (5.8). Hence with these values of δy_j and δu_j,

$$G_{1j}(y+\delta y_j, u+\delta u_j) + G_{2j}(y+\delta y_j, u+\delta u_j) + G_{3j}(y,u) \qquad \dots\dots(5.14)$$

(rejecting all terms of degree greater than the seventh) represents Δ_j correct to the third order. This process may be obviously repeated until we reach the expansion of Δ_j correct to the $(n-1)$th order. (Notice that, of course, the only new terms to be calculated on passing from order m to order $m+1$ are those of order $m+1$, all terms of lower order remaining unchanged.) Then, finally,

$$\sum_{\nu=1}^{n} \Gamma_{\nu j}(y+\delta y_j, u+\delta u_j) \qquad \dots\dots(5.15)$$

(rejecting all terms of degree higher than the $(2n+1)$th) is the desired expansion of $\Delta\Lambda_j^*$ correct to the nth order.

Alternatively we might calculate $\delta y'_j$ and $\delta u'_j$ correct to the nth order and then directly determine $\Lambda_j^{*\prime}$. Though this method might be somewhat shorter in practice (particularly for large n), it would not yield directly the separate contributions by each surface to the final aberration.

§ 6. *g*-POLYNOMIALS

The explicit expansion of Δ is greatly facilitated by the use of certain simple polynomials $g_n(x)$ defined by

$$\sqrt{(1-t)(1-xt)} = \sum_{n=0}^{\infty} g_n(x) t^n, \qquad \dots\dots(6.1)$$

where x, t are independent variables whose range is suitably restricted so as to ensure the convergence of (6.1).

Replacing t by t/x in (6.1)

$$\sqrt{(1-t/x)(1-t)} = \sum_{n=0}^{\infty} g_n(x)x^{-n}t^n \equiv \sum_{n=0}^{\infty} g_n(1/x)t^n.$$

$$\therefore\quad g_n(x) = x^n g_n(1/x).$$

Hence

$$y^n g_n(x/y) \equiv x^n g_n(y/x) \qquad \text{......(6.2)}$$

is a polynomial symmetrical in x and y.

Expanding the square roots on the left-hand side of (6.1), it follows easily that

$$\left.\begin{aligned} g_n(x) &= (-1)^n \sum_{\nu=0}^{n} \binom{\frac{1}{2}}{n-\nu}\binom{\frac{1}{2}}{\nu} x^\nu \\ \text{(or, also,}\quad g_n(x) &= (-1)^n \binom{\frac{1}{2}}{n} F(-n,\ -\tfrac{1}{2};\ \tfrac{3}{2}-n;\ x), \end{aligned}\right\} \text{......(6.3)}$$

where $F(\alpha,\ \beta;\ \gamma;\ x)$ denotes the hypergeometric function of Gauss).

Setting $x = +1$ in (6.1) we have at once

$$\left.\begin{aligned} &g_n(+1) = 0, \qquad (n > 1). \\ \text{Similarly}\quad &g_n(-1) = 0, \qquad (n \text{ odd}). \end{aligned}\right\} \text{......(6.4)}$$

The recurrence formula satisfied by the $g_n(x)$ is

$$(n+1)g_{n+1}(x) = (n-\tfrac{1}{2})(x+1)g_n(x) - (n-2)xg_{n-1}(x). \qquad \text{......(6.5)}$$

In particular

$$\left.\begin{aligned} &g_0(x) = 1, \qquad g_1(x) = -\tfrac{1}{2}(x+1), \\ &g_2(x) = -\tfrac{1}{8}(x-1)^2, \quad g_3(x) = -\tfrac{1}{16}(x-1)^2(x+1), \\ &g_4(x) = -\tfrac{1}{128}(x-1)^2(5x^2+6x+5), \\ &g_5(x) = -\tfrac{1}{256}(x-1)^2(x+1)(7x^2+2x+7). \end{aligned}\right\} \text{......(6.6)}$$

§ 7. EXPANSION OF Δ

We have

$$\Delta = \sin U' + \sin I' - \sin U - \sin I,$$

which, by (1.3),

$$\begin{aligned} &= \cos U \sin I \cos I' - \cos U \cos I \sin I' + \sin U \cos I \cos I' \\ &\qquad + \sin U \sin I \sin I' - \sin I + \sin I' - \sin U. \end{aligned} \qquad \text{......(7.1)}$$

For convenience, in this paragraph, let

$$\left.\begin{aligned} &(L-r)/r = x; \quad kx = Nx \quad N' = y; \quad \sin U = z, \\ \text{so that}\quad &\sin I = xz; \quad \sin I' = yz. \end{aligned}\right\} \text{......(7.2)}$$

Therefore, since $\cos I = (1-\sin^2 I)^{\frac{1}{2}}$, etc.,

$$\begin{aligned} \Delta = z\{&x\sqrt{(1-z^2)(1-y^2z^2)} - y\sqrt{(1-z^2)(1-x^2z^2)} \\ &+ \sqrt{(1-x^2z^2)(1-y^2z^2)} + xyz^2 - x + y - 1\}, \end{aligned} \qquad \text{......(7.3)}$$

or, in terms of the polynomials of §7,

$$\Delta = z\{xyz^2 - x + y - 1 + \sum_{n=0}^{\infty}[xg_n(y^2) - yg_n(x^2) + x^{2n}g_n(y^2/x^2)]z^{2n}\}. \qquad \ldots\ldots(7.4)$$

$$\therefore\quad \Delta = \sum_{n=1}^{\infty}\delta_n z^{2n+1}, \qquad \ldots\ldots(7.5)$$

where

$$\left.\begin{aligned}
\delta_1 &= \tfrac{1}{2}(x-y)(x+1)(y-1),\\
\delta_2 &= \tfrac{1}{8}(x-y)(x+1)(y-1)(1-x+y+x^2+xy+y^2),\\
\delta_3 &= \tfrac{1}{16}(x-y)(x+1)(y-1)(1-x+y+x^2+y^2-x^3+y^3+x^4+x^3y\\
&\qquad\qquad\qquad\qquad +x^2y^2+xy^3+y^4),
\end{aligned}\right\} \ldots\ldots(7.6)$$

and generally

$$\delta_n = xg_n(y^2) - yg_n(x^2) + x^{2n}g_n(k^2), \qquad n \geqslant 2.$$

Writing $\delta_0 = x - y + 1$, we have in particular

$$\delta_2 = \tfrac{1}{8}\delta_1\{3(x^2+y^2+1) - \delta_0{}^2\}. \qquad \ldots\ldots(7.7)$$

It is evident that every $\delta_n (n > 1)$ has δ_1 as a factor, since δ_n vanishes when $x = -1$, $y = +1$, and $k = 1$, in virtue of (6.4).

Absorbing z^{2n+1} in δ_n we obtain the explicit form of the G_1, G_2, ... of (5.10); thus

$$\left.\begin{aligned}
G_1 &= \tfrac{1}{2}(\sin I + \sin U)(\sin I - \sin I')(\sin I' - \sin U),\\
G_2 &= \tfrac{1}{4}G_1(\sin^2 U - \sin U \sin I + \sin U \sin I' + \sin^2 I\\
&\qquad\qquad + \sin I \sin I' + \sin^2 I'),\\
&\quad . \quad . \quad . \quad . \quad . \quad . \quad . \quad . \quad . \quad . \quad ., \text{ etc.}
\end{aligned}\right\} \ldots\ldots(7.8)$$

To obtain the $G_\nu(y, u)$ of (5.11) we need only replace $\sin U$, $\sin I$, $\sin I'$ by the values of u, i, i' of the associated ray, giving

$$\left.\begin{aligned}
G_1(y,u) &= \tfrac{1}{2}(i+u)(i-i')(i'-u),\\
G_2(y,u) &= \tfrac{1}{8}G_1(y,u)\{3(i^2+u^2+i'^2)-u'^2\}, \text{ by (7.7)},\\
G_3(y,u) &= \tfrac{1}{8}G_1(y,u)(u^4 - iu^3 + i'u^3 + i^2u^2 + i'^2u^2 - i^3u + i'^3u + i^4\\
&\qquad\qquad + i^3i' + i^2i'^2 + ii'^3 + i'^3)\\
&= \tfrac{1}{2}u^2G_2(y,u) + \tfrac{1}{8}G_1(y,u)\left\{u(i'^3 - i^3) - ii'u^2 + \frac{i^5 - i'^5}{i - i'}\right\}\\
&\quad . \quad . \quad . \quad . \quad . \quad . \quad . \quad . \quad . \quad . \quad ., \text{ etc.}
\end{aligned}\right\} \ldots\ldots(7.9)$$

where i, u, ... are given by (4.11). Thus, for instance,

$$\begin{aligned}
G_1(y,u) = \tfrac{1}{2}\{(i+u)_p y_1 + (i+u)_q u_1\}\{(i-i')_p y_1\\
+ (i-i')_q u_1\}\{(i'-u)_p y_1 + (i'-u)_q u_1\}.
\end{aligned} \qquad \ldots\ldots(7.10)$$

The case of a plane surface is easily disposed of. It is only necessary to calculate rG_ν in place of G_ν (so that instead of the vanishing factor $(i+u)$ in G_ν we now have $r(i+u) = y$, which remains finite), and to allow for this by substituting Ni_p for c_p and Ni_q for c_q at this surface in (5.8), etc.

§ 8. EXPANSION OF ΔΛ*

We have

$$\Delta\Lambda^* = \Delta(\Lambda \sec U) = \sec U \Delta\Lambda + \Lambda\Delta \sec U + (\Delta\Lambda)(\Delta \sec U),$$

$$\therefore\quad \Delta\Lambda^* = \sec U' \Delta\Lambda + \Lambda\Delta \sec U. \qquad \ldots\ldots(8.1)$$

If we desire to carry out the computations to a high order, much labour will evidently be saved if we express the Γ_ν as far as possible in terms of the G_ν since the latter are to be calculated in any case. This may be done as follows:

By (7.5), remembering that $\delta_0=x-y+1$,

$$\sin U'=\sum_{\nu=0}^{\infty}\delta_\nu z^{2\nu+1}; \qquad \ldots\ldots(8.2)$$

also

$$\sec U=(1-\sin^2 U)^{-\frac{1}{2}}$$

$$\left.\begin{aligned} \therefore\quad \sec U&=1+\tfrac{1}{2}z^2+\tfrac{3}{8}z^4+\tfrac{5}{16}z^6+\ldots \\ \text{and}\quad \sec U'&=1+\tfrac{1}{2}\delta_0{}^2z^2+(\delta_0\delta_1+\tfrac{3}{8}\delta_0{}^4)z^4 \\ &\quad+(\tfrac{1}{2}\delta_1{}^2+\delta_0\delta_2+\tfrac{3}{2}\delta_0{}^3\delta_1+\tfrac{5}{16}\delta_0{}^6)z^6+\ldots \end{aligned}\right\}\ldots\ldots(8.3)$$

$$\begin{aligned} \therefore\Delta\Lambda^*&=c_0\{1+\tfrac{1}{2}\delta_0{}^2z^2+(\delta_0\delta_1+\tfrac{\ }{8}\delta_0\ )\ {}^4+\ldots\}\{\delta_1z^3+\delta_2z^5+\delta_3z^7+\ldots\}+\Lambda\Delta\sec U \\ &=c_0\{\delta_1z^3+(\delta_2+\tfrac{1}{2}\delta_0{}^2\delta_1)z^5+(\delta_3+\tfrac{1}{2}\delta_0{}^2\delta_2+\delta_0\delta_1{}^2+\tfrac{3}{8}\delta_0{}^4\delta_1)z^7+\ldots\}+\Lambda\Delta\sec U. \end{aligned}$$

$$\ldots\ldots(8.4)$$

Combining the various powers of z with the factors which multiply them, and replacing the resulting sines of the angles by the corresponding quantities of the associated ray, we obtain

$$\left.\begin{aligned} \Gamma_1&=c_0G_1+\tfrac{1}{2}\lambda_0(u'^2-u^2) \\ \Gamma_2&=c_0(G_2+\tfrac{1}{2}u'^2G_1)+\lambda_0(u'G_1+\tfrac{3}{8}\overline{u'^4-u^4}) \\ \Gamma_3&=c_0(G_3+\tfrac{1}{2}u'^2G_2+u'G_1{}^2+\tfrac{3}{8}u'^4G_1)+\lambda_0(u'G_2+\tfrac{1}{2}G_1{}^2 \\ &\qquad\qquad+\tfrac{3}{2}u'^3G_1+\tfrac{5}{16}\overline{u'^6-u^6}) \\ &\quad.\ .\ .\ .\ .\ .\ .\ .\ .\ .\ .\text{, etc.} \end{aligned}\right\}\ldots\ldots(8.5)$$

In practice Γ_1 and Γ_2 are particularly important. Let us consider these in particular. We have by (8.5), (7.9)

$$\Gamma_1=\tfrac{1}{2}c_0(i+u)(i-i')(i'-u)+\tfrac{1}{2}(i-i')(u+u')\lambda_0.$$

Also

$$\begin{aligned} G_2+\tfrac{1}{2}u'^2G_1&=G_1\{\tfrac{1}{2}u'^2+\tfrac{3}{8}(u^2+i^2+i'^2)-\tfrac{1}{8}u'^2\} \\ &=\tfrac{3}{8}G_1(u^2+i^2+i'^2+u'^2) \end{aligned}$$

and

$$G_1+\tfrac{3}{8}(u'^4-u^4)=\tfrac{1}{8}(i-i')\{4u'(i+u)(i'-u)+3(u+u')(u^2+u'^2)\},$$

which may be rearranged, giving

$$u'G_1+\tfrac{3}{8}(u'^4-u^4)=\tfrac{1}{8}(i-i')\{\tfrac{3}{2}(u+u')(u^2+i^2+i'^2+u'^2)+(i+u)(i-i')(u'-3u)\}.$$

Hence if we write

$$\left.\begin{aligned} \gamma_1&=\tfrac{1}{2}c_0(i+u)(i-i')(i'-u), \\ \gamma_2&=\tfrac{1}{2}(i-i')(u+u')\lambda_0=\tfrac{1}{2}(u'^2-u^2)\lambda_0, \\ \gamma_3&=\tfrac{3}{8}(u^2+i^2+i'^2+u'^2), \\ \gamma_4&=\tfrac{1}{4}(u'-3u)\lambda_0/c_0, \end{aligned}\right\}\ldots\ldots(8.6)$$

we have finally

$$\left.\begin{aligned} \Gamma_1&=\gamma_1+\gamma_2, \\ \Gamma_2&=(\gamma_1+\gamma_2)\gamma_3+\gamma_1\gamma_4, \end{aligned}\right\}\ldots\ldots(8.7)$$

which is the form most convenient for computation. (Notice that at every surface λ_0 may be replaced by λ_{01} at once.)

Correct to the second order, the contribution by the jth surface to $N'_j u'_{0f} v'$ is then given by

$$(\gamma_{1j}+\gamma_{2j}) \\ +\left\{(\gamma_{1j}+\gamma_{2j})\gamma_{3j}+\gamma_{1j}\gamma_{4j}+\frac{1}{N_1}\frac{\partial(\gamma_{1j}+\gamma_{2j})}{\partial u_1}\sum_{\nu=1}^{j-1}\frac{c_{p\nu}}{c_{0\nu}}\gamma_{1\nu}-\frac{1}{N_1}\frac{\partial(\gamma_{1j}+\gamma_{2j})}{\partial y_1}\sum_{\nu=1}^{j-1}\frac{c_{q\nu}}{c_{0\nu}}\gamma_{1\nu}\right\} \qquad \ldots\ldots(8.8)$$

§9. CHANGE OF POSITION OF OBJECT OR OF FOCAL PLANE

Since the ray RR′ (§3) is quite arbitrary, it follows that the position of the object enters into the Γ_ν of §8 only through the coefficients c_0 and λ_0. In fact, using the extended definition of v' of §3, we are in every case only interested in the perpendicular distance from the principal axis of the point in which R′ intersects a chosen focal plane, the position of which is defined by l'_{0f}, where the suffix 0 is now used to refer to a paraxial ray having the required l'_{0f} as its final axial intersection length. That is, if we are interested in the performance of the optical system for widely differing positions of the object (or, more generally, for widely differing positions of the plane of reference), we need only compute v'_p and v'_q separately (i.e. v' corresponding to the rays $(y_{01}, u_{01})\equiv(1,0)$ and $(0,1)$ respectively). For then, by (5.4),

$$N'_f u'_{0f} v' = y_{01}\sum_{j=1}^{f}\Delta\Lambda^*_{pj} + u_{01}\sum_{j=1}^{f}\Delta\Lambda^*_{qj}. \qquad \ldots\ldots(9.1)$$

Here y_{01} and u_{01} are connected by the condition that $y_{0f}/u'_{0f}=l'_{0f}$. Hence writing (9.1) in the form

$$u'_{0f}v' = y_{01}u'_{pf}v'_p + u_{01}u'_{qf}v'_q, \qquad \ldots\ldots(9.2)$$

and applying (4.11) and (4.14), it follows that

$$v' = \frac{N'_f}{N_1}\{(l'_{0f}u'_{qf}-y_{qf})u'_{pf}v'_p-(l'_{0f}u'_{pf}-y_{pf})u'_q v'_q\}. \qquad \ldots\ldots(9.3)$$

According to this equation, if the reference plane be moved through a distance $\delta l'_{0f}$, v' changes by the amount

$$\delta v' = \frac{N'_f}{N_1}u'_{pf}\,u_{qf}(v'_p-v'_q)\delta l'_{0f}. \qquad \ldots\ldots(9.4)$$

Notice that the actual magnitude of $\delta l'_{0f}$ is not restricted to be small.

The amount of labour involved in calculating both v'_p and v'_q is not much greater than that involved in calculating v' alone. We shall indicate how this is to be done most easily, considering only primary and secondary terms. (Higher orders are not essentially different.) Thus, from (8.6) we first determine in the ordinary way the quantities γ_1, γ_2, γ_3 and γ_4 with $(y_{01}, u_{01})\equiv(1,0)$, i.e. we determine the four quantities γ_{1p}, γ_{2p}, γ_{3p}, γ_{4p} and hence the three products $\gamma_{1p}\gamma_3$, $\gamma_{2p}\gamma_3$ and $\gamma_{1p}\gamma_{4p}$.

Let $c_q/c_p=\theta$. Then, since

$$\lambda_q = -\gamma_1\lambda_p/u_1, \qquad \ldots\ldots(9.5)$$

we have

$$\left.\begin{aligned} \gamma_{1q} &= \theta\gamma_{1p}, \\ \gamma_{2q} &= -y_1\gamma_{2p}/u_1, \\ \gamma_{1q}\gamma_3 &= \theta\gamma_{1p}\gamma_3, \\ \gamma_{2q}\gamma_3 &= -y_1\gamma_{2p}\gamma_3/u_1, \\ \gamma_{1q}\gamma_{4q} &= -y_1\gamma_{1p}\gamma_{4p}/u_1. \end{aligned}\right\} \quad \ldots\ldots(9.6)$$

(Notice that the δy_j already involve γ_{1q}.) Thus, having determined v'_p, it will be seen (remembering that the δy_j and δu are unchanged) that the only new multiplications required are those of the coefficients of $\gamma_{1p}\gamma_3$ by θ; apart from these only a number of additions is required.

§ 10. THE DIAPHRAGM

A pencil of rays is frequently specified by the position of the object point and the position and aperture of the diaphragm. The "extreme rays" of the pencil (assuming that there is no vignetting) are the rays grazing the rim of the diaphragm. (The aperture of the latter is supposed to be circular.) For a given position of the diaphragm there exists therefore a definite relationship between the values of y and u (i.e. y_1 and u_1) specifying principal rays. To determine this let the diaphragm be situated a distance d behind the surface immediately preceding it, say the jth. Then, paraxially, the desired relationship is given by

$$l \equiv d = \frac{y_{pj}y + y'_{qj}u}{u'_{pj}y + u'_{qj}u}, \qquad \ldots\ldots(10.1)$$

$$y = \frac{u'_{qj}d - y_{qj}}{y_{pj} - u'_{pj}d} = p_1 u, \text{ say.} \qquad \ldots\ldots(10.2)$$

(p_1 is simply the paraxial location of the centre of the entrance pupil with respect to the first surface.) However, we have strictly

$$L' \equiv d = \frac{y_j + y_{pj}\delta y'_j + y_{qj}\delta u'}{u' + u'_{pj}\delta u' + u'_{qj}\delta u'},$$

which may be written

$$y = p_1 u - \delta y_j' + p_1 \delta u_j'. \qquad \ldots\ldots(10.3)$$

To the first order the $\delta y_j'$ and $\delta u_j'$ may be calculated by setting $y = p_1 u$, ($\delta y_j'$ and $\delta u_j'$ have already been computed for *general* values of y_1 and u_1), the error so committed being only of the second order. Hence, correct to the second order,

$$y = p_1 u + p_3 u^3, \qquad \ldots\ldots(10.4)$$

where p_3 is a polynomial of the forth degree in p_1. This process may be continued to any desired order. Writing (10.4) in the form

$$y/u - p_1 = (L_{pr})_1 - p_1 = p_3 u^2 + \ldots, \qquad \ldots\ldots(10.5)$$

we see that the right-hand side of (10.5) gives the variation of the location with respect to the first surface of the centre of the entrance pupil, due to the imperfections of the optical system, as a function of the inclination to the axis of the incident principal ray.

Similarly the relation between y and u for the extreme rays, corresponding to (10.2), is

$$y = p_1 u \pm \frac{e}{y_p - u'_p d}, \qquad \text{......(10.6)}$$

where e is the radius of the aperture of the diaphragm. Higher approximations, corresponding to (10.5), may of course be determined.

In the present notation, the stop-number of the system, defined as the ratio of the posterior focal length $f'(=1/u'_{pf})$ to the diameter of the entrance pupil, is given by

$$\text{stop number} = \frac{y_{pf} - u'_{pf} d}{2u'_{pf} e}. \qquad \text{......(10.7)}$$

§11. v', AND SPHERICAL ABERRATION

(*a*) Let us assume that v' has been computed (§§5–8) and is available in the final form

$$\begin{aligned} v' = {} & a_0 y^3 + a_1 y^2 u + a_2 y u^2 + a_3 u^3 + b_0 y^5 + b_1 y^4 u + b_2 y^3 u^2 \\ & + b_3 y^2 u^3 + b_4 y u^4 + b_5 u^5 + \text{higher terms}. \qquad \text{......(11.1)} \end{aligned}$$

(11.1) here refers to the last surface of the optical system considered (which may of course be any intermediate surface of an actual system), the coefficients being evaluated for a definite position of the object. We shall take the plane of reference to be the paraxial focal plane.

To gain information about the system, which can be easily visualized, it will frequently be desirable (though by no means essential) to plot v' as a function of y and u. If the object is situated at infinity it is advisable to plot v' as a function of y for various fixed values of u, whilst if the object, of height h, is situated at l_{01}, one may plot v' against u for various fixed values of h; y and u in this case are related by the condition

$$(l_{01} - L_1) \tan U_1 = \text{const.} = h,$$

or in terms of the associated ray,

$$y = l_{01} u - h\sqrt{(1-u^2)}. \qquad \text{......(11.2)}$$

The position of the diaphragm may often be decided upon by inspection of the graphs so obtained.

(*b*) If the object is situated at infinity (as is frequently the case with photographic objectives) the *spherical aberration* is given by (11.1) on making $u=0$, i.e.

$$\text{spher. ab.} = (v')_{=0} = a_0 y^3 + b_0 y^5 + \dots . \qquad \text{......(11.3)}$$

This equation gives the radius of the disc of confusion projected by the system on a screen placed in the position of the focal plane. In practice we may also measure the spherical aberration by the value of the expression

$$[(l'_{0f} - L'_f) \sin U'_f]_{u=0}, \qquad \text{......(11.4)}$$

which is more convenient from the point of view of the computation of higher orders.

Thus for the *tertiary spherical aberration* we require essentially the calculation of $G_1(y, u)$ omitting the term in u^3; of $G_2(y, u)$ rejecting all terms except those in

y^6 and y^4u; and of the term in y^7 in $G_8(y,u)$. (Since the $\delta y'_j$ and $\delta u'_j$ are then in any case known to the second order, $\sin U'_j$, and hence $(v')_{u=0}$ may, if desired, be calculated subsequently directly from (11.4). The difference between these results is, however, in general, quite negligible.)

The great simplicity apparent in the calculation of the higher-order spherical aberration *ab initio*, as indicated above, is there due to the fact that one of the independent variables, namely u, is zero. Hence to obtain the same simplicity when the object is not at infinity but at l_{01}, say, we must proceed somewhat differently, viz. by introducing the independent variable

$$\bar{y}_1 = y_1 - l_{01}u_1 \qquad \ldots\ldots(11.5)$$

in place of y_1. Equation (5.7) then becomes

$$\sin U_j = u_{pj}\left(\bar{y} - \sum_{\nu=1}^{j-1} \frac{1}{N_1}(c_{q\nu} + l_{01}c_{p\nu})\Delta_\nu\right) + (u_{qj} + u_{pj}l_{01})\left(u + \sum_{\nu=1}^{j-1} \frac{1}{N_1} c_{p\nu}\Delta_\nu\right). \qquad \ldots\ldots(11.6)$$

We have therefore again a set of equations of the type (5.8), (5.9), etc., except that where previously any quantity referring to the ray (0,1) appeared we now have in its place the corresponding quantity referring to the ray (l_{01}, 1). Accordingly the computations now begin with the tracing of the two rays (l_{01},1) and (1,0). And since one of the independent variables is now zero, the calculations are similar in every detail to those in the case where the object point is situated at infinity.

If, as will often be the case, the primary and secondary terms are already known, it may nevertheless be worth while to calculate them again by the method above. For in this way a good check is obtained on equation (11.1), from which the spherical aberration is obtained by setting $y = l_{01}u$, so that *all* the coefficients appearing in it are checked in this way.

(*c*) In practice one will generally limit oneself to the computation of the exact primary and secondary aberrations; partly because the information so obtained will be sufficient in many cases, and partly because the evaluation of the *general* tertiary (and higher) terms is rather lengthy. As we have seen, the computation of the tertiary spherical aberration is, however, relatively simple. Consequently it will frequently be advisable to carry it out. For obviously (taking the object to be at infinity) when the inclination of the incident pencil (i.e. u_1) is sufficiently small, the difference between the actual aberration and the sum of the primary and secondary terms is in general dominated by the next higher term in (11.1) not involving u; the latter being the tertiary spherical aberration. Similarly when l_{01} is finite.

If the plane of reference is other than the paraxial focal plane, the considerations above are not essentially altered. Thus, if the system were perfect, the radius of the disc of confusion would be given by a simple term involving y and u linearly. In the actual system the radius of the disc of confusion is, therefore, the sum of this linear term and v' (extended definition).

§ 12. DISTORTION

From the definition of § 3 it will be seen that the distortion is represented by v' when y is replaced by its value in terms of u as given by (10.4). We shall restrict ourselves in this and the next paragraph to the first and second orders, the extension to all orders being obvious. Thus

$$\text{Distortion} = (a_0 p_1^3 + a_1 p_1^2 + a_2 p_1 + a_3) u^3 + \{(b_0 p_1^5 + b_1 p_1^4 + b_2 p_1^3 + b_3 p_1^2 + b_4 p_1 + b_5) + p_3(3a_0 p_1^2 + 2a_1 p_1 + a_2)\} u^5. \qquad \ldots\ldots(12.1)$$

Therefore, if

$$\left.\begin{aligned} A &= \sum_{\nu=1}^{3} a_\nu p^{3-\nu} \\ \text{and} \qquad B &= \sum_{\nu=1}^{5} b_\nu p^{5-\nu}, \end{aligned}\right\} \ldots\ldots(12.2)$$

this may be written more compactly

$$\text{Distortion} = Au^3 + \left(B + p_3 \frac{dA}{dp_1}\right) u^5. \qquad \ldots\ldots(12.3)$$

As might be expected, the term in p_3 will in practice often be found to be negligible compared with the other terms, in which case we have simply

$$\text{Distortion} = Au^3 + Bu^5. \qquad \ldots\ldots(12.4)$$

§ 13. COMA AND CURVATURE OF FIELD

In this paragraph we take for the sake of simplicity an object situated at infinity. This implies no restriction in principle. (For objects finitely situated we only require the additional application of equation (11.2): see (13.5)). In equations in which several rays of a pencil are involved, quantities without suffix refer to the principal ray, whilst, as before, the suffixes *a* and *b* refer to the extreme rays.

It may be easily verified that according to the definition of § 3, the coma, C', is given by

$$C' = \left\{\frac{v_a' + v_b'}{2} - v'\right\} + \frac{v_a' - v_b'}{2}\left\{\frac{2\tan U' - (\tan U_a' + \tan U_b')}{\tan U_a' - \tan U_b'}\right\}, \qquad \ldots\ldots(13.1)$$

whilst the curvature of field, W', is given by

$$W' = \frac{v_a' - v_b'}{\tan U_a' - \tan U_b'}. \qquad \ldots\ldots(13.2)$$

(13.1) may therefore be written

$$C' = \{\tfrac{1}{2}(v_a' + v_b') - v'\} - W'\{\tfrac{1}{2}(\tan U_a' + \tan U_b') - \tan U'\}. \qquad \ldots\ldots(13.3)$$

In this equation, since the lowest terms of the factor of W' are of the third degree, W' need in general only be evaluated to the $(n-1)$th order if C' is required to the nth order. Thus, when $n=2$, since $\delta y_f'$ and $\delta u_f'$ are known to the first order, the calculation of $\sin U_f'$ and hence of $\tan U_f'$ to this order presents no difficulty. Therefore (omitting the suffix f), let

$$\tan U' = u_p' y + u_q' u + u_p'(t_0 y^3 + t_1 y^2 u + t_2 y u^2 + t_3 u^3). \qquad \ldots\ldots(13.4)$$

We have assumed the incident pencil to consist of parallel rays;

$$\left.\begin{aligned} \therefore\quad y_a &= y + w, \\ y_b &= y - w, \end{aligned}\right\} \ldots\ldots(13.5)$$

where w is the semi-aperture of the incident pencil. (13.5) applies because $y-y_a[=(L_{a1}-L_1)\sin U_1]$ is the perpendicular distance between the a ray and the principal ray; and similarly for the b ray. (The fact that, if the pencil is actually limited physically by the diaphragm, the principal ray will not in general lie precisely halfway between the extreme rays at the first surface is of no practical consequence.)

Now to the required order, by (13.2), (13.4), (13.5), and (10.2),

$$W'=\frac{1}{u_p'}\{(3a_0p_1^2+2a_1p_1+a_2)u^2+a_0w^2\} \qquad \ldots\ldots(13.6)$$

and

$$\tfrac{1}{2}(\tan U_a'+\tan U_b')-\tan U'=u_p'(3t_0p_1+t_1)uw^2. \qquad \ldots\ldots(13.7)$$

Also, by (11.1) and (10.4),

$$\begin{aligned}\tfrac{1}{2}(v_a'+v_b')-v'=(3a_0p_1+a_1)uw^2+\{&(10b_0p_1^3+6b_1p_1^2+3b_2p_1+b_3)\\&+3a_0p_3\}u^3w^2+(5b_0p_1+b_1)uw^4.\end{aligned} \qquad \ldots\ldots(13.8)$$

$$\begin{aligned}\therefore\quad C'=(3a_0p_1+a_1)uw^2+\{&(10b_0p_1^3+6b_1p_1^2+3b_2p_1+b_3)\\&+3a_0p_3-(3a_0p_1^2+2a_1p_1+a_2)(3t_0p_1+t_1)\}u^3w^2\\&+\{(5b_0p_1+b_1)-a_0(3t_0p_1+t_1)\}uw^4.\end{aligned} \qquad \ldots\ldots(13.9)$$

As in the case of distortion, it will frequently be found in practice that the terms in p_3, t_0, t_1 may be neglected. If so, (13.9) may be written, in terms of (12.2),

$$C'=A_2uw^2+(B_2u^3w^2+B_4uw^4), \qquad \ldots\ldots(13.10)$$

where

$$A_n=\frac{1}{n!}\cdot\frac{d^nA}{dp^n},$$

and

$$B_n=\frac{1}{n!}\frac{d^nB}{dp^n}. \qquad \ldots\ldots(13.11)$$

By means of (13.2), a formula analogous to (13.9) may be written down, giving W' correct to the required order. From our present point of view this is of no great interest (see end of § 3). Accordingly we content ourselves with observing that if the terms containing p_3, t_0, t_1, t_2 can again be neglected, the equation for W' analogous to (13.10) becomes

$$u_p'W'=(A_1u^2+A_3w^2)+(B_1u^4+B_3u^2w^2+B_5w^4). \qquad \ldots\ldots(13.12)$$

§ 14. PRINCIPLES OF AN ALTERNATIVE METHOD

It is interesting from a theoretical point of view that whereas previously we made use of the *two* quasi-invariants $\Delta\Lambda$ and $\Delta\Lambda^*$, each of which splits up into two (quasi-invariant) parts, i.e.

$$\left.\begin{aligned}\Delta\Lambda_p&=c_p\Delta,\\ \Delta\Lambda_q&=c_q\Delta,\end{aligned}\right\} \qquad \ldots\ldots(14.1)$$

and

$$\left.\begin{aligned}\Delta\Lambda_p^*&=c_p(\sec U'\Delta+\sin U\Delta(\sec U))-c_p^*\sin I\Delta(\sec U),\\ \Delta\Lambda_q^*&=c_q(\sec U'\Delta+\sin U\Delta(\sec U))-c_q^*\sin I\Delta(\sec U),\end{aligned}\right\} \qquad \ldots\ldots(14.2)$$

where

$$c^*=Nru \qquad \ldots\ldots(14.3)$$

(together with their corresponding sums D_p, D_q and D_p^*, D_q^* respectively), we can also proceed in a way which avoids the use of the former altogether.

If we now take the associated ray of the arbitrary ray R to be $(L_1 \tan U_1, \tan U_1)$ we can write down a set of equations, by (5.1), similar to (4.13), but with the sines of the angles replaced by their tangents, and with the $\Delta\Lambda$ replaced by the $\Delta\Lambda^*$. Write

$$\left.\begin{aligned} \delta y_j &= -\frac{1}{N_1}\sum_{\nu=1}^{j-1} \Delta\Lambda_{q\nu}^*, \\ \delta u_j &= +\frac{1}{N_1}\sum_{\nu=1}^{j-1} \Delta\Lambda_{p\nu}^*, \end{aligned}\right\}\quad\ldots\ldots(14.4)$$

and similarly $\delta y_j^{*\prime}$ and $\delta u_j^{*\prime}$, as before. Then in place of (5.9) we have now

$$\left.\begin{aligned} \tan U_j &= u_{pj}(y+\delta y_j^*)+u_{qj}(u+\delta u_j^*), \\ L_j \tan U_j &= y_{pj}(y+\delta y_j^*)+y_{uj}(u+\delta u_j^*), \\ \sec U_j \sin I_j &= i_{pj}(y+\delta y_j^*)+i_{qj}(u+\delta u_j^*), \\ & \quad . \quad . \quad . \quad . \quad . \quad . \quad . \quad . \quad . \quad ., \text{ etc.} \end{aligned}\right\}\quad\ldots\ldots(14.5)$$

$\Delta\Lambda_p^*$ and $\Delta\Lambda_q^*$ are now to be regarded as expanded in series of ascending powers of $\tan U$. If, as before, we absorb, in the nth term of these series, $\tan^{2n+1} U$ in the factor that multiplies it, then the nth term will be composed solely of the products of quantities given by (14.5). Hence we may proceed as before.

Although $\Delta\Lambda$ is no longer explicitly contained in these equations, it is doubtful whether their practical application would be more convenient than that of the formulae developed earlier.

§ 15. EXAMPLE OF COMPUTATIONS

(*a*) The system used for the purpose of illustrating the practicability of the methods above is a slightly altered design of a corrected Cooke Triplet as given by Hardy and Perrin (1932, Chap. 21). The specifications of the system are

Surface	1	2	3	4	5	6
r	+20·05	−128·3	−58·8	+18·9	+311·3	−66·2
N'	1·6162	1	1·5725	1	1·6162	1
d'	3·896	1·63	0·93	13·42	3·03	–

$(f' = 96{\cdot}729)$; $d = 4{\cdot}0$ (behind 4th surface)
Max. stop-number of system $= f'/5{\cdot}6$. ……(15.1)

The object is assumed to be situated at infinity, so that we are essentially computing v_p'. Moreover the factor $N_j' u'_{0j}$ may be replaced by $1/f'$ wherever it occurs where f' is the focal length of the system.

(*b*) *Table* 1

This gives the complete detailed computation for v' (primary and secondary). Little comment is needed, as the computing scheme is arranged so as to explain itself. (A lowered number after a nought following the decimal point gives the total number of noughts following the latter.) A current symbol, t_ν, is attached to such quantities as recur at a later stage of the computation. The entries are

Table 1

	$j\to$		1	2	3	4	5	6	$f'\Sigma\{$
p trace	l_p		∞	48·6921	24·6892	50·1798	942·331	528·503	
	u_p		0	0·0190154	0·0351802	0·0169942	0·0$_3$892248	0·00158183	
	$(l_p-r)/r=x_p$			−1·37952	−1·41989	1·65502	2·02708	−8·98343	
	$x_pu_p=i_p$		0·0498753	−0·0262325	−0·0499518	0·0281257	0·00180866	−0·0142102	
	$Ni_p/N'=i_p'$		0·0308596	−0·0423970	−0·0317658	0·0442277	0·00111908	−0·0229666	
	$(i+u-i')_p=u_p'$		0·0190157	0·0351802	0·0169942	0·0$_3$892248	0·00158183	0·0103382	
	$i_p'/u_p'=x_p'$		1·62285	−1·20514	−1·86921	49·5688	0·707462	−2·22153	
	$(x_p'+1)r=l_p'$		52·5881	26·3192	51·1098	955·751	531·533	80·8654	
q trace	l_q		0	−3·8960	−4·06883	−7·08442	−17·3842	−32·1276	
	u_q		1·0	0·618735	0·988422	0·653469	1·167810	0·697701	
	$(l_q-r)/r=x_q$		−1·0	−0·969634	−0·930802	−1·37484	−1·05584	−0·514688	
	$x_qu_q=i_q$		−1·0	−0·599466	−0·920026	−0·898413	−1·23303	−0·359099	
	$Ni_q/N'=i_q'$		−0·618735	−0·969634	−0·585072	−1·41275	−0·762916	−0·580375	
	$(i+u-i')_q=u_q'$		0·618735	0·988422	0·653469	1·167810	0·697701	0·918978	
	$i_q'/u_q'=x_q'$		−1·0	−0·980991	−0·895333	−1·20975	−1·09346	−0·631544	
	$(x_q'+1)r=l_q'$		0	−2·43883	−6·15442	−3·96421	−29·0976	−24·3918	
	$(u+i)_p$	t_1	0·0498753	−0·0072168	−0·0147716	0·0451199	0·00270091	−0·0126284	
	$(i-i')_p$	t_2	0·0190157	0·0161645	−0·0181859	−0·0161020	0·0$_3$689578	0·00875634	
	$(i'-u)_p$	t_3	0·0308596	−0·0614127	−0·0669459	0·0272335	0·0$_3$226834	−0·0245484	
	$\frac{1}{4}(u'-3u)_p$	t_4	0·00475392	−0·0010050	−0·00753671	−0·0149809	−0·0$_3$486167	0·0$_3$919616	
	$Nri_p=c_p$		1·0	5·43953	2·93716	0·835903	0·563036	1·52039	
	$(u+i)_q$	t_5	0	0·0187887	0·0683966	−0·244944	−0·0652151	0·338602	
	$(i-i')_q$	t_6	−0·381265	0·369687	−0·334954	0·514341	−0·470109	0·221277	
	$(i'-u)_q$	t_7	−0·161874	−0·158837	−1·57349	−2·06622	−1·93073	−1·27808	
	$\frac{1}{4}(u'-3u)_q$	t_8	−0·595316	−0·0398832	−0·196771	−0·237048	−1·24580	−0·193064	
	$Nri_q=c_q$		−20·05	124·404	54·0975	−26·7011	−383·841	38·4208	
	$c_q/c_p=\theta$		−20·05	22·8704	18·4183	−31·9428	−681·734	25·2704	

γ_3	u_p^2	t_9	0	$0{\cdot}0_3361597$	0·00123764	$0{\cdot}0_3288803$	$0{\cdot}0_679611$	$0{\cdot}0_525022$		
	i_p^2		0·00248755	$0{\cdot}0_3688144$	0·00249518	$0{\cdot}0_3791056$	$0{\cdot}0_532713$	$0{\cdot}0_3201930$		
	$i_p'^2$		$0{\cdot}0_3952316$	0·00179750	0·00100907	0·00195609	$0{\cdot}0_512523$	$0{\cdot}0_3527463$		
	$u_p'^2$	t_{10}	$0{\cdot}0_3361597$	0·00123764	$0{\cdot}0_328803$	$0{\cdot}0_679611$	$0{\cdot}0_525022$	$0{\cdot}0_3106878$		
	$\frac{3}{8}\Sigma$	t_{11}	0·00142555	0·00153183	0·00188651	0·00113878	$0{\cdot}0_529332$	$0{\cdot}0_3314540$		
	u_pu_q	t_{12}	0	0·0117657	0·0347729	0·0111052	0·00104198	0·00110364		
	i_pi_q		−0·0498753	0·0157381	0·0459569	−0·0252685	−0·00223012	0·00510287		
	$i_p'i_q'$		−0·0190939	0·0411095	0·0185853	−0·0624828	$-0{\cdot}0_3853766$	0·0133292		
	$u_p'u_q'$	t_{13}	0·0117657	0·0347729	0·0111052	0·00104198	0·00110364	0·00950054		
	$\frac{3}{4}\Sigma$	t_{14}	−0·0429027	0·0775396	0·0828152	−0·0567031	$-0{\cdot}0_3703704$	0·0217772		
	u_q^2	t_{15}	1·0	0·382833	0·976979	0·427021	1·36378	0·486787		
	i_q^2		1·0	0·359936	0·846447	0·807146	1·52035	0·128952		
	$i_q'^2$		0·382833	0·940189	0·342309	1·99588	0·582041	0·336835		
	$u_q'^2$	t_{16}	0·382833	0·976979	0·427021	1·36378	0·486787	0·844520		
	$\frac{3}{8}\Sigma$	t_{17}	1·03713	0·997477	0·972284	1·72268	1·48236	0·673910		
γ_2	$\frac{1}{2}(t_{10}-t_9)$	t_{18}	$0{\cdot}0_3180798$	$0{\cdot}0_2438023$	$-0{\cdot}0_3474420$	$-0{\cdot}0_3144004$	0·0685303	$0{\cdot}0_4521877$		
	$(t_{13}-t_{12})$	t_{19}	0·0117657	0·0230072	−0·0236676	−0·0100632	$0{\cdot}0_461666$	0·00839690		
	$\frac{1}{2}(t_{16}-t_{15})$	t_{20}	−0·308583	0·297073	−0·274979	0·468380	−0·438497	0·178866		
γ_1	$\frac{1}{2}c_pt_1t_2t_3$	t_{21}	$0{\cdot}0_4146338$	$0{\cdot}0_4194847$	$-0{\cdot}0_4264111$	$-0{\cdot}0_5826944$	$0{\cdot}0_9118943$	$0{\cdot}0_5206356$		
	$\frac{1}{2}c_pt_5t_6t_7$	t_{24}	0	−0·0300064	0·0529399	0·108798	−0·0166638	−0·0727958		
	t_5/t_1		0	−2·60347	−4·63027	− 5·42874	− 24·1456	−26·8128		
	t_6/t_2		−20·05	22·8704	18·4183	−31·9428	− 681·734	25·2704		
	t_7/t_3		−52·4548	25·8639	23·5039	−75·8707	−8511·63	52·0636		
	Σ	t_{25}	−72·5048	46·1308	37·2919	−113·242	−9217·51	50·5212		

Table 1—*continued*

	$j\rightarrow$		1	2	3	4	5	6	$f'\Sigma_1^f$	
γ_1	t_1/t_5		—	−0·384102	−0·215970	−0·184205	−0·0414154	−0·0372956		
	t_2/t_6		—	0·0437247	0·0542940	−0·0313060	−0·0014668	0·0395719		
	t_3/t_7		—	0·0386640	0·0425461	−0·0131803	−0·0$_3$11750	0·0192073		
	Σ	t_{26}	—	−0·301714	−0·119130	−0·228691	−0·0429997	0·0214836		
	$t_{21}t_{25}$	t_{22}	−0·00106102	0·0$_3$898846	−0·0$_3$984922	0·0$_3$936450	−0·0$_5$109633	0·0$_3$104253		
	$t_{24}t_{26}$	t_{23}	0·0153907	0·00905335	−0·00630673	−0·0248812	0·0$_3$716538	−0·00156392		
$\gamma_1+\gamma_2$	t_{21}	t_{21}							0·0$_3$145259	a_0
	$t_{22}+t_{18}$	t_{27}	−0·0$_3$880226	0·00133687	−0·00145934	0·0$_3$792446	−0·0$_6$24330	0·0$_3$156441	−0·0052286	a_1
	$t_{23}+t_{19}$	t_{28}	0·0271564	0·0320605	−0·0299744	−0·0349444	0·0$_3$778204	0·00683298	0·18468	a_2
	$t_{24}+t_{20}$	t_{29}	−0·308583	0·267066	−0·222039	0·577178	−0·455161	0·106071	−3·4308	a_3
	θt_{21}	(t_{68})	−0·0$_3$293409	0·0$_3$445623	−0·0$_3$486447	0·0$_3$264149	−0·0$_7$8106	0·0$_4$521471		
	θt_{22}		0·0212735	0·0205569	−0·0181406	−0·0299128	0·0$_3$747406	0·00263453		
	θt_{23}		−0·308583	0·207053	−0·116159	0·794774	−0·488488	−0·0395209		
	θt_{24}		0	−0·686258	0·975061	−3·47532	11·3603	−1·83958		
δu	$\Sigma_1^{j-1}t_{21}$	t_{30}	0	0·0$_4$146338	0·0$_4$341186	0·0$_5$770747	−0·0$_6$561971	−0·0$_6$561852		
	$\Sigma_1^{j-1}t_{22}$	t_{31}	0	−0·00106102	−0·0$_3$162178	−0·00114710	−0·0$_3$210650	−0·0$_3$211746		
	$\Sigma_1^{j-1}t_{23}$	t_{32}	0	0·0153907	0·0244440	0·0181373	−0·00674389	−0·00602735		
	$\Sigma_1^{j-1}t_{24}$	t_{33}	0	0	−0·0300064	0·0229335	0·131732	0·115068		
$-\delta y$	$\Sigma^{j-1}\theta t_{21}$	t_{34}	0	−0·0$_3$293409	0·0$_3$152215	−0·0$_3$334237	−0·0$_4$708388	−0·0$_4$701649		
	$\Sigma_1^{j-1}\theta t_{22}$	t_{35}	0	0·0212735	0·0418305	0·0236900	−0·00622291	−0·00547550		
	$\Sigma^{j-1}\theta t_{23}$	t_{36}	0	−0·308583	−0·101530	−0·217689	0·577085	0·0885970		
	$\Sigma_2^{j-1}\theta t_{24}$	t_{37}	0	0	−0·686258	0·288804	−3·18651	8·17376		
	$t_{21}t_{11}$		0·0$_7$208612	0·0$_7$298473	−0·0$_7$498249	−0·0$_8$941706	0·0$_{15}$3	0·0$_9$649072		
	$t_{30}t_{27}$		0	0·0$_7$195635	−0·0$_7$497907	0·0$_8$610776	0·0$_{11}$13673	−0·0$_{10}$878968		
	$-3t_{34}t_{21}$	(t_{58})	0	0·0$_7$171510	0·0$_7$120605	−0·0$_8$829185	0·0$_{13}$250	0·0$_9$434369		

Σ	t_{38}	$0\cdot0_{7}208612$	$0\cdot0_{7}665614$	$-0\cdot0_{7}875551$	$-0\cdot0_{7}116012$	$0\cdot0_{11}13926$	$0\cdot0_{9}995544$	$-0\cdot0_{5}103856$	b_0
$t_{27}t_{11}$		$-0\cdot0_{5}125480$	$0\cdot0_{5}204786$	$-0\cdot0_{5}275306$	$0\cdot0_{6}902421$	$-0\cdot0_{12}7$	$0\cdot0_{7}492070$		
$t_{21}t_{14}$		$-0\cdot0_{6}627831$	$0\cdot0_{5}151084$	$-0\cdot0_{5}218724$	$0\cdot0_{6}468903$	$-0\cdot0_{13}8$	$0\cdot0_{7}449386$		
$t_{21}t_{4}$		$0\cdot0_{7}695682$	$-0\cdot0_{7}195822$	$0\cdot0_{6}199053$	$0\cdot0_{6}123884$	$-0\cdot0_{13}578$	$0\cdot0_{8}189768$		
$t_{31}t_{27}$		0	$-0\cdot0_{5}141845$	$0\cdot0_{6}236673$	$-0\cdot0_{6}909015$	$0\cdot0_{10}51251$	$-0\cdot0_{7}331258$		
$2t_{30}t_{28}$		0	$0\cdot0_{6}938337$	$-0\cdot0_{5}204537$	$-0\cdot0_{6}538666$	$-0\cdot0_{9}874656$	$-0\cdot0_{8}767825$		
$-3t_{35}t_{21}$		0	$-0\cdot0_{5}124353$	$0\cdot0_{5}331437$	$0\cdot0_{6}587707$	$0\cdot0_{11}222$	$0\cdot0_{7}338971$		
$-2t_{34}t_{27}$		0	$0\cdot0_{6}784498$	$0\cdot0_{6}444266$	$0\cdot0_{6}529729$	$-0\cdot0_{10}341$	$0\cdot0_{7}219534$		
Σ	t_{39}	$-0\cdot0_{5}181306$	$0\cdot0_{5}259998$	$-0\cdot0_{5}279131$	$0\cdot0_{5}116496$	$-0\cdot0_{9}8559$	$0\cdot0_{6}111090$	$-0\cdot0_{4}70536$	b_1
$t_{28}t_{11}$		$0\cdot0_{4}387127$	$0\cdot0_{4}491113$	$-0\cdot0_{4}565470$	$-0\cdot0_{4}397939$	$0\cdot0_{8}228$	$0\cdot0_{5}214924$		
$t_{27}t_{14}$		$0\cdot0_{4}377$	$0\cdot0_{3}103660$	$-0\cdot0_{3}120856$	$-0\cdot0_{4}449342$	$0\cdot0_{9}17$	$0\cdot0_{5}340685$		
$t_{21}t_{17}$		$0\cdot0_{4}151771$	$0\cdot0_{4}194356$	$-0\cdot0_{4}256791$	$-0\cdot0_{4}142456$	$0\cdot0_{9}18$	$0\cdot0_{5}139065$		
$t_{22}t_{4}$		$-0\cdot0_{5}504403$	$-0\cdot0_{6}903341$	$0\cdot0_{5}742307$	$-0\cdot0_{4}140289$	$0\cdot0_{9}5330$	$0\cdot0_{7}958732$		
$t_{21}t_{8}$		$-0\cdot0_{5}871176$	$-0\cdot0_{6}777114$	$0\cdot0_{5}519695$	$0\cdot0_{5}196025$	$-0\cdot0_{9}1481$	$-0\cdot0_{6}398399$		
$t_{32}t_{27}$		0	$0\cdot0_{4}205753$	$-0\cdot0_{4}356722$	$0\cdot0_{4}143728$	$0\cdot0_{8}16408$	$-0\cdot0_{6}942927$		
$2t_{31}t_{28}$		0	$-0\cdot0_{4}680340$	$0\cdot0_{5}972237$	$0\cdot0_{4}801694$	$-0\cdot0_{6}327857$	$-0\cdot0_{5}289371$		
$3t_{30}t_{29}$		0	$0\cdot0_{4}117246$	$-0\cdot0_{4}227270$	$0\cdot0_{4}133457$	$0\cdot0_{6}767361$	$-0\cdot0_{6}178788$		
$-3t_{36}t_{21}$		0	$0\cdot0_{4}180380$	$0\cdot0_{5}804455$	$-0\cdot0_{5}540050$	$-0\cdot0_{9}206$	$-0\cdot0_{6}548476$		
$-2t_{35}t_{27}$		0	$-0\cdot0_{4}568799$	$0\cdot0_{3}122090$	$-0\cdot0_{4}375460$	$-0\cdot0_{8}3028$	$0\cdot0_{5}171319$		
$-\ t_{34}t_{28}$		0	$0\cdot0_{5}940683$	$0\cdot0_{5}456254$	$-0\cdot0_{4}116797$	$0\cdot0_{7}54540$	$0\cdot0_{6}479436$		
Σ	t_{40}	$0\cdot0_{4}778980$	$0\cdot0_{3}105358$	$-0\cdot0_{3}120531$	$-0\cdot0_{4}577806$	$0\cdot0_{6}49547$	$0\cdot0_{5}427293$	$0\cdot0_{3}93953$	b_2
$t_{29}t_{11}$		$-0\cdot0_{3}43990$	$0\cdot0_{3}409101$	$-0\cdot0_{3}418879$	$0\cdot0_{3}657278$	$-0\cdot0_{5}13351$	$0\cdot0_{4}333635$		
$t_{28}t_{14}$		$-0\cdot00116508$	$0\cdot00248596$	$-0\cdot00248234$	$0\cdot00198146$	$-0\cdot0_{6}5476$	$0\cdot0_{3}148803$		
$t_{27}t_{17}$		$-0\cdot0_{3}912904$	$0\cdot00133350$	$-0\cdot00141889$	$0\cdot00136513$	$-0\cdot0_{6}3607$	$0\cdot0_{3}105427$		
$t_{23}t_{4}$		$0\cdot0_{4}731662$	$-0\cdot0_{5}909863$	$0\cdot0_{4}475320$	$0\cdot0_{3}372743$	$-0\cdot0_{6}34836$	$-0\cdot0_{5}143820$		
$t_{22}t_{8}$		$0\cdot0_{3}631645$	$-0\cdot0_{4}358489$	$0\cdot0_{3}193804$	$-0\cdot0_{3}221983$	$0\cdot0_{5}136581$	$-0\cdot0_{4}201276$		
$t_{33}t_{27}$		0	0	$0\cdot0_{4}437896$	$0\cdot0_{4}181735$	$-0\cdot0_{7}32050$	$0\cdot0_{4}180029$		
$2t_{32}t_{28}$		0	$0\cdot0_{3}986867$	$-0\cdot00146539$	$-0\cdot00126760$	$-0\cdot0_{4}104963$	$-0\cdot0_{4}823696$		
$3t_{31}t_{29}$		0	$-0\cdot0_{3}850091$	$0\cdot0_{3}108029$	$-0\cdot00198624$	$0\cdot0_{3}287638$	$-0\cdot0_{4}673801$		
$-3t_{37}t_{21}$		0	0	$-0\cdot0_{4}543745$	$0\cdot0_{5}716474$	$0\cdot0_{8}114$	$-0\cdot0_{4}506012$		
$-2t_{36}t_{27}$		0	$0\cdot0_{3}825071$	$-0\cdot0_{3}296334$	$0\cdot0_{3}345014$	$0\cdot0_{6}2808$	$-0\cdot0_{4}277204$		
$-\ t_{35}t_{28}$		0	$-0\cdot0_{3}682041$	$0\cdot00125384$	$0\cdot0_{3}827830$	$0\cdot0_{5}48427$	$0\cdot0_{4}374140$		

Table 1—*continued*

$j\rightarrow$		1	2	3	4	5	6	$f'\Sigma\{_1$	
Σ	t_{41}	−0·00181307	0·00446342	−0·00448921	0·00209897	$0{\cdot}0_{3}281009$	$0{\cdot}0_{4}933736$	0·061374	b_3
$t_{29}t_{14}$		0·0132390	0·0207082	−0·0183882	−0·0327278	$0{\cdot}0_{3}320298$	0·00230992		
$t_{28}t_{17}$		0·0281646	0·0319796	−0·0291436	−0·0601982	0·00115358	0·00460482		
$t_{24}t_{4}$		0	$0{\cdot}0_{4}301565$	$-0{\cdot}3_{3}398993$	−0·00162990	$0{\cdot}0_{5}810138$	$-0{\cdot}0_{4}669442$		
$t_{23}t_{8}$		−0·00916233	$-0{\cdot}0_{3}361077$	0·00124098	0·00589803	$-0{\cdot}0_{3}892665$	$0{\cdot}0_{3}301936$		
$2t_{33}t_{28}$		0	0	0·00179885	$-0{\cdot}0_{2}160279$	$0{\cdot}0_{3}205028$	0·00157264		
$3t_{32}t_{29}$		0	0·0123310	−0·0162826	0·0314054	0·00920866	−0·00191798		
$-2t_{37}t_{27}$		0	0	−0·00200297	$-0{\cdot}0_{3}457723$	$-0{\cdot}0_{5}1551$	−0·00255743		
$-\ t_{36}t_{28}$		0	0·00989334	−0·00304330	−0·00760701	$-0{\cdot}0_{3}449090$	−0·00605381		
Σ	t_{42}	0·0322413	0·0745813	−0·0662198	−0·0669200	0·00955236	0·00364158	−1·2694	b_4
$t_{29}t_{17}$		−0·320039	0·266392	−0·215885	0·994295	−0·674712	0·0714821		
$t_{24}t_{8}$		0	0·00119675	−0·0104170	−0·0257904	0·0207598	0·0140542		
$3t_{33}t_{29}$		0	0	0·0199878	0·0397101	−0·179877	0·0366189		
$-t_{37}t_{28}$		0	0	−0·0205702	0·0100921	0·00247976	−0·0558512		
Σ	t_{43}	−0·320039	0·267589	−0·226883	1·018306	−0·831349	0·0663041	−2·5221	b_5

Table 2

	$j\rightarrow$		1	2	3	4	5	6	$f'\Sigma\{_1$	
c_0G_2	$t_{11}-\frac{1}{2}t_{10}$	t_{44}	0·00124475	$0{\cdot}0_{3}910301$	0·00174211	0·00113838	$0{\cdot}0_{5}1682$	$0{\cdot}0_{3}261101$		
	$t_{14}-t_{13}$	t_{45}	−0·0546684	0·0427668	0·0717100	−0·0577451	−0·00180735	0·0122767		
	$t_{21}t_{44}$	t_{46}	$0{\cdot}0_{7}182155$	$0{\cdot}0_{7}177898$	$-0{\cdot}0_{7}460110$	$-0{\cdot}0_{8}941376$	$0{\cdot}0_{15}200$	$0{\cdot}0_{9}53880$		
	$t_{22}t_{44}$		$-0{\cdot}0_{5}132071$	$0{\cdot}0_{6}820656$	$-0{\cdot}0_{5}171584$	$0{\cdot}0_{5}106604$	$-0{\cdot}0_{11}1844$	$0{\cdot}0_{7}272207$		
	$t_{21}t_{45}$		$-0{\cdot}0_{6}800008$	$0{\cdot}0_{6}833299$	$-0{\cdot}0_{5}189394$	$0{\cdot}0_{6}477520$	$-0{\cdot}0_{12}215$	$0{\cdot}0_{7}253336$		
	Σ	t_{47}	$-0{\cdot}0_{5}212072$	$0{\cdot}0_{5}165395$	$-0{\cdot}0_{5}360978$	$0{\cdot}0_{5}154356$	$-0{\cdot}0_{11}2059$	$0{\cdot}0_{7}525543$		

c_0G_3	$\frac{1}{2}t_{46}t_9$	t_{48}	0	$0\cdot0_{11}321637$	$-0\cdot0_{10}284725$	$-0\cdot0_{11}135937$	$0\cdot0_{22}7961$	$0\cdot0_{13}674093$		
	$i_p'(i_p')^2$	t_{49}	$0\cdot0_4293881$	$-0\cdot0_4762086$	$-0\cdot0_4320539$	$0\cdot0_4865134$	$0\cdot0_8140142$	$-0\cdot0_4121140$		
	$i_p(i_p^2)$	t_{50}	$0\cdot0_3124067$	$-0\cdot0_4180517$	$-0\cdot0_3124639$	$0\cdot0_4222490$	$0\cdot0_8591667$	$-0\cdot0_5286947$		
	$u_p(t_{49}-t_{50})$	t_{51}	0	$-0\cdot0_5110589$	$0\cdot0_5325716$	$0\cdot0_5109212$	$-0\cdot0_{11}402872$	$-0\cdot0_7146232$		
	$-i_pi_p't_9$	t_{52}	0	$-0\cdot0_6402161$	$-0\cdot0_5196384$	$-0\cdot0_6359254$	$-0\cdot0_{11}161134$	$-0\cdot0_9816618$		
	$(i_p^2)t_{50}$	t_{53}	$0\cdot0_6308623$	$-0\cdot0_7124222$	$-0\cdot0_6310997$	$0\cdot0_7176002$	$0\cdot0_{13}193552$	$-0\cdot0_9579432$		
	$(i_p')^2t_{49}$	t_{54}	$0\cdot0_7279868$	$-0\cdot0_6136985$	$-0\cdot0_7323446$	$0\cdot0_6169228$	$0\cdot0_{14}175500$	$-0\cdot0_8638969$		
	$(t_{53}-t_{54})/t_2$	t_{55}	$0\cdot0_4147581$	$0\cdot0_5770596$	$0\cdot0_4153224$	$0\cdot0_5941672$	$0\cdot0_{10}255231$	$0\cdot0_6663549$		
	$\frac{1}{8}(t_{51}+t_{52}+t_{55})$	t_{56}	$0\cdot0_5184476$	$0\cdot0_6774739$	$0\cdot0_5207698$	$0\cdot0_5126870$	$0\cdot0_{11}248539$	$0\cdot0_7810136$		
	$t_{21}t_{56}+t_{48}$	t_{57}	$0\cdot0_{10}269959$	$0\cdot0_{10}183119$	$-0\cdot0_{10}833274$	$-0\cdot0_{10}118509$	$0\cdot0_{21}3751$	$0\cdot0_{12}167850$		
δ	$t_{22}t_{30}$	t_{59}	0	$0\cdot0_7131536$	$-0\cdot0_7336041$	$0\cdot0_8721766$	$0\cdot0_{12}6159$	$-0\cdot0_{10}58575$		
	$t_{46}+t_{58}+t_{59}$	t_{60}	$0\cdot0_7182155$	$0\cdot0_7480944$	$-0\cdot0_7675546$	$-0\cdot0_7104879$	$0\cdot0_{12}6411$	$0\cdot0_991459$	$-0\cdot0_510463$	2nd ord.
	θt_{60}	t_{61}	$-0\cdot0_6365221$	$0\cdot0_5109994$	$-0\cdot0_5124424$	$0\cdot0_6335015$	$-0\cdot0_94372$	$0\cdot0_723112$		
	$\Sigma_1^{j-1}t_{60}$	t_{62}	0	$0\cdot0_7182155$	$0\cdot0_7663099$	$-0\cdot0_612447$	$-0\cdot0_7117326$	$-0\cdot0_7117319$		
	$\Sigma_1^{j-1}t_{61}$	t_{63}	0	$-0\cdot0_6365221$	$0\cdot0_6734714$	$-0\cdot0_6509529$	$-0\cdot0_6174514$	$-0\cdot0_6174951$		
	$(t_{34})^2$	t_{64}	0	$0\cdot0_786089$	$0\cdot0_723169$	$0\cdot0_6111714$	$0\cdot0_849118$	$0\cdot0_849231$		
	$-t_{30}t_{34}$	t_{65}	0	$0\cdot0_842937$	$-0\cdot0_851933$	$0\cdot0_825761$	$-0\cdot0_{10}39385$	$-0\cdot0_{10}39421$		
	$(t_{30})^2$	t_{66}	0	$0\cdot0_921415$	$0\cdot0_811641$	$0\cdot0_{10}59405$	$0\cdot0_{12}3158$	$0\cdot0_{12}3157$		
	$-3t_{21}t_{63}$		0	$0\cdot0_{10}21349$	$0\cdot0_{10}58214$	$-0\cdot0_{10}12641$	$0\cdot0_{16}60$	$0\cdot0_{11}10831$		
	$t_{22}t_{62}$		0	$0\cdot0_{10}163729$	$-0\cdot0_{10}653101$	$-0\cdot0_{11}11656$	$0\cdot0_{13}1286$	$-0\cdot0_{11}12231$		
	$3t_{21}t_{64}$		0	$0\cdot0_{11}50322$	$-0\cdot0_{11}18357$	$-0\cdot0_{11}27714$	$0\cdot0_{17}18$	$0\cdot0_{13}30477$		
	$2t_{22}t_{65}$		0	$0\cdot0_{11}77188$	$0\cdot0_{10}102298$	$0\cdot0_{11}48248$	$0\cdot0_{16}86$	$-0\cdot0_{14}8220$		
	$t_{23}t_{66}$		0	$0\cdot0_{11}19388$	$-0\cdot0_{11}73416$	$-0\cdot0_{11}147807$	$0\cdot0_{15}226$	$-0\cdot0_{15}4937$		
	$-5t_{46}t_{34}$		0	$0\cdot0_{10}26098$	$0\cdot0_{10}35018$	$-0\cdot0_{10}15732$	$0\cdot0_{19}70$	$0\cdot0_{12}18902$		
	$t_{47}t_{30}$		0	$0\cdot0_{10}24204$	$-0\cdot0_9123161$	$0\cdot0_{10}11897$	$0\cdot0_{17}11$	$-0\cdot0_{13}2950$		
	t_{57}		$0\cdot0_{10}269959$	$0\cdot0_{10}18312$	$-0\cdot0_{10}833274$	$-0\cdot0_{10}118509$	$0\cdot0_{21}3751$	$0\cdot0_{12}167850$		
	Σ	t_{67}	$0\cdot0_{10}269959$	$0\cdot0_9121026$	$-0\cdot0_9177514$	$-0\cdot0_{10}28917$	$0\cdot0_{13}1324$	$0\cdot0_{12}20920$	$-0\cdot0_856284$	3rd ord.

reduced to six significant figures (the original calculations were generally carried out to seven). In the case of a corrected system it is important that the number of significant figures carried should exceed by at least two the number of significant figures desired in the final result. Since no trigonometrical tables are required, this creates no practical difficulty. It may, however, be convenient at times to "modify" the dimensions of the system by dividing all the given radii and distances by the focal length (or a similar convenient quantity). This avoids the continual occurrence of a great number of noughts after the decimal point.

Altogether it will be seen that the computations can be rapidly carried out if a high-speed calculating machine is available. For each surface there are 113 entries consisting entirely of simple additions and multiplications. Many of these can be further speeded up by observing that some of the coefficients repeatedly appear multiplied by various other coefficients. Thus it will be seen that in the last part of table 1, t_{28}, for instance, appears 11 times, i.e. multiplied by t_{11}, t_{14}, t_{17}, t_{34}, t_{35}, t_{36}, t_{37}, $2t_{30}$, $2t_{31}$, $2t_{32}$, $2t_{33}$ respectively.

The *first-order contributions* by the different surfaces appear in the rows t_{21}, t_{27}, t_{28}, t_{29}; whilst the *second-order contributions* appear in the rows $t_{38}, \ldots, t_{43}$ (disregarding the factor f' by which they should be multiplied to give the actual contributions as defined). Hence the final result is

$$\begin{aligned} v' = {} & +0{\cdot}0_3145259y^3 - 0{\cdot}0_252286y^2u + 0{\cdot}18468yu^2 - 3{\cdot}4308u^3 \\ & - 0{\cdot}0_5103856y^5 - 0{\cdot}0_470536y^4u + 0{\cdot}0_393953y^3u^2 \\ & + 0{\cdot}061374y^2u^3 - 1{\cdot}2694yu^4 - 2{\cdot}5221u^5. \qquad \ldots\ldots(15.2) \end{aligned}$$

(*c*) *Table* 2

This gives the additional computations required to determine the secondary and tertiary spherical aberrations, measured by $(l'_{pf} - L_f')\sin U_f'$ (see (11.4)). There are only 33 entries per surface; t_{60} and t_{67} are the contributions by the individual surfaces to the secondary and tertiary aberrations respectively (except again for the factor f'). The final result is

$$\text{Sph. ab.} = +0{\cdot}0_314526y^3 - 0{\cdot}0_510463y^5 - 0{\cdot}0_856284y^7. \qquad \ldots\ldots(15.3)$$

Since
$$\delta u_f' = \left(\sum_1^f t_{21}\right)y^3 + \left(\sum_1^f t_{60}\right)y^5,$$

and
$$-\delta y_f' = \left(\sum_1^f t_{68}\right)y^3 + \left(\sum_1^f t_{61}\right)y^5,$$

we can determine $\sin U_f'$ at once, by (5.9), correct to the second order. Hence the spherical aberration measured by $(v')_{u=0}$ may be calculated. Thus

$$\sec U_f' = 1 + 0{\cdot}0_453439y^2 + 0{\cdot}0_720476y^4.$$

$$\therefore \quad \text{Sph. ab.} = +0{\cdot}0_314526y^3 - 0{\cdot}0_510386y^5 - 0{\cdot}0_856813y^7. \qquad \ldots\ldots(15.4)$$

The difference between the results (15.3) and (15.4) is negligible in practice, as will generally be the case.

(*d*) *Figures* 1–5

These are drawn, as explained in §11, on the basis of (15.2) and (15.4), i.e. v' is plotted against y for fixed values of u. (The units correspond to $f' = 96{\cdot}729$; i.e. they represent approximately percentages of the focal length.) In this way the

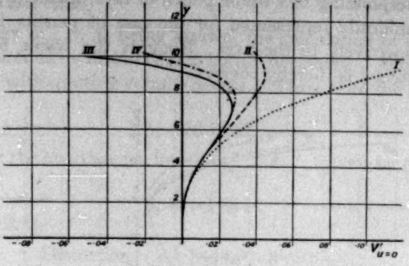

Figure 1. Sph.

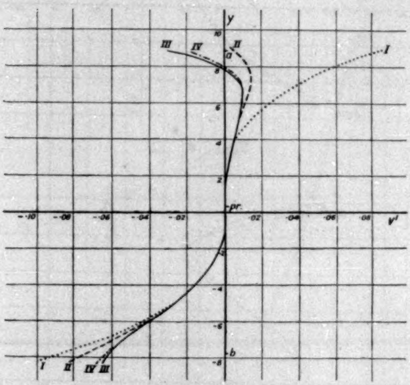

Figure 2. 3°.

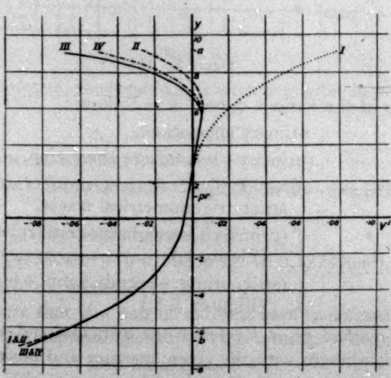

Figure 3. 6°.

values of v' corresponding to a whole pencil of rays, incident parallel at the first surface, are graphically represented for the case of pencils inclined at 0°, 3°, 6°, 12°, 18°, respectively to the axis. Roughly the whole field for which the objective is designed is thereby covered.

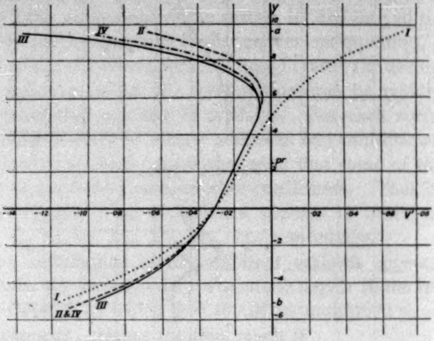

Figure 4. 12°.

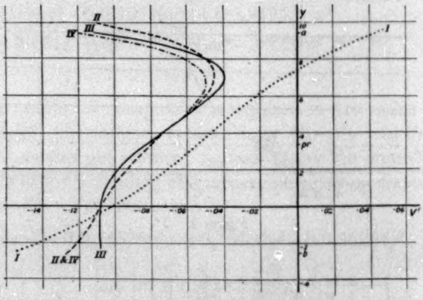

Figure 5. 18°.

The meaning of the various curves is as follows:

Curve I, ·········, primary aberration.
Curve II, – – – – – –, (primary + secondary) aberration.
Curve III, ————, curve obtained from a number of strict trigonometrical traces.
(Figures 1–5.)

Curve IV, – · – · – · –, (primary + secondary + tertiary) sph. abn. (Figure 1.)
(strict primy. + secndy.) abn. + terty. sph. abn. (Figures 2–5.)

The values of y marked *pr*, *a*, *b* refer to the principal and extreme rays corresponding to the diaphragm with the given aperture and position. (As has been pointed out, these are not involved in the calculation of v'.)

(*e*) ***Distortion and coma***

The coefficients $a_0, \ldots, b_5$ being known, the calculation of distortion, coma, etc., is so simple that its inclusion here is hardly necessary. Accordingly we shall content ourselves with quoting certain results. Thus, with the given diaphragm position,

$$p_1 = 10{\cdot}9523. \qquad \ldots\ldots(15.5)$$

Putting $y = p_1 u$ in the expressions for $-\delta y_4'$, $+\delta u_4'$, (given by $(t_{30})_5, \ldots, (t_{37})_5$), we have

$$p_3 = +2{\cdot}6444. \qquad \ldots\ldots(15.6)$$

Substituting in (12.1),

$$\text{Distortion} = -1{\cdot}8444u^3 - 8{\cdot}6839u^5. \qquad \ldots\ldots(15.7)$$

Notice the large value of the secondary term.

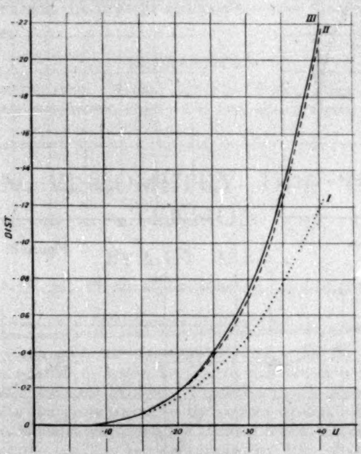

Figure 6.

As has been mentioned, the term in p_3 is often negligible in practice. Actually in this case

$$p_3 A_1 u^5 = +0{\cdot}3237u^5. \qquad \ldots\ldots(15.8)$$

For the coma we obtain, by (13.9),

$$C' = -0{\cdot}0_3 45580uw^2 + (0{\cdot}027238u^3w^2 - 0{\cdot}0_3 12949uw^4). \qquad \ldots\ldots(15.9)$$

(If the terms in p_3, t_0, t_1 be neglected, we find

$$C' = -0{\cdot}0_3 45580uw^2 + (0{\cdot}028985u^3w^2 - 0{\cdot}0_3 12741uw^4), \qquad \ldots\ldots(15.10)$$

which, again, is nearly the same as (15.9).)

We may note here that if a pair of extreme rays is defined by a particular value of w, then the corresponding effective stop-number of the system is given by

$$\text{stop-number} = 48{\cdot}4/w. \qquad \ldots\ldots(15.11)$$

(*f*) *Figure* 6. This is a graphical representation of (15.7).

(*g*) *Figures* 7–10

In these, by means of (15.9), coma is plotted against w for various fixed values of u. (The meaning of curves I, II and III is in each case as explained in § 15 (d)).

It will be seen that from a practical point of view the primary coma gives no useful information about the residual coma in the image, whilst the inclusion of the secondary coma gives a very fair representation of the actual state of affairs. In fact, the curves strongly suggest that, in the process of correction, virtual elimination of primary coma was aimed at by the designer, leaving, however, large secondary coma. Thus for fixed u (at any rate up to $U_1 = 12°$), the coma is virtually given by a single term proportional to the *fourth power* of the aperture of the pencil, whereas the primary term alone would predict a residual coma proportional to the *square* of the aperture.

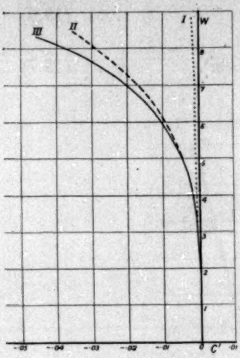

Figure 7. 3°.

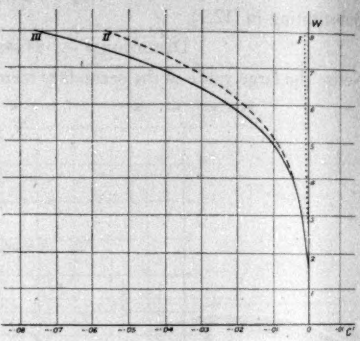

Figure 8. 6°.

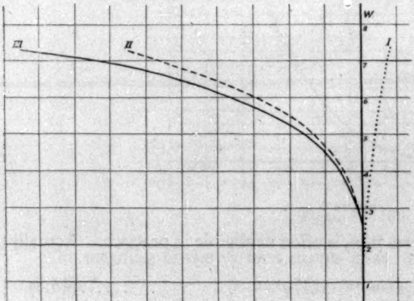

Figure 9. 12°.

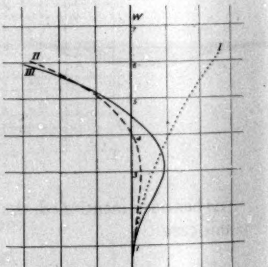

Figure 10. 18°.

If a direct measure of the contribution to the coma by any individual surface is required, this may be obtained from table 1 by means of a formula analogous to (13.9) or (13.10), with the *a*s replaced by t_{21}, t_{27}, t_{28}, t_{29} and the *b*s replaced by $t_{38}, \ldots, t_{43}$, respectively.

§ 16. CONCLUSION

It has been shown how, by means of relatively short and straightforward computations, the tangential aberrations of higher order than the first can be obtained for a given system. In principle, the properties of the system are completely characterized for arbitrary positions of the object and the plane of reference (and of the diaphragm) by two expressions D_p^* and D_q^*, or one such expression D^* if the object and plane of reference have fixed positions. For the calculations of D_p^* and D_q^* it is convenient, though not essential, to make use of two expressions D_p and D_q, similarly defined, the latter being needed correct only to the order next lower than that to which the D_p^* and D_q^* are required. All four expressions are sums of certain expressions, of which one is contributed by each surface of the system, and all of them vanish identically in the paraxial region.

It is hoped to extend the present analysis to cover the case of arbitrary skew rays at a later date.

REFERENCES

Conrady, 1929. *Applied Optics and Optical Design.*
Hardy and Perrin, 1932. *The Principles of Optics.*

ERRORS IN VISCOMETRY DUE TO SURFACE TENSION

By GUY BARR,
National Physical Laboratory, Teddington

MS. received 17 *April* 1946

ABSTRACT. In viscometers of the Ostwald type used for the determination of kinematic viscosities relative to water, surface tension causes a reduction of the head available and increases the time of flow. The correction is greater for water than for organic liquids, but is not proportional to the surface tension. Earlier estimates of the correction are shown to be suspect, and the classical tables of Bashforth and Adams are applied to show how the capillary rise in a measuring bulb of specified size (3·85 ml.) and form varies during the discharge. The calculated corrections for two liquids with surface tensions differing rather more than those of water and benzol diverge by 0·5% when a mean head of 10 cm. is assumed, and a simple experiment demonstrates that this estimate is probably low owing to effects of drainage on the shape of the meniscus. Two methods are proposed for eliminating the correction during the calibration of viscometers.

§ 1. INTRODUCTION

The possibility that errors in measurement of relative viscosity may occur when liquids of different surface tension are tested in instruments of Ostwald (or similar) type has frequently been discussed (Barr, 1931) and much more frequently overlooked. The calculation of the necessary correction for viscometers having bulbs of a given shape and size should be feasible when the surface tension is known, but several attempts have been based on inadequate theory. Since the blown bulbs of a U-tube instrument are not likely to be geometrically perfect, the method used by Bénard (1907), in which the effect of surface tension is measured at successive levels of the liquid in the bulb, would be more suitable for general use; this method is not, however, readily applicable with great accuracy to a completed viscometer, and could hardly be used with oils and opaque liquids that wet glass.

The desirability of either avoiding or correcting for the effects of surface tension has increased in recent years with the demand for higher precision in the measurement of kinematic viscosity, especially of oils. As absolute determinations have been considered impracticable for routine work, there is fairly general agreement that the viscosity of water at 20° c. be adopted as a standard, for which the value 1·007 cs. is provisionally accepted, and that all viscosities be relative to this standard. The writer is in accord with this tendency, but it must be recognized that two disadvantages attach to the selection:—

(*a*) If water gives a flow time of 200 seconds in a viscometer that may be calibrated by its means to $\pm 0{\cdot}1\%$, an oil with a viscosity of only 1000 cs. will require a flow time of over 55 hours. This direct comparison may, of course, be avoided by calibrating a series of viscometers by a step-up procedure, but with three instruments, allowing a maximum time of 2000 seconds for the calibrating liquids of intermediate viscosity, the cumulative errors, for two determinations of the same accuracy in each tube, will amount to $\pm\sqrt{6\times(0{\cdot}1)^2} = \pm 0{\cdot}24\%$.

(*b*) Water has an exceptionally high surface tension (72·7 dynes/cm. at 20°), while the value for most mineral oils is about 30 dynes/cm. If the surface-tension correction with water in a viscometer amounts to only $0{\cdot}5\%$ and the correction is proportional to surface tension, the error in a comparison between water and oil will be some $0{\cdot}3\%$; actually it will be shown later that the correction falls more rapidly, so that the error will be greater.

§ 2. RECENT CALCULATIONS OF AN APPROXIMATE CORRECTION FOR SURFACE TENSION

Mention may be made of three attempts later than those cited by Barr (1931) to obtain an estimate of the magnitude of the effect of surface tension on the hydrostatic head in a viscometer. In the first (Barr, 1933) the "capillary" rises, h_σ, at various levels in a bulb of the shape specified for B.S. viscometers were deduced from a table due to Sugden (1921) and were subtracted from the hydrostatic head h operating during the outflow of successive elements of volume δV. Summation of $\delta V/h$ and of $\delta V/(h-h_\sigma)$ over the whole discharge gave quantities proportional to the total time of efflux without and with correction for surface tension (σ). For bulbs of 1 ml. and 4·7 ml. capacity the corrections were calculated as $2{\cdot}1\%$ and $0{\cdot}8\%$ respectively, for water fillings. This calculation is invalidated by the omission of any attempt to allow for the effect of the slope of the walls of the 45° cones on the capillary rise.

In a long paper dealing with the use of his "suspended level" in viscometry, Ubbelohde (1936) analysed the effect of surface tension in a spherical bulb on the assumption that, when the radius at the line of contact of the meniscus with the wall is r, the capillary rise is simply $2\sigma\cos\theta/(r\rho g)$, where θ is the deviation of the wall from the vertical, g is the acceleration due to gravity, and ρ is the density of the liquid (more strictly ρ is the density of the liquid minus that of air). For the whole bulb he thus finds that the operative head is reduced by $2\sigma/(R\rho g)$, where

R is the radius of the bulb. Relying on this value, he deduces a radius for a hemispherical "suspended level" at the lower end of the capillary such that the correction should be eliminated. The calculation ignores the variations in shape of the meniscus during its passage down the bulb. The experimental comparisons of viscosities of benzol and water, determined (i) by applying the indicated correction to results obtained with a plane "suspended level", and (ii) by using the hemispherical level, differ by 0·7% (or by nearly 2% if kinetic-energy corrections are similar in the two series).

Jones and Fornwalt (1938) used a method of summation similar to that indicated by Barr (1933) for the effect of surface tension in two viscometers: one (T) with a cylindrical length of 3·8 cm., radius 0·90 cm., and conical ends, and one (F) with a cylindrical length of 5·6 cm., radius 0·85 cm., and hemispherical ends: the discharge in the first case was into a lower reservoir of radius 3·6 cm., and in the latter into one with a radius equal to that of the bulb. They assumed again that capillary rises are inversely proportional to radius, but they allowed for variations of slope of the wall by postulating that the rise was also proportional to $(1-\sin\theta)/\cos\theta$; no explanation of this postulate is given. Since their calculations indicated corrections of 0·44% and of 0·02% for comparisons of the viscosity of water and methanol in instruments T and F, respectively, and experiment gave a difference of 0·4% in the relative times of flow, they concluded that the correction was practically eliminated by the substitution of hemispherical for conical ends in the measuring bulb and the provision of a recipient bulb of the same diameter.

§ 3. APPLICATION OF THE TABLES OF BASHFORTH AND ADAMS

Gross errors may be inherent in any estimation of the effect of surface tension on viscometry when it is assumed that the capillary rise is proportional to surface tension and inversely proportional to density and to radius. Thus for water ($\sigma=72{\cdot}7$ dynes/cm., $\rho=0{\cdot}9970$ gm./ml.) and benzol ($\sigma=28{\cdot}9$ dynes/cm., $\rho=0{\cdot}8774$ gm./ml.) at 20° c. the capillary rises in tubes of three different radii r cm. may be obtained from Sugden's tables as—

	$r=0{\cdot}2$	$r=0{\cdot}4$	$r=0{\cdot}8$	$r=1{\cdot}6$
Water	0·683 cm.	0·273 cm.	0·067 cm.	0·0046 cm.
Benzol	0·280 cm.	0·090 cm.	0·010 cm.	0·0002 cm.
Ratio B/W	0·41	0·33	0·15	0·04

The last row gives the ratio of the rises for benzol and water in the same tube; the ratio of the values of σ/ρ is 0·45. Now Sugden's tables were based mainly on the much more comprehensive work of Bashforth and Adams (1883), who showed how the form of the meniscus dividing a liquid from air could be calculated in detail. The contour of a meniscus is defined by the value of a parameter $\beta=b^2\rho g/\sigma$, where b is the radius of curvature at the vertex (O in figure 1); tables (No. II) are given for values of β up to 100, showing the ratio x/b and z/b all round a sessile drop, x being the radius at a vertical distance z from the vertex. If σ and ρ are known, each value of β fixes a value for b and hence a series of values for x and z.

The points of which the co-ordinates x and z are thus listed are at intervals of 5°, from 0° to 180°, of the angle ϕ between the vertical through the axis of revolution of the drop or meniscus and the normal to the surface. Sugden's table refers to the special case $\phi=90°$, which applies to the meniscus of a liquid in a vertical cylinder—when, as is assumed throughout this paper, the contact angle is zero—but the complete work of Bashforth and Adams allows the capillary rise to be found for any small vessel of which the internal surface constitutes a surface of revolution. The simplest form of bulb for calculation is the biconical, but the form specified for B.S. viscometers, viz., a cylinder with conical ends, may be treated by finding the shape of the meniscus at successively lower levels in the bulb when the angle ϕ is first 135° (for the upper cone), then 90° (for the cylindrical part) and finally 45° (for the lower cone). For the small elements of volume enclosed between the fiducial marks on the tubing above and below the bulb, the angle ϕ is 90°, and the capillary rise may be found by either method. A constant a is defined by the relation $a^2=2\sigma/(\rho g)$, where ρ is again strictly the difference in density between the fluids on the inner and outer sides of the meniscus, i.e., in our case, the "apparent" density of the liquid in the viscometer. The capillary rise h_σ is given by $h_\sigma=a^2/b$; Sugden's table gives r/b for various values of r/a, where r is the radius of a vertical tube containing the liquid, while we shall use the x of Bashforth and Adams' tables to refer to the radius of the circle of contact between the meniscus and the bulb.

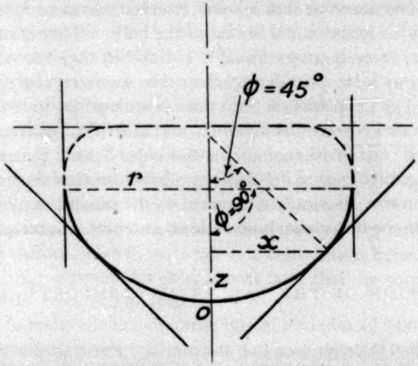

Figure 1. Diagram to illustrate definitions of x, z, r and ϕ. The contour is that of Bashforth and Adams' smallest drop (of mercury resting on the horizontal plane, shown dotted); it has been inverted so that the part below $\phi=90°$ represents the meniscus of a liquid wetting the wall of a vertical cylinder and touching a cone, of 45° semi-vertical angle, below it.

Method of calculation for a specified bulb

The surface-tension correction has been calculated for a bulb consisting of a cylindrical portion with a length equal to its radius, 0·896 cm., connected above and below by 45° (semi-vertical angle) cones to cylindrical tubing of radius

0·21 cm., with timing marks 0·42 cm. beyond the junctions of the tubing with the cones. The form of the bulb is nearly the same as that which was shown by Barr (1933) to give the minimum ratio of wall surface to volume for a cylinder with conical ends; the length of the cylinder is assumed equal to the radius (instead of to 0·8 of the radius) since in practice it is convenient to lengthen it even more. The actual radii result from arbitrary selection of certain round values of β (1 and 100) as minimum and maximum and of a value $a^2=0{\cdot}16$ cm^2 corresponding with a surface tension somewhat higher than that of water (for which $a^2=0{\cdot}149$ cm^2 at 20° c.). The total volume of the bulb was then subdivided by finding the volumes discharged when β assumed the values $\beta=1, 4, 10, 40$ and 100 as the meniscus fell in the upper cone; while the cylindrical part was discharging, β remained constant at 100 and in the lower cone it fell again, to $\beta=1{\cdot}5$, before the junction with the tubing below. In the upper cone, particularly, the lowest point of the meniscus is so much below the circle of contact that a considerable addition must be made to the volume delivered from the frustrum above the plane of this circle; Bashforth and Adams provide a table (No. III) which gives the value of this addition, in terms of b, for all values of β and of ϕ. For each element of volume discharged, ΔV, the capillary rise h_σ was assumed to be the mean between those characterized by the values of β at the beginning and end of the discharge of that element. The product $\Delta V \, . \, h_\sigma$ was finally summed for the whole bulb volume V and divided by V to give a mean h_σ. Assuming that the recipient bulb has the same diameter as the measuring bulb, the capillary rise in this arm will have the same value as that already calculated for the cylindrical part of the measuring bulb; the excess of h_σ over this value represents the correction to be applied to the mean head causing the flow. The method of calculation may be illustrated by detailing the procedure for the first two elements of volume considered:—

(*a*) The tubing above the upper cone has radius 0·21 cm. and the graduation is 0·42 cm. above the junction, assumed sharp. The meniscus starts with its lowest part in the plane of the graduation (see figure 2, position I) and its shape will remain unchanged until the circle of contact reaches the joint (position II). With $a=0{\cdot}40$ cm. we have $r/a=0{\cdot}525$, whence from Sugden's table $r/b=0{\cdot}9165$ and $b=0{\cdot}229$. The capillary rise in the tube is, therefore, $h_\sigma=a^2/b=0{\cdot}698$ cm. We require to know the distance of the vertex of the meniscus below the plane of the joint and also, for later use, the "bubble" volume v bounded by this plane and the surface of the meniscus. We find first the value of $\beta=2b^2/a^2=0{\cdot}655$. Interpolation in Bashforth and Adams' table II for $\beta=0{\cdot}655$ and $\phi=90°$ gives $x/b=0{\cdot}917$, $z/b=0{\cdot}825$, whence $x=0{\cdot}210$ and $z=0{\cdot}189$ cm. The volume ΔV discharged while h_σ remains at 0·698 cm. is, therefore, $\pi(0{\cdot}21)^2(0{\cdot}42+0{\cdot}19)=0{\cdot}082$ ml. Hence $\Delta V \, . \, h_\sigma=0{\cdot}0590$. Bashforth and Adams' table III gives the volume of the "bubble" as $1{\cdot}47b^3=0{\cdot}0176$ ml.

(*b*) We pass next to the position where $\beta=1$; here $b^2=\frac{1}{2}a^2\beta=0{\cdot}08$ and $b=0{\cdot}282$, whence $h_\sigma=a^2/b=0{\cdot}568$ cm. For $\phi=135°$ the tables give $r/b=0{\cdot}7369$ and $v=2{\cdot}091b^3$, whence $r=0{\cdot}21$ cm. and $v=0{\cdot}0473$ ml. The meniscus has, therefore, become tangential to the cone at the junction with the tubing above it (position III) and the volume run out since the meniscus touched the joint at 90° is $0{\cdot}0473-0{\cdot}0176=0{\cdot}0297$ ml. This volume is considered to have been discharged while the mean capillary rise was $\frac{1}{2}(0{\cdot}698+0{\cdot}568)=0{\cdot}633$ cm.

The radius of the cylindrical part of the bulb was fixed at 0·896 cm. because this value of r results from the figure given by the table for $\beta=100$ at $\phi=90°$; the meniscus touches the upper cone at the same time, when $r=0{\cdot}846$ cm. for $\phi=135°$ (position VII). In this position the lowest point of the meniscus is 0·410 cm. below the circle of contact with the cylindrical wall and 0·536 cm. below the circle of contact with the cone; a surprisingly large fraction of the total content of the bulb is, therefore, discharged before the minimum capillary rise occurs. This minimum persists until the meniscus touches the lower cone (cf. figure 1), after which there is a relatively rapid increase. The variations in capillary rise during discharge are plotted in figure 3 (upper curve).

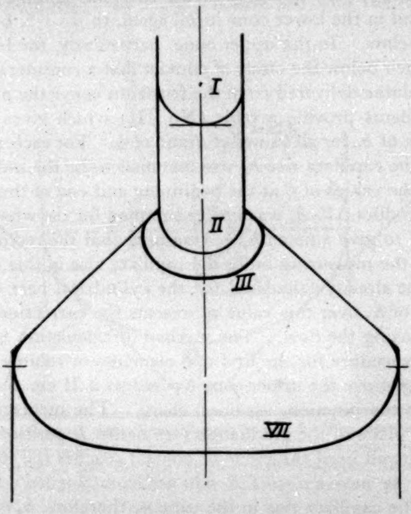

Figure 2. Positions of the meniscus at four stages of the flow from a bulb shaped as in figure 3—not to scale.

The total volume of the bulb between the timing marks, 3·85 ml., was subdivided into 13 elements in all. The sum $\Sigma(\Delta V . h_\sigma)$ divided by 3·85 gave $h_\sigma=0{\cdot}1241$ cm. If the discharge is supposed to be into a recipient cylinder of radius 0·896 cm., in which the capillary rise is 0·0566 cm., the mean amount by which the driving head is reduced is $0{\cdot}1241-0{\cdot}0566=0{\cdot}0675$ cm. Assuming that the average hydrostatic head is 10 cm., the surface-tension correction will therefore amount to some 0·7% when the liquid tested has the surface-tension postulated.

As Bashforth and Adams' tables do not extend beyond $\beta=100$ it is not possible to complete a precise calculation by the above method for a liquid of lower surface tension in the postulated bulb. The positions of seven points on the lower curve of figure 3 were, however, calculated for a liquid for which $a^2=0{\cdot}0625$ (the value of a^2 for benzol at 20° c. is 0·0671). These points refer to positions of the meniscus in the upper and lower cones. The capillary rise in the cylindrical part of the bulb was found from Sugden's table, and the extremities of the horizontal straight line were displaced in the direction of the h_σ axis by an amount arbitrarily estimated to allow for the flattening of the meniscus; the curve was then completed by the dotted portions. Measurements, with a planimeter, of the area between this curve and the ordinate $h_\sigma = 0{\cdot}0057$ and of that between the curve for $a^2 = 0{\cdot}16$ and the ordinate $h_\sigma = 0{\cdot}0566$ gave a ratio 0·29 : 1. The surface-tension correction when $a^2 = 0{\cdot}0625$ and the hydrostatic head is 10 cm. is, therefore, estimated as $0{\cdot}29 \times 0{\cdot}68\% = 0{\cdot}20\%$. The correction falls more rapidly than does a^2, for which the ratio is $0{\cdot}0625/0{\cdot}16 = 0{\cdot}39$.

The correction for water in a larger bulb of the same shape is also not directly obtainable by the use of the tables. For a smaller bulb, of volume 2·3 ml. and maximum radius 0·75 cm., with a recipient of the same radius, the correction is found to be 0·88% (instead of 0·68%) for a hydrostatic head of 10 cm. when $a^2 = 0{\cdot}16$.

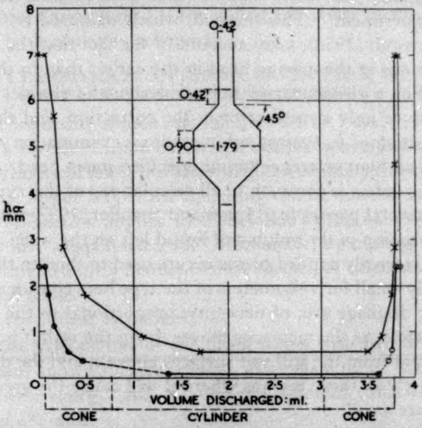

Figure 3. Calculation of surface-tension correction for viscometer bulb of volume: 3·85 ml.

Examination of the curves illustrates the correctness of the common assumption that an increase in the volume or in the maximum diameter of the bulb tends to decrease the effect of surface tension. They show, however, that an increase in the diameter of the tubing above and below the bulb will produce only minor improvement, the main portion of the effect being due to conditions in the upper cone. If adequate drainage occurs with a cone of greater semi-vertical angle than 45°, it might be preferable to adopt an angle of 60°, say, for the upper cone, so that the meniscus more rapidly reached its maximum diameter. Observation shows that some improvement in the drainage from the lower cone is desirable, and the curves suggest that the capillary effect is here so small that a steeper slope, say a 30° cone, might be adopted without undue increase in the surface-tension correction. Such a change would require that the maximum diameter be increased and the parallel portion practically eliminated so as to prevent inconvenient increase in the overall length. A 60° cone and a 30° cone, base to base, would need to have a maximum radius 29% greater than that of the form assumed in the above calculations, in order to have the same content, and would have almost exactly the same length.

§4. CRITICISM OF THE METHOD

A stricter method of calculating the correction for surface tension requires that the height of the measuring bulb above the recipient be known, so that for each element of volume, ΔV, discharged, a quantity $\Delta V/(h-h_\sigma)$ may be deduced which is proportional to the time required for the discharge of that volume. The sum $\Sigma\Delta V/(h-h_\sigma)$ for the whole bulb is then proportional to the flow time observed in an experiment. This method, which was used by Barr (1933) and by Jones and Fornwalt (1938), takes account of the fact that the flow time is less sensitive to variations in the driving head in the earlier than in the later stages of the discharge. For a viscometer of normal design the simpler procedure now adopted will produce only a small error in the correction, and the summation of $\Delta V.h_\sigma$ or the plotting of h_σ against volume allows examination of the behaviour of different bulbs without reference to one specified mean head.

A more serious defect is common to all calculations of this type. It has been demonstrated in several papers (e.g. Jones and Stauffer, 1937) that the "drainage error", due to variation in the volume of liquid left on the walls of the bulb, may be serious when externally applied pressures are used to shorten the flow time, but becomes negligibly small for viscometers of the type here considered, in which the times allowed for drainage are, of necessity, proportional to the viscosity of the liquid. Nevertheless, as the meniscus moves down the wall it must be distorted by the flow of liquid from the still wet surfaces above it and the distortion will be most severe precisely in those regions where it will cause the greatest effect, viz., where diameters are small.

§5. EXPERIMENT TO ILLUSTRATE THE EFFECT OF SURFACE TENSION

A simple experiment has been made to demonstrate the necessity for a surface-tension correction in the use of a No. 0 B.S. viscometer. After determining the time of flow (1348 sec.) for water at 25° c. in the usual manner, the water was blown up until the level was about 1 cm. above the upper timing mark and a volume of 0·02 ml. of a solution of "Wettol" (a wetting agent for photographic use supplied by Messrs. Ilford), of density 1·1010 at 25° c., was added at the surface. Flow was then allowed to proceed and the time observed was 1334 sec., approximataly 1% less than that for water alone. During the flow the Wettol tended to remain at the air-water interface, and probably none of it reached the capillary during the timed interval. When equilibrium had been reached, the contamination of the water surface was shown by the greatly reduced rise of the meniscus in the capillary above the level of the water in the other arm; the exact rise observed, 2·5 cm., is not significant as the extent of dilution is unknown, but pure water gave a rise of about 7·5 cm. (when the levels in the U-tube were lowered to allow the full rise to occur).

The capillary rise for water in the 2-cm. diameter recipient bulb of a No. 0 viscometer is calculated from Sugden's table as 0·034 cm., and would have been reduced to less than 0·002 cm. if Wettol had been added to this surface also. The surface-tension correction with pure water is thus some 0·7% greater than with a liquid having about 1/3 the surface tension of water.

The correction calculated for water in a bulb of only 3·85 ml. capacity was less than 0·7%; for the 6·5 ml. bulb of a No. 0 viscometer it would be appreciably less, and it cannot have been completely eliminated by the addition of Wettol. Hence some factor, such as the distortion—suggested above—of the meniscus by liquid draining from the wall, must have been operative to produce the observed difference of flow times. An attempt is often made, especially in viscometers, such as that of Bingham, which are operated by external pressure, to eliminate the effect of surface tension by constructing the recipient bulb to be of the same shape and size as the timing bulb; if the falling and rising menisci differ in shape the object cannot be completely achieved.

§6. DETERMINATION OR ELIMINATION OF THE SURFACE-TENSION CORRECTION

From the absence of any simple relation between a^2, r and h_a it will be obvious that the need for a surface-tension correction cannot be avoided by selecting such a diameter for a cylindrical lower bulb as will give a capillary rise equal to the mean capillary rise in the upper bulb: the matching can be correct only for one value of a^2. The same objection applies to Ubbelohde's proposal (1936) to eliminate the correction, in his "suspended-level" viscometer, by causing the lower end of the capillary to expand into a hemispherical surface of calculated radius instead of into a horizontal plane.

Two alternatives appear to remain:—

(1) To calibrate viscometers of the usual forms with two or more liquids of known viscosity and known surface tension, using such times of flow as will avoid errors due to kinetic energy, and to state the different constants occurring for different values of a^2; and

(2) To design viscometers so that the maximum surface-tension correction will be negligibly small.

(1) The former procedure presupposes that the viscosities required can be accurately determined by other means. The dynamic viscosity (poises) may be measured in an instrument of the Bingham type, in which external pressures are used that are 30 or more times the variation in hydrostatic pressure in the viscometer during flow. When all the numerous precautions and corrections are taken (including consideration of the "drainage error" which may be marked in this type) accurate results are obtainable, especially if it is necessary only to make them relative to the viscosity of water. The higher pressures used necessitate smaller diameters for the capillary, to minimize kinetic-energy corrections, than in the Ostwald type, and troubles due to suspended matter in the sample and to obstruction of the capillary are exaggerated. For the calibration of an Ostwald-type instrument a further determination, that of density, is required to convert poises to stokes.

(2) If an instrument for comparison of kinematic viscosities can be produced, such that times of flow are proportional to kinematic viscosity to the precision

required, this viscometer, though possibly inconvenient for routine determinations, might be used to determine the relative viscosities required in method (1). Cannon and Fenske (1936), and more recently Cannon (1944), have described "master" viscometers for this purpose, in which the capillary length and mean head are increased to some 45 cm. on the assumption that errors due to surface tension and to kinetic energy will become negligible. Their estimate of the order of the surface-tension correction (0·7 mm. difference in loss of head as between runs with water and oil) suggests that the error in the master instrument should be some 0·15%. But in their fusiform 3 ml. bulb the effect is probably as much as in the 3·85 ml. bulb, for which calculations on the lines indicated above would show an error of more than 0·2%; and the experiment with Wettol points to this being an underestimate. The error would be less if the large diameter of the recipient bulb (3 cm.) were reduced to equal that of the bulb, as in the form described by Cannon for low viscosities. We propose to try the effect of using heads and capillary lengths up to nearly a metre: the correction should then become progressively less, and this will be tested by the variation in the relative times of flow of water and an organic liquid of lower surface tension as the length is increased.

We have found, however, that it is possible to time with good precision the fall of a meniscus in a uniform tube of 1 cm. diameter on which two fine marks have been etched 5 cm. apart. With the same diameter for the other arm of the U-tube the surface-tension correction should be zero, apart from effects of drainage on the shape of the meniscus. The importance of such effects will obviously be much less than in Cannon's "semi-micro" form, which has a bore of 2·5 mm. for the measuring and receiving tubes. The occurrence or absence of sensible correction should again be demonstrable by increasing the length. Since the ratio of initial to final head is greater in this type of instrument than when wide bulbs of similar capacity are provided, it may be desirable, at least in the shorter models, to make use of two recipient tubes in parallel, of the same diameter as the measuring tube. This arrangement, besides reducing the variation in head by a quarter and halving the effect of errors in loading, can be made to avoid the main error due to maladjustment to the vertical of a U-tube viscometer; if the tubes are equidistant from the vertical capillary they are equivalent, as far as concerns the effect of tilt, to a recipient vertically below the upper bulb, as in Cannon and Fenske's "routine" form.

ACKNOWLEDGMENTS

The work described above has been carried out as part of the research programme of the National Physical Laboratory, and this paper is published by permission of the Director of the Laboratory. The author desires to acknowledge the comments and suggestions he received from Mr. F. A. Gould of the Metrology Division, National Physical Laboratory.

REFERENCES

Barr, 1931. *Viscometry* (Oxford: The University Press), pp. 72, 79, 127.

Barr, 1933. World Petroleum Congress, London.

Bénard, 1907. See paragraph 139, Brillouin, *Leçons sur la viscosité* (Paris: Gauthiers-Villars).

Bashforth and Adams, 1883. *Capillary Action* (Cambridge : The University Press).
Cannon, 1944. *Industr. Engng. Chem.* (*Anal. Edn.*), **16**, 708.
Cannon and Fenske, 1936. *Oil Gas J.*, **34**, 45.
Jones and Fornwalt, 1938. *J. Amer. Chem. Soc.*, **60**, 1683.
Jones and Stauffer, 1937. *J. Amer. Chem. Soc.*, **59**, 1630.
Sugden, 1921. *J. Chem. Soc.*, **119**, 1483.
Ubbelohde, 1936. *Oel u. Kohle*, **42**, 949 ; *J. Inst. Pet. Techn.*, **22**, 33.

SOME THERMODYNAMIC RELATIONS OF RIGID HYGROSCOPIC GELS

By F. L. WARBURTON,
Wool Industries Research Association

MS. received 22 *February* 1946

ABSTRACT. In studying the absorption of liquids by rigid gels, certain thermodynamic relations are required in terms of stress components and generalized co-ordinates. These have been derived using the analytical methods of Gibbs as developed by Guggenheim, and the conditions under which they hold are clearly defined. The analysis includes a new derivation of Kirchhoff's relation for the heat of absorption, in which it is shown to be an exact relation between the isopiestic and isothermal heat of absorption and the isopiestic and isosteric variation of equilibrium humidity with temperature, where the pressures concerned are the external pressures on the gel-liquid phase. The effect of internal stresses existing in a homogeneous gel-liquid phase due to the absorption of the liquid is obtained by assuming that the energy of expansion of the gel is the same for expansion due to absorption as for expansion due to external forces. The effect of external shear stresses on vapour pressure is considered, although it is not required in the case of homogeneous gels, since the analysis is similar to that for the internal energy of expansion, and the effect of such stresses is required when dealing with more complex structures such as wool cells.

§ 1. INTRODUCTION

Barkas' work on wood (1945), and in particular on the effect of natural restraints on the wood-water isotherm, has shown the importance of structural rigidity for the vapour pressure isotherms of gels. Wood is an aggregate of cylindrical cells with rigid sheaths which are partly filled with gel substance, and Barkas has been mainly concerned with the effect of the rigid sheath on the water absorption of the gel substance; the restraints on the gel substance are, in this case, external restraints imposed by the sheath. The restraints need not, however, be external restraints, for any energy of swelling of a gel must be reflected in the free energy of the gel-absorbate system, and the isotherm will therefore depend to some extent on the swelling energy. Cassie (1945) has already attempted to estimate the effect of this swelling energy on the water-vapour isotherm of keratin, but his work has been considerably restricted by lack of adequate elastic data for the gel, and of appropriate relationships between the thermodynamic functions and the elastic parameters.

The purpose of this paper is to establish the necessary relations of the thermodynamic functions and the elastic parameters, using Gibbs' method. The first requirement is a transformation from the load variables of thermodynamics to the stress variables of elasticity, and from this the relations of chemical potential and entropy changes to changes of external stress are readily derived. The problem of the relation of chemical potential to the energy of expansion for internal stresses is, however, best approached through the intrinsic energy term, and this and the heat of expansion are derived in terms of the swelling of the gel.

Gibbs' method has the great advantage over the cycle method used by Barkas that it avoids reference to swelling pressures, which are not easily visualized for the internal stresses in the gel itself due to its swelling.

The analysis is only concerned with cases where the stress can be reduced to pressures along the three principal directions and with a fixed amount of gel with varying quantities of absorbed material; the state of the gel is therefore completely specified by the temperature T, the number of moles absorbed, n, and the loads in the three directions $\mathbf{X}$, $\mathbf{Y}$, and $\mathbf{Z}$, or alternatively the stresses X, Y, and Z, and where shear stresses are involved a rectangular block is considered.

§2. RELATION BETWEEN VARIATIONS AT CONSTANT STRESS AND AT CONSTANT LOAD

From the thermodynamic relations expressed in terms of generalized co-ordinates, expressions of the type

$$(\delta B)_{Tn}=(\partial x/\partial A)_{\mathbf{XYZ}}\delta\mathbf{X}+(\partial y/\partial A)_{\mathbf{XYZ}}\delta\mathbf{Y}+(\partial z/\partial A)_{\mathbf{XYZ}}\delta\mathbf{Z} \qquad \ldots\ldots(1)$$

can be obtained (e.g., equations (11) and (12) below), where x, y, z are linear dimensions, A is either n or T and B either the chemical potential, μ, of the absorbed substance or the entropy, S.

It is required to express this in terms of $(\partial x/\partial A)_{XYZ}$ and δX etc., the fifth parameter, determining the state of the gel, remaining constant throughout. If the stresses are small compared with the moduli, one can write $\delta\mathbf{X}=yz\,\delta X$ and $(\partial x/\partial A)_{\mathbf{XYZ}}=(\partial x/\partial A)_{XYZ}$ without appreciable error: but in the general case

$$\delta x=\left(\frac{\partial x}{\partial A}\right)_{XYZ}\delta A+\left(\frac{\partial x}{\partial X}\right)_{AYZ}\delta X+\left(\frac{\partial x}{\partial Y}\right)_{AZX}\delta Y+\left(\frac{\partial x}{\partial Z}\right)_{AXY}\delta Z,$$

$$\therefore\left(\frac{\partial x}{\partial A}\right)_{\mathbf{XYZ}}=\left(\frac{\partial x}{\partial A}\right)_{XYZ}+\left(\frac{\partial x}{\partial X}\right)_{AYZ}\left(\frac{\partial X}{\partial A}\right)_{\mathbf{XYZ}}+\left(\frac{\partial x}{\partial Y}\right)_{AZX}\left(\frac{\partial Y}{\partial A}\right)_{\mathbf{XYZ}}+\left(\frac{\partial x}{\partial Z}\right)_{AXY}\left(\frac{\partial Z}{\partial A}\right)_{\mathbf{XYZ}}, \qquad \ldots\ldots(2)$$

but $\mathbf{X}=yzX$,

$$\therefore\ \delta\mathbf{X}=yz\delta X+X(y\delta z+z\delta y).$$

$$\left(\frac{\partial X}{\partial A}\right)_{\mathbf{XYZ}}=-X\left\{\frac{1}{z}\left(\frac{\partial z}{\partial A}\right)_{\mathbf{XYZ}}+\frac{1}{y}\left(\frac{\partial y}{\partial A}\right)_{\mathbf{XYZ}}\right\}, \qquad \ldots\ldots(3)$$

also

$$\left.\begin{aligned}\left(\frac{\partial x}{\partial X}\right)_{AYZ}&=-\frac{x}{E_x},\\ \left(\frac{\partial x}{\partial Y}\right)_{AZX}&=\sigma_{xy}\frac{x}{E_y},\\ \left(\frac{\partial x}{\partial Z}\right)_{AXY}&=\sigma_{xz}\frac{x}{E_z},\end{aligned}\right\} \qquad \ldots\ldots(4)$$

where E_x is Young's Modulus in the x direction, σ_{xy} is the ratio of the contraction in the x direction to the extension in the y direction for a stress in the y direction. Since a positive value of X denotes a pressure, whereas in defining E_x tensions are regarded as positive, the signs in equations (4) are interchanged with their usual values.

Substituting from (3) and (4) in (2),

$$\left(\frac{\partial x}{\partial A}\right)_{\mathbf{XYZ}} = \left(\frac{\partial x}{\partial A}\right)_{XYZ} + \frac{x}{E_x} X \left\{\frac{1}{z}\left(\frac{\partial z}{\partial A}\right)_{\mathbf{XYZ}} + \frac{1}{y}\left(\frac{\partial y}{\partial A}\right)_{\mathbf{XYZ}}\right\}$$
$$- \sigma_{xy}\frac{x}{E_y} Y \left\{\frac{1}{x}\left(\frac{\partial x}{\partial A}\right)_{\mathbf{XYZ}} + \frac{1}{z}\left(\frac{\partial z}{\partial A}\right)_{\mathbf{XYZ}}\right\}$$
$$- \sigma_{xz}\frac{x}{E_z} Z \left\{\frac{1}{x}\left(\frac{\partial x}{\partial A}\right)_{\mathbf{XYZ}} + \frac{1}{y}\left(\frac{\partial y}{\partial A}\right)_{\mathbf{XYZ}}\right\}, \qquad \ldots\ldots(5)$$

or, rearranging and multiplying by $yz\,\delta X$,

$$yz\left(\frac{\partial x}{\partial A}\right)_{XYZ}\delta X = yz\,\delta X\left(1 + \frac{\sigma_{xy}}{E_y}Y + \frac{\sigma_{xz}}{E_z}Z\right)\left(\frac{\partial x}{\partial A}\right)_{\mathbf{XYZ}}$$
$$+ zx\,\delta X\left(\frac{\sigma_{xz}}{E_z}Z - \frac{1}{E_x}X\right)\left(\frac{\partial y}{\partial A}\right)_{\mathbf{XYZ}} + xy\,\delta X\left(\frac{\sigma_{xy}}{E_y}Y - \frac{1}{E_x}X\right)\left(\frac{\partial z}{\partial A}\right)_{\mathbf{XYZ}};$$

similarly

$$zx\left(\frac{\partial y}{\partial A}\right)_{XYZ}\delta Y = yz\,\delta Y\left(\frac{\sigma_{yz}}{E_z}Z - \frac{1}{E_y}Y\right)\left(\frac{\partial x}{\partial A}\right)_{\mathbf{XYZ}}$$
$$+ zx\,\delta Y\left(1 + \frac{\sigma_{yx}}{E_x}X + \frac{\sigma_{yz}}{E_z}Z\right)\left(\frac{\partial y}{\partial A}\right)_{\mathbf{XYZ}} + xy\,\delta Y(\ldots\ldots)\left(\frac{\partial z}{\partial A}\right)_{\mathbf{XYZ}}$$

and

$$xy\left(\frac{\partial z}{\partial A}\right)_{XYZ}\delta Z = yz\,\delta Z\left(\frac{\sigma_{zy}}{E_y}Y - \frac{1}{E_z}Z\right)\left(\frac{\partial x}{\partial A}\right)_{\mathbf{XYZ}}$$
$$+ (\ldots\ldots)\left(\frac{\partial y}{\partial A}\right)_{XYZ} + xy\,\delta Z\left(1 + \frac{\sigma_{zx}}{E_x}X + \frac{\sigma_{zy}}{E_y}Y\right)\left(\frac{\partial z}{\partial A}\right)_{\mathbf{XYZ}}.$$

Adding the three equations gives

$$yz\left(\frac{\partial x}{\partial A}\right)_{XYZ}\delta X + zx\left(\frac{\partial y}{\partial A}\right)_{XYZ}\delta Y + xy\left(\frac{\partial z}{\partial A}\right)_{XYZ}\delta Z$$
$$= \left(\frac{\partial x}{\partial A}\right)_{\mathbf{XYZ}} yz\left\{\delta X - \frac{Y}{E_y}(\delta Y - \sigma_{xy}\delta X - \sigma_{zy}\delta Z) - \frac{Z}{E_z}(\delta Z - \sigma_{xz}\delta X - \sigma_{yz}\delta Y)\right\}$$
$$\left(\frac{\partial y}{\partial A}\right)_{\mathbf{XYZ}} zx\left\{\delta Y - \frac{X}{E_x}(\ldots\ldots) - \frac{Z}{E_z}(\ldots\ldots)\right\}$$
$$+ \left(\frac{\partial z}{\partial A}\right)_{\mathbf{XYZ}} xy\{\ldots\ldots\}. \qquad \ldots\ldots(6)$$

But $\delta \mathrm{X} = yz\,\delta X + Xyz\left(\frac{\delta z}{z} + \frac{\delta y}{y}\right)$, where δz and δy are due to arbitary changes in stress at constant A, and

$$\frac{\delta z}{z} = -\frac{1}{E_z}\delta Z + \frac{\sigma_{zy}}{E_y}\delta Y + \frac{\sigma_{zx}}{E_x}\delta X = -(\delta Z - \sigma_{yz}\delta Y - \sigma_{xz}\delta X)/E_z, \qquad \ldots\ldots(7)$$

since $\sigma_{zy}/E_y = \sigma_{yz}/E_z$, etc. (Love, 1920, p. 105).

$$\therefore\ \delta\mathbf{X} = yz\{\delta X - X(\delta Y - \sigma_{xy}\delta X - \sigma_{zy}\delta Z)/E_y - X(\delta Z - \sigma_{yz}\delta Y - \sigma_{xz}\delta X)/E_z\}, \qquad \ldots\ldots(8)$$

and similarly for $\delta\mathbf{Y}$ and $\delta\mathbf{Z}$, so that if $X = Y = Z$

$$\begin{aligned} yz(\partial x/\partial A)_{XYZ}\,\delta X + zx(\partial y/\partial A)_{XYZ}\,\delta Y + xy(\partial z/\partial A)_{XYZ}\,\delta Z \\ = (\partial x/\partial A)_{\mathbf{XYZ}}\,\delta\mathbf{X} + (\partial y/\partial A)_{\mathbf{XYZ}}\,\delta\mathbf{Y} + (\partial z/\partial A)_{\mathbf{XYZ}}\,\delta\mathbf{Z}. \end{aligned} \qquad \ldots\ldots(9)$$

Hence when the initial stress is a pure hydrostatic pressure, (1) gives

$$\begin{aligned} (\delta B)_{Tn} &= xyz\left\{\frac{1}{x}\left(\frac{\partial x}{\partial A}\right)_{XYZ}\delta X + \frac{1}{y}\left(\frac{\partial y}{\partial A}\right)_{XYZ}\delta Y + \frac{1}{z}\left(\frac{\partial z}{\partial A}\right)_{XYZ}\delta Z\right\} \\ &= V\left\{\frac{1}{x}\left(\frac{\partial x}{\partial A}\right)_{XYZ}\delta X + \frac{1}{y}\left(\frac{\partial y}{\partial A}\right)_{XYZ}\delta Y + \frac{1}{z}\left(\frac{\partial z}{\partial A}\right)_{XYZ}\delta Z\right\}. \end{aligned} \qquad \ldots\ldots(10)$$

When the stress is a pure hydrostatic pressure we can express the variations in B at constant temperature and composition in terms of variation of linear dimensions at constant stress and independent variations in the stress components. When $\delta X = \delta Y = \delta Z = \delta P$ the relation can be obtained more simply from the ordinary thermodynamic relation for fluids (e.g. Guggenheim (1933), equations (151) and (153)) by the relation

$$(1/V)(\partial V/\partial A)_P = (1/x)(\partial x/\partial A)_P + (1/y)(\partial y/\partial A)_P + (1/z)(\partial z/\partial A)_P.$$

When the initial stress involves pure shear stress the error involved is that of neglecting $(X-Y)z\,\delta y + (X-Z)y\,\delta z$ in comparison with $\delta\mathbf{X}$, which is small if $(X-Y)$ etc. are small compared with the moduli.

§3. DERIVATION OF THE GENERAL RELATIONS IN TERMS OF GENERALIZED CO-ORDINATES

For a rectangular block of gel of the type considered, the general equation is given by Fowler and Guggenheim (1939), p. 60, as $\delta F = -S\,\delta T - \Sigma\mathbf{X}\,\delta x + \mu\,\delta n$, where F is the Helmholtz free-energy, and if we define $\mathcal{G}$ as $F + \Sigma\mathbf{X}x$ by analogy with the definition of Gibbs' function G*,

$$\delta\mathcal{G} = -S\,\delta T + \Sigma x\,\delta\mathbf{X} + \mu\,\delta n,$$

hence

$$S = -(\partial\mathcal{G}/\partial T)_{n\mathbf{XYZ}}, \quad x = (\partial\mathcal{G}/\partial\mathbf{X})_{nT\mathbf{YZ}}, \text{ etc.,} \quad \text{and } \mu = (\partial\mathcal{G}/\partial n)_{T\mathbf{XYZ}};$$

hence $$(\partial S/\partial\mathbf{X})_{nT\mathbf{YZ}} = -(\partial^2\mathcal{G}/\partial T\,\partial\mathbf{X}) = -(\partial x/\partial T)_{n\mathbf{XYZ}}$$

and $$(\partial\mu/\partial\mathbf{X})_{nT\mathbf{YZ}} = (\partial x/\partial n)_{T\mathbf{XYZ}}.$$

For variations at constant temperature and composition

$$\begin{aligned} (\delta S)_{nT} &= (\partial S/\partial\mathbf{X})_{nT\mathbf{YZ}}\,\delta\mathbf{X} + (\partial S/\partial\mathbf{Y})_{nT\mathbf{ZX}}\,\delta\mathbf{Y} + (\partial S/\partial\mathbf{Z})_{nT\mathbf{XY}}\,\delta\mathbf{Z}, \\ &= -(\partial x/\partial T)_{n\mathbf{XYZ}}\,\delta\mathbf{X} - (\partial y/\partial T)_{n\mathbf{XYZ}}\,\delta\mathbf{Y} - (\partial z/\partial T)_{n\mathbf{XYZ}}\,\delta\mathbf{Z} \end{aligned} \qquad \ldots\ldots(11)$$

and

$$(\delta\mu)_{nT} = (\partial x/\partial n)_{T\mathbf{XYZ}}\,\delta\mathbf{X} + (\partial y/\partial n)_{T\mathbf{XYZ}}\,\delta\mathbf{Y} + (\partial z/\partial n)_{T\mathbf{XYZ}}\,\delta\mathbf{Z}. \qquad \ldots\ldots(12)$$

---

* $\mathcal{G}$ is not identical with G since in the case of a pure hydrostatic pressure $\Sigma\mathbf{X}x = yzXx + zxYy + xyZz = 3PV$.

When the initial stress is a pure hydrostatic pressure these can be transformed by the relations obtained in the previous section:

$$(\delta S)_{nT} = -V\left\{\frac{1}{x}\left(\frac{\partial x}{\partial T}\right)_{nXYZ}\delta X + \frac{1}{y}\left(\frac{\partial y}{\partial T}\right)_{nXYZ}\delta Y + \frac{1}{z}\left(\frac{\partial z}{\partial T}\right)_{nXYZ}\delta Z\right\}, \quad \ldots\ldots(11.1)$$

$$(\delta \mu)_{nT} = V\left\{\frac{1}{x}\left(\frac{\partial x}{\partial n}\right)_{TXYZ}\delta X + \frac{1}{y}\left(\frac{\partial y}{\partial n}\right)_{TXYZ}\delta Y + \frac{1}{z}\left(\frac{\partial z}{\partial n}\right)_{TXYZ}\delta Z\right\}, \quad \ldots\ldots(12.1)$$

but $(1/x)(\partial x/\partial T)_{nXYZ}$ is the coefficient of thermal expansion in the x direction, α_x and $(1/x)(\partial x/\partial n)_{TXYZ}$ is the isothermal swelling per mole in the x direction at constant pressure $= s_x$; hence

$$(\delta S)_{nT} = -V(\alpha_x \delta X + \alpha_y \delta Y + \alpha_z \delta Z) \quad \ldots\ldots(11.2)$$

and

$$(\delta \mu)_{nT} = V(s_x \delta X + s_y \delta Y + s_z \delta Z). \quad \ldots\ldots(12.2)$$

Equation (12.2) can be used to calculate the effect of shear stress on vapour pressure, and the variation of vapour pressure of a hygroscopic gel initially subject to a pure hydrostatic pressure (or when shear stresses are small compared with the rigidity) with any variation in its state. Equation (11.2) can be used to calculate the contribution of the energy of expansion to the heat of absorption of the moisture by the gel. These will be considered separately.

§4. EFFECT OF CHANGES IN STATE OF A GEL INITIALLY SUBJECT TO A PURE HYDROSTATIC PRESSURE ON THE EQUILIBRIUM VAPOUR PRESSURE

Equation (12.2) gives the variation in μ at constant temperature and composition with changes in the stress components; the net variation when temperature and composition may also change is therefore given by

$$\delta\mu = (\partial\mu/\partial n)_{PT}\delta n + (\partial\mu/\partial T)_{Pn}\delta T + V(s_x \delta X + s_y \delta Y + s_z \delta Z), \quad \ldots\ldots(13)$$

since constant X, Y and Z when $X = Y = Z$ is identical with constant pressure. If μ_V is the chemical potential of the vapour in equilibrium with the absorbed component in the gel, $\mu_V = \mu$ at all times.

The only parameters on which μ_V depends are the vapour pressure p and the temperature T. Equilibrium can only be maintained if T is the same for both phases.

$$\therefore\ \delta\mu = \delta\mu_V = (\partial\mu_V/\partial p)_T \delta p + (\partial\mu_V/\partial T)_p \delta T. \quad \ldots\ldots(14)$$

Combining (13) and (14),

$$(\partial\mu/\partial n)_{PT}\delta n + (\partial\mu/\partial T)_{Pn}\delta T + V(s_x \delta X + s_y \delta Y + s_z \delta Z) = (\partial\mu_V/\partial p)_T \delta p + (\partial\mu_V/\partial T)_p \delta T.$$

We have (Guggenheim, 1933, p. 35)

$$(\partial\mu/\partial T)_{Pn} = -(\partial S/\partial n)_{PT}, \qquad (\partial\mu_V/\partial p)_T = v, \qquad (\partial\mu_V/\partial T)_p = -S_V,$$

where v = molar volume of the vapour.

$$\therefore\ (\partial\mu/\partial n)_{PT}\delta n - (\partial S/\partial n)_{PT}\delta T + V(s_x \delta X + s_y \delta Y + s_z \delta Z) = v\,\delta p - S_V \delta T. \quad \ldots\ldots(15)$$

Considering first isothermal changes at constant stress:

$$(\partial\mu/\partial n)_{PT}\delta n = v\,\delta p$$

$$\therefore\ (\partial\mu/\partial n)_{PT} = v(\partial p/\partial n)_{PT}.$$

The general equation for isothermal changes is

$$V(s_x\delta X+s_y\delta Y+s_z\delta Z)=v\,\delta p-v(\partial p/\partial n)_{XYZT}\,\delta n. \qquad \ldots\ldots(16)$$

This is identical with equation (13) in the paper by Barkas (1945) on swelling stresses in rigid gels, but the derivation given here shows that it is only rigid if the initial stress is a pure hydrostatic pressure. This can also be written

$$V\left\{(s_x+s_y+s_z)\left(\frac{\delta X+\delta Y+\delta Z}{3}\right)+(s_x-s_y)\left(\frac{\delta X-\delta Y}{3}\right)\right.$$
$$\left.+(s_y-s_z)\left(\frac{\delta Y-\delta Z}{3}\right)+(s_z-s_x)\left(\frac{\delta Z-\delta X}{3}\right)\right\}=s\,\delta p-v\left(\frac{\partial p}{\partial n}\right)_{XYZT}\delta n,$$

thus separating the effect of changes in hydrostatic pressure and shear stresses.

Equation (15) can also be used to determine the variation of vapour pressure with temperature keeping the composition constant. This can be done even if the absorbed liquid is in more than one form, as equilibrium must be maintained between these forms, and, therefore, according to the phase rule, in discussing equilibrium with external conditions the absorbed liquid can be treated as a single component. In this case the only variation on the L.H.S. of equation (15) is in T, whereas for the vapour phase the pressure must be allowed to alter to maintain equilibrium.

$$\therefore\quad -\left(\frac{\partial S}{\partial n}\right)_{PT}\delta T=v\,\delta p-S_V\,\delta T,$$

$$\therefore\quad S_V-\left(\frac{\partial S}{\partial n}\right)_{PT}=v\left(\frac{\partial p}{\partial T}\right)_{nP}=\frac{RT}{p}\left(\frac{\partial p}{\partial T}\right)_{nP}$$

(if the vapour behaves as a perfect gas);

$$\therefore\quad T\left\{S_V-\left(\frac{\partial S}{\partial n}\right)_{PT}\right\}=RT^2\left(\frac{\partial}{\partial T}\ln p\right)_{nP},$$

but

$$T\left(\frac{\partial S}{\partial n}\right)_{PT}=\left(\frac{\partial H}{\partial n}\right)_{PT}-\mu$$

(Guggenheim, pp. 37 and 38), where H is the heat content of the gel;

$$\therefore\quad H_V-\left(\frac{\partial H}{\partial n}\right)_{PT}+(\mu-\mu_V)=RT^2\left(\frac{\partial}{\partial T}\ln p\right)_{nP},$$

but $\mu=\mu_V$,

$$\therefore\quad H_V-\left(\frac{\partial H}{\partial n}\right)_{PT}=RT^2\left(\frac{\partial}{\partial T}\ln p\right)_{nP}. \qquad \ldots\ldots(17)$$

This may be combined with the relation obtained by Guggenheim (1933, p. 64), using a similar analysis, for the equilibrium vapour pressure of a pure liquid maintained at constant hydrostatic pressure, which may be written

$$H_V-H_L=RT^2\left(\frac{\partial}{\partial T}\ln p_0\right)_{nP}, \qquad \ldots\ldots(18)$$

where H_L is the molar total heat of the liquid and p_0 the pressure of the vapour in equilibrium with the pure liquid. Whence—since for a perfect gas H_V is independent of the pressure at constant temperature—

$$H_L-\left(\frac{\partial H}{\partial n}\right)_{PT}=\boldsymbol{R}T^2\left\{\frac{\partial}{\partial T}\ln\left(\frac{p}{p_0}\right)\right\}_{nP}.$$

The heat absorbed when 1 mole of liquid is absorbed by a large quantity of gel at constant temperature and pressure is given by the increase in total heat

$$\left(\frac{\partial}{\partial n}\Delta H\right)_{PT},$$

where

$$(\partial\Delta H/\partial n)_{PT}=(\partial H/\partial n)_{PT}-H_L.$$

$$\therefore\quad\left(\frac{\partial}{\partial n}\Delta H\right)_{PT}=-\boldsymbol{R}T^2\left(\frac{\partial}{\partial T}\ln\frac{p}{p_0}\right)_{nP}=-\boldsymbol{R}T^2\left(\frac{\partial}{\partial T}\ln h\right)_{nP},\quad\ldots\ldots(19)$$

where h is the relative humidity of the vapour in equilibrium with the liquid absorbed by the gel.

The above equation is identical with Kirchhoff's relation for the heat of dilution of a dilute solution, but the above derivation shows that it is perfectly general and makes clear precisely what quantity is given by $\boldsymbol{R}T^2(\partial/\partial T\ln h)_{nP}$. Previous derivations of the relation by Shorter (1924) and Hedges (1926) have either directly applied the relation for dilute solutions on general thermodynamic reasoning or have been based on the assumption that the volume swelling per mole was identical with the molar volume of the pure liquid, which does not hold for keratin at low regains. It should be noted that the heat of absorption Q as defined by Hedges and Shorter $=-(\partial\Delta H/\partial n)/M$, where M is the molecular weight.

Equation (17) has also been derived by earlier workers, notably Kruyt and Modderman (1930) and Brunauer (1943), who applied it to the heat of absorption of gases by charcoal, etc., and who give it as $\boldsymbol{R}T^2(\partial/\partial T\ln p)_n=q$, where q is variously defined, whereas in equation (17) the heat is accurately defined in terms of generally understood thermodynamic quantities. The relation of this to the observed heat of absorption in any experimental arrangement is a matter for thermodynamic analysis of the exact procedure employed, and will differ for different experimental arrangements.

In the case of direct absorption by a gel from the pure liquid, the usual procedure is to immerse a given quantity of the gel containing n moles of the absorbed liquid in a calorimeter containing the pure liquid and observe the heat evolved. Since in this case the pressure on the liquid and the gel remain constant throughout and the rise in temperature is negligibly small (although the quantity actually measured), the heat evolved is clearly,

$$-\int_n^{\text{sat}}\left(\frac{\partial\Delta H}{\partial n}\right)_{PT}dn,$$

where the integral covers the range from the initial content of absorbate to saturation. For an amount of gel containing $100M$ grams of the dry substance, where M is the molecular weight of the absorbed liquid, n is the regain C

(amount of absorbate per 100 g. of dry substance), and hence the amount of heat evolved per gram of the dry substance is

$$-(1/100M)\int_{C}^{\text{sat}}\left(\frac{\partial\Delta H}{\partial n}\right)_{PT}dC$$

$$=-(1/1800)\int_{C}^{\text{sat}}\left(\frac{\partial\Delta H}{\partial n}\right)_{PT}dC \text{ for water.} \qquad \ldots\ldots(20)$$

In the case of direct absorption of the pure liquid by the gel, the heat evolved is thus directly related to the quantity given by Kirchhoff's relation, which has been shown to be an exact relation between the heat absorbed when 1 mole of absorbed substance is absorbed by a large quantity of gel material at constant temperature and pressure on the one hand, and the isosteric variation of equilibrium humidity at constant hydrostatic pressure on the gel, on the other hand.

§ 5. EFFECT OF GENERAL EXPANSION OF GEL ON THE INTRINSIC ENERGY AND THE CONTRIBUTION OF THE ENERGY OF EXPANSION TO THE TOTAL HEAT OF ABSORPTION

Equation (11.2) expresses the effect on the entropy of varying the stress components on a rigid gel initially under a pure hydrostatic pressure. This can be used to calculate the change in intrinsic energy δU, when the gel is expanded by the application of external forces by the same amount as when an additional mole of liquid is absorbed at constant temperature and pressure. Experiment does not directly give the changes in stress required to do this, and equation (11.2) must be transformed by expressing the changes in stress in terms of changes in the geometric parameters x, y, and z. This can be done by means of the ordinary elastic equations (for rhombic symmetry):

$$\left.\begin{aligned}
-\frac{\delta x}{x}&=\frac{\delta X}{E_x}-\sigma_{xy}\frac{\delta Y}{E_y}-\sigma_{xz}\frac{\delta Z}{E_z},\\
-\frac{\delta y}{y}&=-\sigma_{yx}\frac{\delta X}{E_x}+\frac{\delta Y}{E_y}-\sigma_{yz}\frac{\delta Z}{E_z},\\
-\frac{\delta z}{z}&=-\sigma_{zx}\frac{\delta X}{E_x}-\sigma_{yz}\frac{\delta Y}{E_y}+\frac{\delta Z}{E_z}.
\end{aligned}\right\} \qquad \ldots\ldots(21)$$

The negative sign appears on the L.H.S., as the conventional definition of E assumes that tensions are positives, whereas in the thermodynamic convention tensions are regarded as negative pressures.

These three equations can be transformed to another set expressing the stresses in terms of the resulting strains. Writing A_x for $\delta X/E_x$, this becomes

$$\left.\begin{aligned}
-DA_x&=(1-\sigma_{zy}\sigma_{yz})\,\delta x/x+(\sigma_{xy}+\sigma_{xz}\sigma_{zy})\,\delta y/y+(\sigma_{xz}+\sigma_{xy}\sigma_{yz})\,\delta z/z,\\
-DA_y&=(1-\sigma_{xz}\sigma_{zx})\,\delta y/y+(\sigma_{yz}+\sigma_{yx}\sigma_{xz})\,\delta z/z+(\sigma_{yx}+\sigma_{yz}\sigma_{zx})\,\delta x/x,\\
-DA_z&=(1-\sigma_{xy}\sigma_{yx})\,\delta z/z+(\sigma_{zx}+\sigma_{zy}\sigma_{yx})\,\delta x/x+(\sigma_{zy}+\sigma_{zx}\sigma_{xy})\,\delta y/y,
\end{aligned}\right\} \qquad \ldots\ldots(22)$$

where D is a determinant of which the value is

$$D=1-\sigma_{xy}\sigma_{yx}-\sigma_{xz}\sigma_{zx}-\sigma_{yz}\sigma_{zy}-\sigma_{xy}\sigma_{yz}\sigma_{zx}-\sigma_{yx}\sigma_{zy}\sigma_{xz}.$$

A similar transformation for colour equations is given by J. Guild (1924). These values can be substituted in equation (12.2), giving

$$\begin{aligned}(\delta S)_{nT} = (V/D)[E_x\alpha_x\{(1-\sigma_{zy}\sigma_{yz})\,\delta x/x + (\sigma_{xy}+\sigma_{xz}\sigma_{zy})\,\delta y/y \\ +(\sigma_{xz}+\sigma_{xy}\sigma_{yz})\,\delta z/z\} + E_y\alpha_y\{(1-\sigma_{xz}\sigma_{zx})\,\delta y/y + \ldots\} + E_z\alpha_z\{\ldots\ldots\}].\end{aligned} \qquad \ldots\ldots(23)$$

If U is the intrinsic energy, $\delta U = T\delta S - \Sigma \mathbf{X}\,\delta x$ at constant composition; or, when the initial stress is pure hydrostatic pressure,

$$\delta U = T\delta S - P\delta V;$$

$$\therefore \quad (\delta U)_{nT} = (TV/D)[E_x\alpha_x\{\ldots\ldots\} + E_y\alpha_y\{\ldots\ldots\} + E_z\alpha_z\{\ldots\ldots\}] - P\delta V.$$

If we assume that the internal energy of differential expansion is the same whether the expansion is due to external forces or absorption of liquid,* the contribution of the expansion to the total heat or, more strictly, the total heat of absorption, when there is no heat of reaction between the absorbed liquid and the gel when absorption takes place at constant temperature and pressure, is given by

$$(\delta H)_{\text{expansion}} = (TV/D)[E_x\alpha_x\{\ldots\ldots\} + E_y\alpha_y\{\ldots\ldots\} + E_z\alpha_z\{\ldots\ldots\}] - P\delta V + P\delta V,$$

since at constant pressure $\delta(PV) = P\delta V$. Expressing this per mole,

$$\begin{aligned}(\partial H/\partial n)_{\text{expansion}} &= (TV/D)[E_x\alpha_x\{(1-\sigma_{zy}\sigma_{yz})(1/x)(\partial x/\partial n)_{PT} + \ldots\ldots\} + \ldots\ldots] \\ &= (TV/D)[E_x\alpha_x\{(1-\sigma_{zy}\sigma_{yz})s_x + (\sigma_{xy}+\sigma_{xz}\sigma_{zy})s_y + \ldots\ldots\} + \ldots\ldots],\end{aligned} \qquad \ldots\ldots(24)$$

writing s_x for $(\partial x/\partial n)/x$, etc., in each of the terms in the equation.

If there is symmetry about the z axis,

$$\sigma_{xy} = \sigma_{yx} = \sigma_{xx},$$

$$\sigma_{zy} = \sigma_{zx},$$

$$\sigma_{yz} = \sigma_{xz},$$

and $\quad s_y = s_x, \quad \alpha_x = \alpha_y, \quad$ and $E_x = E_y$.

The expression for D then reduces to

$$D = (1+\sigma_{xx})(1-\sigma_{xx}-2\sigma_{xz}\sigma_{zx})$$

and

$$\begin{aligned}(\partial H/\partial n)_{\text{expansion}} &= (TV/D)[E_x\alpha_x\{(1-\sigma_{xz}\sigma_{zx})s_x + (\sigma_{xx}+\sigma_{xz}\sigma_{zx})s_x \\ &\qquad +(\sigma_{xz}+\sigma_{xx}\sigma_{xz})s_z\} + E_x\alpha_x\{\ldots\ldots\} + E_z\alpha_z\{(1-\sigma_{xx}^2)s_z + 2(\sigma_{zx}+\sigma_{zx}\sigma_{xx})s_x\}] \\ &= [TV/(1+\sigma_{xx})(1-\sigma_{xx}-2\sigma_{xz}\sigma_{zx})][2E_x\alpha_x\{(1+\sigma_{xx})s_x + \sigma_{xz}(1+\sigma_{xx})s_z\} \\ &\qquad + E_z\alpha_z\{(1+\sigma_{xx})(1-\sigma_{xx})s_z + 2\sigma_{zx}(1+\sigma_{xx})s_x\}] \\ &= [TV/(1-\sigma_{xx}-2\sigma_{xz}\sigma_{zx})][2E_x\alpha_x(s_x+\sigma_{xz}s_z) + E_z\alpha_z\{2\sigma_{zx}s_x + (1-\sigma_{xx})s_z\}],\end{aligned} \qquad \ldots\ldots(25)$$

but

$$E_x\sigma_{xz} = E_z\sigma_{zx},$$

---

* This assumption is the simplest one, and would appear to be justified by the fact that it gives heats of the correct order when this is the principal source of change in intrinsic energy on absorption of water.

therefore an alternative form is

$$(\partial H/\partial n)_{\text{expansion}}=\{TV/(1-\sigma_{xx}-2\sigma_{xz}\sigma_{zx})\}[2E_x\{\alpha_x s_x + \sigma_{xz}(\alpha_x s_z+\alpha_z s_x)\}+E_z\alpha_z s_z(1-\sigma_{xx})]. \quad \ldots\ldots(26)$$

For most hygroscopic gels s_z is only about 3% of s_x, and it is probable that the same is true of α_z and α_x (as it certainly is for wood). In this case, the last term in the square brackets can be omitted and we have

$$(\partial H/\partial n)_{\text{expansion}}=2TVE_x\{\alpha_x s_x+\sigma_{xz}(\alpha_x s_z+\alpha_z s_x)\}/(1-\sigma_{xx}-2\sigma_{zx}\sigma_{xz}). \quad \ldots\ldots(27)$$

It should be emphasized that the above analysis assumes that the gel is homogeneous in the limited sense that external stresses can produce the same distortions at every point as absorption of the liquid.

§6. APPLICATION TO THE STUDY OF THE ABSORPTION OF WATER BY TEXTILE FIBRES

Urquhart and Williams (1924) determined the variation in the equilibrium vapour pressure of cotton with temperature and regain and give the results in the form of a series of iso-humidity curves. From these it is seen that at high relative humidities the equilibrium regain passes through a minimum as the temperature increases, the temperature corresponding to this minimum increasing as the humidity decreases. At these minima the relative humidity in equilibrium with the corresponding regain is a maximum, i.e. $(\partial/\partial T \ln h)_{nP}$ is positive for lower temperatures and negative for higher temperatures. Hence, from equation (19), $(\partial\Delta H/\partial n)_{PT}$ for the particular high regain concerned is negative for lower temperatures and positive for high temperatures.

A somewhat similar result was obtained by Speakman, Stott and Chang (1933) for wool. They found that the saturation regain and that for 97·5% R.H. showed a minimum at temperatures between 40 and 50° C. and also, as might be expected, that the swelling in water was a minimum at about the same temperature. The change in sign of the value of $(\partial\Delta H/\partial n)_{PT}$ with increase in temperature is most easily explained by the assumption that $(\partial\Delta H/\partial n)_{PT}$ consists of two components of opposite sign, and that either the value of each changes with temperature or the contribution of each to the total value of $(\partial\Delta H/\partial n)_{PT}$ changes. Such an assumption is made by Cassie (1945), who attributes the value of $(\partial\Delta H/\partial n)_{PT}$ as observed by Hedges to two components—a negative component changing rapidly with regain, due to the heat of reaction between the gel and the water, and a positive component due to the heat required to expand the gel. Combining this assumption with the theory of Peirce (1929) and others, that the absorbed water consists of two portions, one of which has no heat of reaction, it is seen that $(\partial\Delta H/\partial n)_{PT}$ for this portion is positive, while for the remainder it is negative. If equation (19) is applied separately to these two portions it is seen that the relative humidity in equilibrium with one portion decreases with increase in temperature, and for the other portion increases, if the proportions of the two components remain the same. Equilibrium can in fact only be maintained by taking into account the first term on the L.H.S. of equation (15), which will have two components, and adding the relation that the sum of the changes in δn for the two portions is zero. When this is done, equation (19) is found to hold for the water as a whole, as deduced from the phase rule, but the proportion of the component with a positive value of $(\partial \Delta H/\partial n)_{PT}$ will increase with rise in temperature, thus tending to make $(\partial \Delta H/\partial n)_{PT}$, for the water as a whole, become less negative as the temperature rises, in accordance with the experimental results quoted.

At high regains and temperatures, when practically all the water is absorbed without heat of reaction, $(\partial \Delta H/\partial n)_{PT}$ should approach the heat of expansion of the gel as given by equation (27). However, the comparison requires a knowledge of the transverse value of Young's Modulus, E_x, as well as the three principal values of Poisson's ratio for a material showing radial symmetry. Unfortunately it is impossible to obtain these constants for textile fibres, and an accurate comparison can only be made by the use of a material like horn keratin, which is obtainable in bulk, and shows similar absorption properties to wool keratin. Until full experimental data for horn keratin are available, the best comparison that can be made is between $(\partial \Delta H/\partial n)_{PT}$, calculated from Urquhart and Williams' isostere for cotton at 19·9% regain, which corresponds to about 98% R.H., and for which full experimental values are given, and $(\partial H/\partial n)_{\text{expansion}}$ calculated on certain assumptions for the value of the elastic constants, etc., of cotton. The assumptions are:

(1) E_x for cotton is about 10^4 bars, which is approximately the value for horn keratin and the gel material of wood at high regains (W.I.R.A. and Barkas, 1945, p. 55).

(2) α_x is that for beech across the grain, $=6\times10^{-5}$ (Kaye and Laby).

(3) $2V\{s_x+\sigma_{xz}(s_z+s_x\alpha_z/\alpha_x)\}=$ molar volume of water $=18$ c.c.

(4) $\sigma_{xx}=\sigma_{xz}=\sigma_{zx}=\frac{1}{4}$ (value of σ_{xz} for keratin (W.I.R.A.)).

Substituting in equation (27) for $T=360°$ K. $=87°$ C.,

$$(\partial H/\partial n)_{\text{expansion}}=\frac{360\times10^{10}\times18\times6\times10^{-5}}{1-\frac{1}{4}-\frac{1}{8}}\times2{\cdot}4\times10^{-8}\text{ cals/mole}$$

$$=160\text{ cal/mole.}$$

Urquhart and Williams' data give the equilibrium vapour pressure of cotton at 19·9% regain when it is absorbing water at three temperatures, 70, 80, and 90° C. These can be converted into equilibrium humidities with the aid of saturation vapour pressures at these temperatures as given by the Smithsonian Meteorological Tables and the logarithm of h plotted against the reciprocal of the temperature. $(\partial \Delta H/\partial n)$ at any temperature is then given by the slope of the curve. The value found at 90° C. is 64 cal/mole, which is of the same order of magnitude as the heat of expansion obtained from elastic constants.

Urquhart and Williams also give the absorption and desorption isosteres at 12% regain in the form of curves of the logarithm of the vapour pressure against the reciprocal of the temperature, obtaining a greater (negative) slope for desorption than absorption, showing that $(\partial H/\partial n)_{PT}$ is less positive for desorption than absorption.

This is consistent with the assumption of Barkas (1942) and Cassie (1945) that the hysteresis of the absorption isotherm is a reflection of the elastic hysteresis of the gel, as on this assumption the heat of expansion will be less for desorption than absorption.

The absorption isotberm gives the change in the thermodynamic potential or Gibbs' function when one mole of the absorbate is transferred from the liquid in bulk to a large quantity of the gel at constant temperature and pressure. The general expression for the change in this function is given as

$$\Delta G = \Delta H - T\Delta S;$$

differentiating with respect to n gives the change in chemical potential under the conditions mentioned above, i.e.,

$$\Delta\mu = (\partial\Delta G/\partial n)_{PT} = (\partial\Delta H/\partial n)_{PT} - T(\partial\Delta S/\partial n)_{PT}.$$

The study of the isotherm is thus resolved into a study of the two components of the change in Gibbs' function. The analysis of the entropy term involves statistical considerations and is outside the scope of this paper. The energy term can be obtained experimentally either from the heat of wetting or from the isostere, and can therefore be analysed independently of the entropy term. The change in total heat ΔH can be written

$$\Delta H = \Delta U + \Delta PV$$

and the change in intrinsic energy can be split into two portions: ΔU_1 the change in intrinsic energy due to the reaction between the liquid and the gel, and ΔU_2 the change due to the expansion of the gel. The ΔPV term involves the change in the value of PV for the gel, and also for the liquid, so that, differentiating,

$$\left(\frac{\partial\Delta H}{\partial n}\right)_{PT} = \left(\frac{\partial\Delta U_1}{\partial n}\right)_{PT} + \left(\frac{\partial\Delta U_2}{\partial n}\right)_{PT} + P\left(\frac{\partial V}{\partial n}\right)_{PT} - PV_L, \quad \ldots\ldots(28)$$

where $(\partial V/\partial n)_{PT}$ refers to the gel and V_L is the molar volume of the liquid in bulk. The second term is that obtained from the elastic properties of the gel, and hence the second and third terms are equivalent to $(\partial H/\partial n)_{\text{expansion}}$. If the absorbed liquid takes two forms with different energies of reaction, the differentiation takes place under conditions of equilibrium between the two forms. It is generally assumed that the liquid in one of these forms is localized, and in the other form relatively mobile. If A is the number of moles of liquid in the mobile form and B the number in the localized (bound) form,

$$\left(\frac{\partial\Delta U_1}{\partial n}\right)_{PT} = \left(\frac{\partial\Delta U_1}{\partial A}\right)_{BPT}\left(\frac{\partial A}{\partial n}\right)_{PT} + \left(\frac{\partial\Delta U_1}{\partial B}\right)_{APT}\left(\frac{\partial B}{\partial n}\right)_{PT}, \quad \ldots\ldots(29)$$

$$\therefore\ \left(\frac{\partial\Delta H}{\partial n}\right)_{PT} = \left(\frac{\partial\Delta U_1}{\partial A}\right)_{BPT}\left(\frac{\partial A}{\partial n}\right)_{PT} + \left(\frac{\partial\Delta U_1}{\partial B}\right)_{APT}\left(\frac{\partial B}{\partial n}\right)_{PT} + \left(\frac{\partial H}{\partial n}\right)_{\text{expansion}} - PV_L. \quad \ldots\ldots(30)$$

At low contents of the absorbate it is generally assumed that all the liquid is absorbed in the bound form, i.e. when $n=0$,

$$\left(\frac{\partial A}{\partial n}\right)_{PT} = 0 \quad \text{and} \quad \left(\frac{\partial B}{\partial n}\right)_{PT} = 1;$$

$$\therefore\quad \left(\frac{\partial \Delta H}{\partial n}\right)_{PT,n=0} = \left(\frac{\partial \Delta U_1}{\partial B}\right)_{APT} + \left(\frac{\partial H}{\partial n}\right)_{\text{expansion}} - PV_L. \quad \ldots\ldots(31)$$

Hence the value of $(\partial \Delta U_1/\partial B)$ can be determined at low contents. If it is further assumed, as has been done by Cassie (1945), following Pierce (1929), that $(\partial \Delta U_1/\partial A)$ is zero and that $(\partial \Delta U_1/\partial B)$ is a constant, substitution of the value of the latter in equation (30) enables $\partial B/\partial n$ to be found for all values of n. The values of B so obtained can be used in analysing the entropy term on statistical and other theories.

ACKNOWLEDGMENTS

The author is indebted to Dr. A. B. D. Cassie for much helpful discussion of the subject, and to Mr. B. H. Wilsdon, Director of Research, and the Council of the Wool Industries Research Association for permission to publish this paper.

REFERENCES

Barkas, W. W., 1942. *Trans. Faraday Soc.*, **38**, 207.
Barkas, W. W., 1945. *Swelling Stresses in Gels*, F.P.R. Special Report, No. 6 (H.M.S.O.)
Brunauer, S., 1943. *The Adsorption of Gases and Vapours* (Oxford : The University Press), **1**, 222.
Cassie, A. B. D., 1945. *Trans. Faraday Soc.*, **41**, 458–64.
Fowler, R. H. and Guggenheim, E. A., 1939. *Statistical Thermodynamics* (Cambridge : The University Press).
Guggenheim, E. A., 1933. *Modern Thermodynamics* (London : Methuen & Co.).
Guild, J., 1924–5. *Trans. Opt. Soc.*, **26**, 99 and 100.
Hedges, J. J., 1926. *Trans. Faraday Soc.*, **22**, 178.
Kaye and Laby, 1936. *Physical and Chemical Constants*, 8th Edition (London : Longmans & Co.).
Kruyt, H. R. and Modderman, J. G., 1930. *Chem. Rev.* **7**, 278–82.
Love, A. E. H., 1920. *Mathematical Theory of Elasticity*, 3rd Edition (Cambridge : The University Press).
Peirce, F. T., 1929. *J. Text. Inst.*, **20**, T. 133.
Shorter, S. A., 1924. *J. Text. Inst.*, **15**, T. 328.
Speakman, J. B., Stott, E. and Chang, H., 1933. *J. Text. Inst.*, **24**, T. 284.
Urquhart, A. R. and Williams, A. M., 1924. *J. Text. Inst.*, **15**, T. 559–72.
W.I.R.A. Unpublished work.

OPTICAL PROBLEMS OF THE ROTATING-PRISM CINEMATOGRAPH PROJECTOR

By J. KUDAR

Communicated by Professor A. F. C. Pollard. MS. received 4 March 1946

ABSTRACT. The most characteristic optical aberration in the rotating-prism non-intermittent cinematograph projector, the non-linearity of the image shift, can be eliminated by a suitable periodic variation of the direction of the illuminating beam. In addition to a description of this unusual method of optical correction, other aberrations of the image formation by the rotating prism are discussed, such as the prismatic astigmatism and the tangential and sagittal prismatic coma.

§ 1. INTRODUCTION

In cinematograph projectors with non-intermittent film movement, an optical device is used for producing a stationary projected image from the uniformly moving film. This may be an arrangement of rotating or oscillating mirrors, or a rotating polygonal prism. A ray suffers parallel displacement by refraction in a plane parallel plate, represented by opposite sides of the rotating prism (cf. figure 1); a polygonal prism of suitable dimensions and speed of rotation can, therefore, produce a stationary image. However, the parallel shift is not a linear function of the angle of incidence, and this gives rise to considerable optical aberrations. A theory of these was worked out by H. Dennis Taylor (1937) and applied especially for high-speed cinematographic cameras with rotating prism. The use of such cameras in practice is made possible by the circumstance that the light is cut off by a rotating shutter between two consecutive images in those positions of the prism where the angles of incidence, and thus the aberrations, would be too large. This limitation of the angle of incidence is impracticable in the case of projectors, because it would involve a frequency of interruption equal to the number of images per second. With the usual number of 24 images/sec., this would cause troublesome flicker*; a dark period in the middle of the projection of an image, applied for doubling the flicker frequency, would cut out most of the time available for the projection of the image if its length were made comparable with that dark period between two images which would result from the exclusion of large angles. In addition, it would result in the loss of the optically most perfect interval. Increasing the number of sides of the polygon would reduce the greatest angle of incidence, but the natural limitation to the circumference of the rotating prism prevents sufficiently good correction by this means. It seems more promising, therefore, to investigate optical possibilities for correcting or compensating the non-linearity of the image shift.

Detailed consideration shows that, for practical reasons, it would be very difficult to attempt correction by means of rotating or oscillating optical elements between the film and the projection objective or in front of the objective. Fortunately, however, the non-linearity of the image shift can be eliminated by a very unusual method of correction, without introducing any constructional parts between the film and the objective or in front of the objective. This can be understood by means of figures 1 and 2. Figure 1 shows small pencils of rays coming from the film F parallel to the optic axis A–A of the projection objective O and deviated by refraction in the prism (of which p and p′ are opposite parallel sides).

---

* With modern intermittent projectors, the number of interruptions is two or three times the number of images.

§2. DETAILED THEORY

Let D be the distance between the sides p and p′, n the refractive index of the prism, x the angle of incidence which is equal to the angle between the objective axis and the prism face normal and y the angle of refraction. The parallel shift h of the rays due to the refraction is

$$h=\frac{D\sin(x-y)}{\cos y}=D\sin x\left(1-\frac{\cos x}{\sqrt{(n^2-\sin^2 x)}}\right)=D\frac{n-1}{n}\left[x+\left(\frac{n+1}{2n^2}-\frac{1}{6}\right)x^3+\ldots\right], \qquad \ldots\ldots(1)$$

where the terms in x^5 and higher powers of x can be neglected for practical purposes. Equation (1) shows that the non-linear aberration of the parallel shift, represented by the term with x^3, is positive. A small pencil from any point M of the film produces an astigmatic image M′–M″ which is nearer to the optic axis by the distance (1) than the original point M.

Let now figure 2 represent another case in which narrow parallel pencils of the illuminating rays remain perpendicular, not to the film, but to the face p of the rotating prism. Let again x be the angle between the axis of the projection and the prism face normal. In this case there is no parallel shift, but, seen from the objective O, a point M of the film appears as an anastigmatic image M′ produced by the refraction at the prism. For pencils of small aperture the distance between M and M′ is

$$\mathrm{MM}'=D\frac{n-1}{n}. \qquad \ldots\ldots(2)$$

Relatively to the point M, the image M′ is nearer to the objective axis by the distance

$$h'=\mathrm{MM}'.\sin x=D\frac{n-1}{n}\left(x-\frac{x^3}{6}+\ldots\right). \qquad \ldots\ldots(3)$$

Equation (3) represents the compensation of the movement of the film in the case shown by figure 2, while equation (1) represents the same for the case of figure 1. Both cases involve non-linear aberrations, as shown by the presence of the terms with x^3; the essential difference, however, is that the sign of the aberration is different.

Figures 1 and 2 represent extreme cases in which the movement of the film is over-compensated or under-compensated. By a suitable choice of conditions, therefore, an intermediate case can be obtained in which the aberration term in x^3 disappears. The condition for this is provided by the following rule: the ratio of the angle of incidence of the principal ray illuminating a point of the film to the angle between the prism face normal and the objective axis must be constant during the rotation of the prism. This ratio is 1 in the case of figure 1, and 0 in the case of figure 2; the non-linear aberration disappears at an intermediate value which depends on the refractive index of the prism.

This optical condition for the elimination of the non-linear aberration of the image shift can be fulfilled, for example, by introducing between the film and the

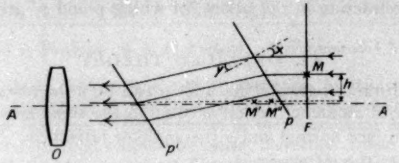

Figure 1.

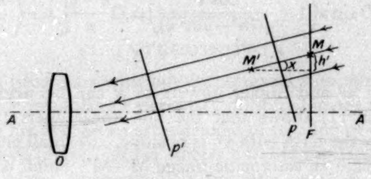

Figure 2.

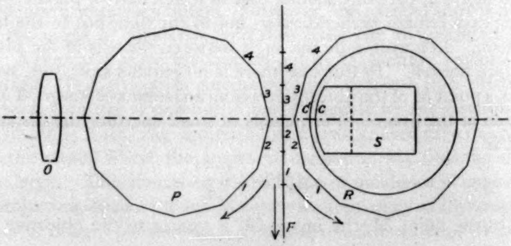

Figure 3.

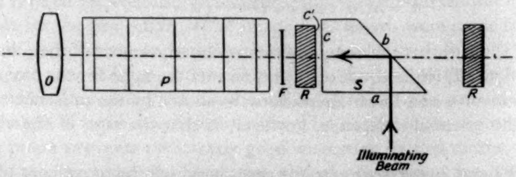

Figure 4.

light source a rotating optical device that influences the direction of the illuminating beam without taking part directly in the formation of the projected image by the objective. Figures 3 and 4 show a schematic arrangement of the projector with a suitable beam-deflecting device satisfying the optical condition just mentioned. In figure 3, O is the projection objective, P the rotating polygonal prism which produces a stationary image from the uniformly moving film F, R a rotating hollow polygonal prism which is the moving component of the beam-deflecting device. Inside R is the stationary component S with a cylindrical surface c concentric with the cylindrical inner surface c′ of the rotating component R. The uniform movement of the film F and the uniform rotation of P and R (as shown by the arrows) are mechanically synchronized and the consecutive pictures 1, 2, 3, 4 on the film correspond to the prism faces 1, 2, 3, 4 of P and R. The illuminating beam crosses the plane face a of the fixed prism S, the diagonal face b of which is a reflecting plane surface. The beam thus reflected at right angles crosses the concentric surfaces c and c′ and leaves the moving faces (2, 3 in figure 3) of the rotating polygonal prism R for traversing the film F, the rotating prism P and the objective O. The illuminating beam is more or less deflected according to the varying angle of refraction at the prism faces of the rotating polygon R. It is easily seen that the ratio of the angle of incidence of the principal ray traversing a point of the film to the angle between the prism face normal of P and the objective axis is approximately constant and less than 1. If this ratio has a suitable value, the non-linearity of the image shift is eliminated.

§ 3. FURTHER ABERRATIONS

In what follows, other aberrations produced by the rotating prism P will be discussed which, although less striking than the non-linearity of the image shift, must nevertheless be considered in any practical solution of the problem. These aberrations can be classified in two groups: (*a*) those which are essentially independent of the angular aperture of the illuminating beam, and (*b*) those which are proportional to the first and second powers of this angular aperture.

(*a*) The non-linearity of the image shift belongs to those aberrations which are essentially independent of the aperture; another is the chromatic variation of the image shift, which does not exceed the practically tolerable limit. A further aberration may arise as a consequence of film shrinkage, in which case the length of the film per image would become less than that on which the design of the prism is based. An optical compensation of film shrinkage by an automatically responding device is of course desirable when using considerably shrunk films in non-intermittent projectors; however, it would be difficult to discuss this question before treating the optical problems of the image formation in the standard case of non-shrunk film.

(*b*) The illuminating rays crossing the film have wide apertures in practical cases; consequently, the aberrations depending on the aperture need detailed investigation. These aberrations, which determine the quality of the projection if linearity of the image shift is achieved, will be treated in the following discussion of the image formation by wide-angle pencils starting from any point of the film.

Lens calculations, based on the approximation $\sin\alpha = \alpha - \alpha^3/6$, give account of the following five aberrations (apart from the chromatic error): spherical aberration, coma, astigmatism, curvature of field and distortion. It is possible to design the projection objective and the prism behind it, in the position in which the optic axis is perpendicular to the prism faces, together as a well-corrected lens system. Then the rotation of the prism produces periodic aberrations which have no axial symmetry and are to be related to the tangential and sagittal sections of the rotating prism. These prismatic aberrations are obviously analogous to the five lens aberrations above mentioned. For instance, the non-linearity of the image shift is an effect corresponding to the distortion in lens optics. There is a prismatic astigmatism, while the field curvature of lens optics corresponds here to the varying positions of the plane of the astigmatic image. Finally, the periodically varying prismatic coma is also a very interesting and practically important aberration. The analogy between these periodic aberrations due to the rotating prism and the axially symmetrical aberrations of lens optics becomes immediately obvious by considering the variation of the former during the rotation of the prism. Thus the axially symmetrical aberrations due to the prism, when its two faces are just perpendicular to the optic axis, will change continuously to the tangential and sagittal prismatic aberrations.

§4. TANGENTIAL RAY-TRACE

We begin by tracing tangential rays through the prism. Thus figure 5 is crossing the prism axis at right angles. Let M be a point on the film; p, p′, two parallel faces of the prism; x, the angle between the objective axis and the prism face normal; e–e, the second principal plane of the objective; MO, a ray through M parallel to the objective axis, crossing the principal plane e–e at O after traversing the prism faces p, p′. Let further B_+ and B_- be points of intersection of the plane e–e with two other rays from M; $+\tau$ and $-\tau$, the angle between these rays and MO; M′, virtual intersection of the rays MB_+ and MB_-; M'_+, virtual intersection of the rays MO and MB_+; M'_-, virtual intersection of the rays MO and MB_-; t–t, a plane through M′ parallel to e–e and to the film plane.

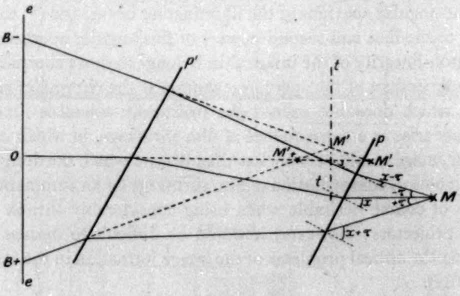

Figure 5.

We calculate first $M'O_+$ and M'_-O, i. e. the distances of these virtual image points from the principal plane. Let m be the distance of M from e–e. The parallel shift of the ray MO is

$$D \sin x\left(1 - \frac{\cos x}{\sqrt{(n^2 - \sin^2 x)}}\right) \qquad \ldots\ldots(4)$$

and the parallel shift of MB_+

$$D \sin(x+\tau)\left[1 - \frac{\cos(x+\tau)}{\sqrt{(n^2 - \sin^2(x+\tau))}}\right], \qquad \ldots\ldots(5)$$

wherein D is again the diameter of the inscribed cylinder in the prism. Then the distance OB_+ is

$$m \tan \tau + D \sin x\left(1-\frac{\cos x}{\sqrt{(n^2-\sin^2 x)}}\right) - D \sin(x+\tau)\left[1-\frac{\cos(x+\tau)}{\sqrt{(n^2-\sin^2(x+\tau))}}\right]\frac{1}{\cos\tau}. \qquad \ldots\ldots(6)$$

Introducing $t_+ = \mathrm{OM}'_+$, we obtain

$$t_+ = \frac{\mathrm{OA}_+}{\tan\tau} = m + D\frac{\sin x}{\tan\tau}\left(1-\frac{\cos x}{\sqrt{(n^2-\sin^2 x)}}\right) - D\frac{\sin(x+\tau)}{\sin\tau}\left[1-\frac{\cos(x+\tau)}{\sqrt{(n^2-\sin^2(x+\tau))}}\right], \qquad \ldots\ldots(7)$$

which, breaking off the series of the trigonometric functions after the second power, results in

$$t_+ = m - D\frac{n-1}{n}\left[1+\left(\frac{3}{2}\cdot\frac{n+1}{n^2}-\frac{1}{2}\right)x^2+\frac{3}{2}\cdot\frac{n+1}{n^2}x\tau+\frac{n+1}{2n^2}\tau^2\right]. \qquad \ldots\ldots(8)$$

Equation (8) reveals several aberrations:

The term in τ^2, being independent of the rotation of the prism, is simply the spherical aberration, and is the same as in the position when the prism faces are at right angles to the optic axis. The term in x^2 represents the position of the image formed by an infinitesimal pencil of rays in the tangential section through the prism. Finally, the term in $x\tau$ is a measure of the varying prismatic coma. It is of practical importance to find the intersection M′ of the rays MB_+ and MB_-. The distance of M′ from e–e is

$$m - D\frac{n-1}{n}\left[1+\left(\frac{3}{2}\cdot\frac{n+1}{n^2}-\frac{1}{2}\right)x^2+\frac{n+1}{2n^2}\tau^2\right] \qquad \ldots\ldots(9)$$

and the distance of M′ from the film plane

$$D\frac{n-1}{n}\left[1+\left(\frac{3}{2}\cdot\frac{n+1}{n^2}-\frac{1}{2}\right)x^2+\frac{n+1}{2n^2}\tau^2\right]. \qquad \ldots\ldots(10)$$

The term in τ^2 is of no importance, because the spherical aberration of the prism (in the perpendicular position to the optic axis) can be corrected by the projection objective.

In the image plane t–t the tangential coma produces the vertical aberration

$$\frac{\overline{M'_+M'_-}}{2}\,.\tan\tau = D\frac{n-1}{n}\cdot\frac{3}{2}\cdot\frac{n+1}{n^2}x\tau\,.\tan\tau \approx D\,.\,\frac{3}{2}\,\frac{n^2-1}{n^3}x\tau^2. \qquad \ldots\ldots(11)$$

§5. SAGITTAL RAY-TRACE

The tracing of sagittal rays through the prism can be effected by reference to the perspective drawing figure 6. Taking M, a point on the film; MK, a ray parallel to the optic axis; MK′, another ray in a sagittal plane, i. e. in a plane parallel to the prism axis (and parallel to the objective axis, in the particular case of figure 6); and taking also K and K′, the points of incidence of these rays on the prism face p; V, the point of intersection of the perpendicular from M with the prism face, we get T for the point on this perpendicular for which MK⊥TK and write x, the angle of incidence of the ray MK; α, the angle of incidence of the ray MK′; σ, the angle between MK and MK′; ϑ, the angle between MK′ and K′T; ω, the angle between KT and K′T. We use the sign ∢ for a right angle.

For the triangle KVK′ we have

$$\sin^2\alpha = \sin^2\sigma + \cos^2\sigma \,.\, \sin^2 x. \qquad \ldots\ldots(12)$$

It may be noted that the refracted rays of MK and MK′—which are not shown in figure 6—have no vertical intersection, unless σ is infinitely small. Consequently, there is no Pythagorian equation for the corresponding angles of refraction.

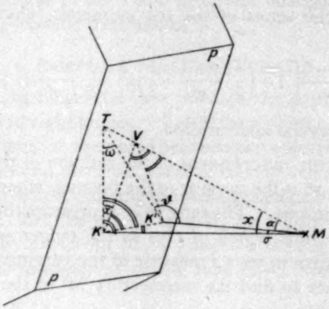

Figure 6.

We find for triangle KTK′

$$\frac{\sin\sigma}{\sin\omega} = \frac{\cos\sigma \,.\, \tan x}{\cos\omega} \qquad \ldots\ldots(13)$$

and for triangle MK′T

$$\frac{\sin\sigma}{\sin\omega} : \frac{\cos\sigma}{\cos x} = \sin\alpha : \sin\vartheta. \qquad \ldots\ldots(14)$$

(13) and (14) give

$$\frac{\sin x}{\cos\omega} = \frac{\sin\alpha}{\sin\vartheta}. \qquad \ldots\ldots(15)$$

The ray MK′, after refraction at two parallel faces of the prism, has suffered a parallel shift of magnitude,

$$d = D\sin\alpha\left(1 - \frac{\cos\alpha}{\sqrt{(n^2 - \sin^2\alpha)}}\right), \qquad \ldots\ldots(16)$$

in the plane of incidence. Produced backwards, the refracted ray intersects the film in a point whose distance from M is

$$d/\sin\vartheta, \qquad \ldots\ldots(17)$$

since the film plane and the triangle KTK′ are parallel. The displacement (17) in the film plane has a vertical component

$$d\cos\omega/\sin\vartheta \qquad \ldots\ldots(18)$$

and a horizontal component

$$d \sin\omega / \sin\vartheta \qquad \ldots\ldots(19)$$

(the prism axis being assumed horizontal).

The vertical component (18) can be obtained from (15) and (16); if the power series for the trigonometrical functions are broken off after the second term, we have

$$d\frac{\cos\omega}{\sin\vartheta} = D\sin x\left(1-\frac{\cos\alpha}{\sqrt{(n^2-\sin^2\alpha)}}\right) \approx D\frac{n-1}{n}x\left[1+\left(\frac{n+1}{2n^2}-\frac{1}{6}\right)x^2+\frac{n+1}{2n^2}\sigma^2\right]. \qquad \ldots\ldots(20)$$

The horizontal component (19) is given by (13) and (15)

$$d\frac{\sin\omega}{\sin\vartheta} = D.\tan\sigma.\cos x\left(1-\frac{\cos\alpha}{\sqrt{(n^2-\sin^2\alpha)}}\right). \qquad \ldots\ldots(21)$$

Let us now consider in the plane MK′K of figure 6 another ray at an angle $-\sigma$ with MK, so that this new ray and the ray MK′ have a point of intersection the distance of which from the film plane is

$$d\frac{\sin\omega}{\sin\vartheta}\cdot\frac{1}{\tan\sigma} = D\cos x\left(1-\frac{\cos\alpha}{\sqrt{(n^2-\sin^2\alpha)}}\right) \approx D\frac{n-1}{n}\left[1+\left(\frac{n+1}{2n^2}-\frac{1}{2}\right)x^2+\frac{n+1}{2n^2}\sigma^2\right]. \qquad \ldots\ldots(22)$$

In (22), the term in σ^2 is the spherical aberration of the prism, which does not change during the rotation, while the term in x^2 gives the position of the image formed by an infinitesimal pencil of rays in the sagittal section of the prism.

The difference between the x^2-terms of (10) and (22),

$$D\frac{n^2-1}{n^3}x^2, \qquad \ldots\ldots(23)$$

is the distance between the tangential and the sagittal points of intersection, i.e. the prismatic astigmatism.

In (20) the term with x^3 is the well known non-linear aberration of the parallel shift, and the term in $x\sigma^2$ is the sagittal coma.

§ 6. CONCLUSION

These aberrations have been calculated for the special example where the principal ray illuminating any point of the film is parallel to the objective axis. The formulae are the same for any other direction of the rays; in the general case, however, x does not mean the angle between the prism face normal and the objective axis, but the angle of incidence of the principal ray from any point on the film. τ and σ are always the tangential and sagittal angular semi-apertures of the wide-angle pencil illuminating a point of the film. In the general case, these aberrations as vector quantities have to be related to the direction of the principal ray in question, not to the axis of the objective.

A more detailed discussion of how the results given in the present paper can be used for the optical correction of the image formation in the rotating prism projector will be published later.

REFERENCE

Taylor, Dennis H., 1937. *Proc. Phys. Soc.*, **49**, 663.

THE ROTATIONAL ANALYSIS OF SOME BANDS OF THE NEAR ULTRA-VIOLET SYSTEM (D–X) OF SILICON MONOSULPHIDE

By R. F. BARROW,
Physical Chemistry Laboratory, University of Oxford

MS. received 25 *May* 1946

ABSTRACT. A rotational analysis has been done of the 0,1, 0,2, 0,3, 0,4, and 1,5 bands of the near ultra-violet band-system ($\nu_e \simeq 35030$ cm.$^{-1}$) of SiS. The transition responsible for the production of the band-system is of the type D $^1\Pi$ – X $^1\Sigma$. The rotational constants have been derived from two sets of experimental observations : (i) of the bands in absorption, by G. Herzberg, N. Olson and F. J. Wilson (University of Saskatchewan), and (ii) of the bands in emission, by the author. The more important constants are given by

$$B_v'' = 0{\cdot}3036 - 0{\cdot}0014_9\,(v'' + \tfrac{1}{2}), \text{ for the ground state, and}$$
$$B_v' = 0{\cdot}2664 - 0{\cdot}0020_5\,(v' + \tfrac{1}{2}) \text{ for the upper state.}$$

Λ-type doubling in the upper $^1\Pi$ state is negligibly small, at least up to $J=100$. The values of the equilibrium internuclear distances are $r_e'' = 1{\cdot}929$ A. and $r_e' = 2{\cdot}059_5$ A. A brief discussion of the results is given.

§1. INTRODUCTION

The production and vibrational analysis of a near ultra-violet band-system of silicon monosulphide ($\nu_e \simeq 35030$ cm.$^{-1}$) were described some time ago by Barrow and Jevons (1938). Since then, a preliminary account has been given of the rotational analysis of the 0,1, 0,2 and 0,3 bands of this system (Barrow, 1944), which was shown to be due to a transition of the type $^1\Pi - {}^1\Sigma$. The present paper gives the results of a more detailed analysis of these three bands and of the 0,4 and 1,5 bands of the same system.

Two distinct sets of experimental material have been used. When the preliminary analysis of the 0,1, 0,2 and 0,3 bands from my own plates, taken in emission, had been completed, I learned from Professor G. Herzberg that Mr. N. Olson and Mr. F. J. Wilson, working in his laboratory at Saskatchewan on plates of the bands in absorption taken by Olson, had already carried out analyses of the 0,1, 0,2, 0,3, 0,4 and 0,5 bands. Their results proved to be in close agreement with mine. Professor Herzberg then most kindly sent me the detailed measurements and analyses: the results to be given are based, where possible, on the averaged measurements of the two independent sets of investigations.

§2. EXPERIMENTAL METHODS

Olson photographed the bands in absorption. SiS, prepared by the method described by Barrow and Jevons (1938), was sublimed into an electrically-heated T-shaped quartz tube. This consisted of an absorption tube, 15–20 cm. long and 2·5 cm. in internal diameter, fitted with a central T-piece which acted as a reservoir for SiS and through which the whole system could be evacuated and ultimately sealed. Independent heating of the reservoir and of the main tube minimized deposition of SiS on the windows of the latter. The tubes were operated at about 900° c. A hydrogen lamp was used as source of continuous radiation, and the bands were photographed in a second order of a 6-m. concave grating spectrograph on Eastman " 40 " plates.

The experimental arrangements used in developing the SiS system in emission have already been described (Barrow and Jevons, 1938). The region 2800–3100 A. was photographed in a fourth order of the 10-ft. concave grating at Imperial College, London. The grating itself largely absorbed the overlapping fifth order: the overlapping part of the third order was absorbed in a 2-cm. column of an aqueous solution of cobalt and nickel sulphates containing 4·15 g. $CoSO_4 . 7H_2O$ and 14·5 g. $NiSO_4 . H_2O$ dissolved in 100 c.c. water (Bowen, 1942). Ilford "Zenith" plates were used, and exposure times were of the order of two hours.

§ 3. ROTATIONAL ANALYSIS

The 0,1, 0,2, and 0,3 bands were first selected for analysis as their structure is little overlaid by that of other bands. However, the 0,2 band, which appeared to be particularly simple, proved to suffer from considerable overlapping of the branches, and the 0,1 and 0,3 bands were therefore examined first. In no bands were the lines resolved close to the heads, but further away from the heads three branches were apparent, one of which—the *Q* branch—was considerably stronger than either of the others.

By a trial and error study of the first differences, $R(J)-Q(J)\simeq Q(J+1)-P(J+1)$, it turned out to be an easy matter, first to identify the *P* and *R* branches, then to ascertain the absolute *J*-numbering, and finally, using a rough value of D, obtained from the relation $D=-4B^3/\omega$, to get fairly accurate values of the constants B for the 0,1, 0,3 and 0,2 bands.

At this stage I received the data of Olson on the 0,2 and 0,3 bands and of Wilson on the 0,1, 0,4, and 1,5 bands. Their assignments of the lines of the 0,1, 0,2 and 0,3 bands agreed with mine in detail, and, after taking account of a small systematic difference in the wave-numbers of the lines (my values were on an average 0·35 $cm.^{-1}$ lower), means of the wave-numbers of the lines of these three bands were taken. Only Wilson measured the 0,4 and 1,5 bands. The wave-numbers are displayed in table 1.

The procedure adopted for the final evaluation of the constants was as follows. The constants which could be determined with the highest absolute accuracy were obviously those for the upper state with $v'=0$, for which there were measurements of four bands. Either $\Delta_1F'(J)$ or $\Delta_2F'(J)$ differences could have been used: eventually the former,

$$\Delta_1F'(J)=R(J)-Q(J)\simeq Q(J+1)-P(J+1),$$

were chosen after it had been demonstrated that, within the limits of error of the measurements, the differences $R(J)-Q(J)$ were equal to $Q(J+1)-P(J+1)$, up to the highest *J*-values ($J\sim 100$). Thus the Λ-type doubling of the upper $^1\Pi$ state is very small—as would be expected by analogy with the results of the analysis of bands of the similar system of SiO (Saper, 1932).

Table 1 Observed wave numbers of rotational lines (cm.$^{-1}$, *in vac.*)

Asterisks indicate unresolved lines

v', v''	0,1			0,2			0,3			0,4			1,5		
J	$Q(J)$	$R(J)$	$P(J)$	$Q(J)$	$R(J)$	$P(J)$	$Q(J)$	$R(J)$	$P(J)$	$Q(J)$	$R(J)$	$P(J)$	$Q(J)$	$R(J)$	$P(J)$
20	34148·60*	34159·76*	34138·36*	33409·88*		33399·89*	32676·16*	32687·48*	32665·68*	31948·17*		31937·13*	31730·97*		31720·39*
21	47·36*	58·94*	36·32*	08·36*		97·93*	74·97	86·76*	63·54*	46·86*		35·34*	29·51*		18·71*
22	45·52*	57·73*	34·34*	06·79*		95·74*	73·46	85·81*	61·63*	45·50*		33·18*	28·08*		16·75*
23	43·79*	56·68*	31·71	05·25*		93·42*	72·15	84·76*	59·57*	43·84*		31·76*	26·90*		14·73*
24	42·13*	55·36*	29·55	03·45*		91·20*	70·55	83·52*	57·52*	42·27*		29·74*	25·33*		12·79*
25	40·31*	54·07*	27·12	01·71*		88·97*	68·80	82·37*	55·39*	40·58*		27·62*	23·61*		10·69*
26	38·36*	52·87*	24·68	399·89*		86·68*	67·10	81·20*	53·11*	38·90*		25·53*	22·30*		08·43*
27	36·32*	51·57*	22·10	97·93*		84·34*	65·25	80·00*	50·83*	37·13*		23·28*	20·39*	31734·85*	06·18*
28	34·34*	50·11*	19·63	96·24		81·71*	63·54*	78·88*	48·44*	35·34*	31950·40*	21·40*	18·71*	33·52*	03·91*
29	32·51	48·60*	17·07	94·32		79·28*	61·63*	77·60*	45·99*	33·18*	49·54*	18·69*	16·75*	32·33*	01·59*
30	30·08	46·90	14·46	92·12		76·79*	59·57*	75·90*	43·49*	31·76*	48·17*	15·84	14·73*	30·97*	699·31*
31	27·81	44·96	11·65	90·05		73·98*	57·52*	74·38*	40·95*	29·74*	46·86*	13·44	12·79*	29·51*	96·51*
32	25·89*	43·31	08·77	87·76	33405·25*	71·25*	55·39*	72·72*	38·41*	27·62*	45·50*	10·83	10·69*	28·08*	94·01*
33	23·42*	41·38	05·91	85·55	03·45*	68·36*	53·11*	71·11*	35·75*	25·53*	43·84*	08·23	08·43*	26·90*	91·30*
34	20·86*	39·43	02·83	83·17	01·71*	65·48*	50·83*	69·29*	32·94*	23·28*	42·27*	05·54	06·18*	25·33*	88·62*
35	18·33*	37·38	099·77	80·61	399·89*	62·39*	48·44*	67·61*	30·20*	21·40*	40·58*	02·80	03·91*	22·30*	85·82*
36	15·84*	35·32	96·57	78·23	97·93*	59·39*	45·99*	65·68*	27·36*	18·69*	38·90*	899·98	01·59*	20·39*	83·35*
37	13·08*	32·86	93·42	75·62	95·74*	56·34*	43·49*	63·54*		16·91*	37·13*	97·10	699·31*	18·71*	80·48*
38	10·25*	30·84	90·21	73·04	93·42*	53·14*	40·95*	61·65*		14·43*	35·34*	94·21	96·51*	16·75*	77·09*
39	07·36*	28·43	86·74	70·38	91·20*	49·77*	38·41*	59·57*		12·07*	33·18*	91·08	94·01*	14·73*	73·80*
40	04·41*	25·89*	83·31	67·41	88·97*	46·35*	35·75*	57·52*		09·39*	30·85	88·09	91·30*	12·79*	70·63*
41	01·45*	23·42*	79·87	64·63	86·68*	43·06*	32·94*	55·39*	11·59	06·80*	28·76	85·00	88·62*	10·69*	67·49*
42	098·29*	20·86*	76·31	61·92	84·34*	39·57*	30·20*	53·11*	08·20	04·07*	26·65	81·74	85·82*	08·43*	64·15*
43	95·13*	18·33*	72·52	58·84	81·71*	36·09*	27·36*	50·83*	04·79	01·28*	24·42	78·47	83·35*	06·18*	61·05*
44	91·89*	15·84*	68·75	55·88	79·28*	32·41*	24·46	48·44*	01·19	898·43*	22·18	75·12	80·48*	03·91*	57·36*
45	88·64*	13·08*	64·96	52·74	76·79*	28·81*	21·35	45·99*	597·74	95·56*	20·10	71·76	77·09*	01·59*	53·86*
46	85·33*	10·25*	61·17	49·77*	73·98*	24·91*	18·30	43·49*	94·26	92·57*	16·91*	68·33	74·65	699·31*	50·51*
47	81·78*	07·36*	57·45	46·35*	71·25*	21·11*	15·15	40·65	90·34	89·50*	14·43*	64·77	71·65	96·51*	46·69*
48	78·35*	04·41*	53·23	43·06*	68·36*	17·24*	12·01	37·90	86·61	86·46*	12·07*	61·10	68·38	94·01*	43·11*
49	74·92	01·45*	49·20	39·57*	65·48*	13·37*	08·77	35·20	82·93	83·26*	09·39*	57·51	64·92	91·30*	39·45*

50	71·38	098·29*	44·87	36·09*	62·39*	09·34*	05·40	32·40	78·95	79·99*	06·80*	53·76	62·70	88·62*	35·46*
51	67·63	95·13*	40·63	32·41*	59·39*	05·22*	01·97	29·60	75·02	76·80*	04·07*	49·91	59·32	85·82*	31·66*
52	63·80	91·89*	36·48	28·81*	56·34*	01·01*	598·49	26·55	71·05	73·27*	01·28*	45·97	55·66	83·35*	27·79*
53	59·91	88·64*	31·95	24·91*	53·14*	296·78*	94·92	23·45	66·97	69·95*	898·43*	42·08	51·85	80·48*	23·49*
54	56·02	85·33*	27·51	21·11*	49·77*	92·48*	91·31	20·25	62·78	66·43*	95·56*	38·18	48·18	77·09*	19·35*
55	51·94	81·78*	22·94	17·24*	46·35*	88·07*	87·62	17·20	58·60	62·89*	92·57*	34·06	44·66	73·80*	16·25
56	47·78	78·35*	18·51	13·37*	43·06*	83·66*	83·81	13·91	54·30	59·55	89·50*	29·95	40·93	70·63*	12·02
57	43·58	74·29	13·58	09·34*	39·57*	79·24*	79·98	10·58	50·00	55·94	86·46*	25·88	37·14	67·49*	07·44
58	39·42	70·55	08·99	05·22*	36·09*	74·69*	76·12	07·10	45·66	52·13	83·26*	21·55	33·26	64·15*	03·23
59	35·12	66·93	04·03	01·01*	32·41*	69·94*	72·16	03·67	41·01	48·30	79·99*	17·13	29·55	61·05*	598·63
60	30·66	62·96	33999·07	296·78*	28·81*	65·27*	68·05	00·25	36·49	44·41	76·80*	12·85	25·60	57·36*	94·18
61	26·26	58·84	94·12	92·48*	24·91*	60·47*	63·94	596·57	31·78	40·48	73·27*	08·35	21·54	53·86*	89·69
62	21·69	54·81	88·92	88·07*	21·11*	55·58*	59·77	93·07	27·20	36·45	69·95*	04·18*	17·49	50·51*	85·18
63	17·01	50·70	83·95	83·66*	17·24*	50·61*	55·51	88·94	22·40	32·47	66·43*	799·65*	13·27	46·69*	80·54
64	12·33	46·52	78·63	79·24*	13·37*	45·59*	51·18	85·29	17·62	28·28	62·89*	94·80*	09·05	43·11*	75·73
65	07·53	42·15	73·24	74·69*	09·34*	40·41*	46·76	81·47	12·56	23·99	58·73	90·05*	04·83	39·45*	70·94
66	02·53	37·83	67·92	69·94*	05·22*	35·26*	42·17	77·57	07·59	19·75	54·92	85·25*	00·48	35·46*	66·11
67	33997·83	33·49	62·50	65·27*	01·01*	30·01*	37·76	73·58	02·60	15·50	51·13	80·42*	595·85	31·66*	61·07
68	92·74	29·12	57·07	60·47*	296·78*	24·65*	33·17	69·39	497·43	11·08	47·26	75·43*	91·42	27·79*	56·03
69	87·68	24·44	51·39	55·58*	92·48*	19·20*	28·44	65·28	92·26	06·63	43·29	70·36*	86·99	23·49*	50·82
70	82·51	19·84	45·99*	50·61*	88·07*	13·74*	23·71	61·01	86·94	02·07	39·28	65·29*	82·27	19·35*	45·91
71	77·22	15·05	40·23*	45·59*	83·66*	08·19*	19·04	56·74	81·66	797·41	35·21	60·20*	77·58	14·99	40·66
72	71·91	10·21	34·38*	40·41*	78·59	02·63*	14·09	52·45	76·25	92·80	31·09	54·86*	72·82	10·66	35·47
73	66·62	05·45	28·45*	35·26*	74·09	196·89*	09·09	47·90	70·78	87·98	26·94	49·57*	67·92	06·46	29·62
74	61·04	00·46	22·49*	30·01*	69·29	91·15*	04·07	43·29	65·30	83·14	22·59	44·20*	63·02	02·09	24·58
75	55·58	33995·23	16·31*	24·65*	64·45	85·27*	498·97	38·72	59·50	78·24	18·26	38·47*	58·02	597·56	
76	49·88	90·23	10·22*	19·20*	59·59	79·34*	93·75	34·05		73·24	13·67		53·00	92·92	
77	44·33	85·00	03·87*	13·74*	54·67	73·28*	88·50	29·20		68·22	09·12		47·86	88·39	
78	38·57	79·73	897·49*	08·19*	49·55	67·20*	83·20	24·35		63·27	04·18*		42·58	83·86	
79	32·52	74·25	91·05*	02·63*	44·38	61·11*	77·65	19·45		58·06	799·65*		37·47	78·94	
80	26·55	68·91	84·53*	196·89*	39·12	54·83*	72·15	14·65		52·80	94·80*		31·94	74·03	
81	20·58	63·42	77·95*	91·15*	34·09	48·47*	66·60			46·96	90·05*		26·68	69·42	
82	14·40	57·61	71·51	85·27*	28·66	42·20*	60·90			42·08	85·25*		21·24	64·31	
83	08·07	51·86	64·97	79·34*	23·17	35·68*	55·35			36·49	80·42*			59·19	
84	01·96	45·99*	58·31	73·28*	17·71	29·17*	49·60				75·43*				

Table 1—*continued*

Asterisks indicate unresolved lines

v', v''	0,1			0,2			0.3			0,4			1,5		
J	$Q(J)$	$R(J)$	$P(J)$	$Q(J)$	$R(J)$	$P(J)$	$Q(J)$	$R(J)$	$P(J)$	$Q(J)$	$R(J)$	$P(J)$	$Q(J)$	$R(J)$	$P(J)$
85	895·61	40·23*	51·29	67·20*	12·17	22·55*	43·75				70·36*				
86	89·28	34·38*	44·36	61·11*	06·39	15·89					65·29*				
87	82·62	28·45*	37·37	54·83*	00·69	09·24					60·20*				
88	76·14	22·49*	30·29	48·47*	194·76	02·44					54·86*				
89	69·42	16·31*	23·05	42·20*	88·99	095·54					49·57*				
90	62·74	10·22*	15·82	35·68*	82·88	88·39					44·20*				
91	55·78	03·87*	08·37	29·17*	76·78	81·34					38·47*				
92	48·87	897·47*	00·93	22·55*	70·76	74·29									
93	41·94	91·05*	793·53	15·59	64·56	66·94									
94	34·86	84·53*	85·98	08·79	58·12	59·74									
95	27·91	77·95*	78·10	01·89	51·85	52·64									
96	20·35	71·17	70·35	094·99	45·33	45·09									
97	13·19	64·16	62·86	87·89	38·91	37·54									
98	05·67	57·15	54·74	80·74	32·16	29·84									
99	798·24	50·17	47·20	73·54	25·41	22·04									
100	90·65	43·16	38·85	66·29	18·74	14·44									
101	83·34	35·95	30·91	59·09	11·88	06·79									
102	75·48	28·89	22·43	51·64	04·79	32998·64									
103	67·67		14·13	43·99	097·84	90·69									
104	59·71		05·82	36·34	90·79	82·64									
105	51·50			28·74	83·59										
106	43·49			20·99	76·34										
107	35·32			12·99	69·14										
108	27·02			05·19	61·59										
109	18·64			32997·24	54·04										
110	10·47			89·04	46·74										
111	02·06			80·99	38·99										

It is a familiar result that

$$\frac{\Delta_1 F(J)}{(J+1)} = 2B + 4D(J+1)^2 + 6F(J+1)^4 + \ldots, \qquad \ldots\ldots(1)$$

where B, D and F are the constants in the expression for the rotational energy levels,

$$F(J) = B\,.\,J(J+1) + D\,.\,J^2(J+1)^2 + F\,.\,J^3(J+1)^3 + \ldots, \qquad \ldots\ldots(2)$$

and generally, $B \gg D \gg F$.

Thus, a plot of $\dfrac{\Delta_1 F(J)}{J+1}$ against $(J+1)^2$ should—at least for moderate values of J—yield a straight line of intercept $2B$ and of slope $4D$. A selection of $\Delta_1 F_0'(J)$ values for $v' = 0$ is given in table 2, and a plot of $\dfrac{\Delta_1 F_0'(J)}{J+1}$ against $(J+1)^2$ is shown in figure 1. From the latter it appeared safe—in the first instance—to neglect terms in F, and the best straight line was therefore drawn through all the points with $J > 45$, using the centre-of-gravity method. This gave $B_0' = 0{\cdot}2653_3$ and $D_0' = -2{\cdot}85 \times 10^{-7}$ cm.$^{-1}$.

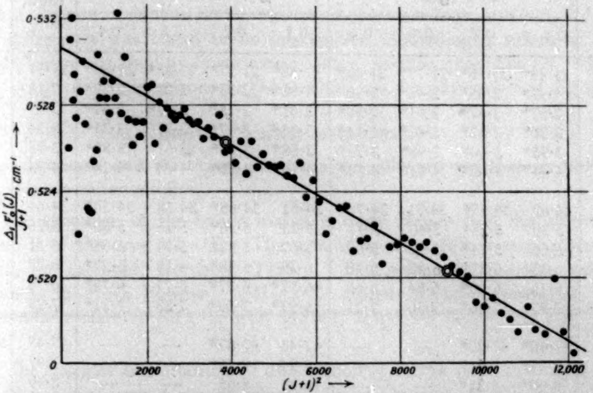

Figure 1. $\dfrac{\Delta_1 F_0'(J)}{J+1}$ as a function of $(J+1)^2$.

The two points ◎ represent the mean values for $J = 45$–76, 77–111: their coordinates are (0·52626, 3868) and (0·52027, 9127), giving $2B_0' = 0{\cdot}5306_6$, $4D_0' = 1{\cdot}14 \times 10^{-6}$.

It was considered that the measurements of the Q-branch lines were more reliable than those of either P- or R-branch lines, and the lower-state constants for the 0,1, 0,2, 0,3, and 0,4 bands were therefore determined from the Q line in the following way. The wave-number of any such line is given by

$$Q(J) = \nu_0 + (B' - B'')\,.\,J(J+1) + (D' - D'')\,.\,J^2(J+1)^2 + \ldots, \qquad \ldots\ldots(3)$$

where ν_0 is the band-origin. Provisional values of B'' and of D'', obtained from $\Delta_1 F''(J)$ and $\Delta_2 F''(J)$ differences, were inserted in (3), and preliminary values of

ν_0, which we may write $\bar{\nu}_0$, calculated for each line, thus

$$\bar{\nu}_0 = Q(J) - \overline{(B'-B'')}\,.\,J(J+1) - \overline{(D'-D'')}\,.\,J^2(J+1)^2 - \ldots, \qquad \ldots\ldots (3\,\text{a})$$

where the horizontal bars indicate provisional values. In general these $\bar{\nu}_0$ values were not quite constant with J, since the $\overline{(B'-B'')}$ and $\overline{(D'-D'')}$ values were not quite correct. If the differences between the true and the provisional values are indicated by Δ's—thus, $\Delta\nu_0 = \nu_0 - \bar{\nu}_0$,—then

$$\Delta\nu_0 = -\Delta(B'-B'')\,.\,J(J+1) - \Delta(D'-D'')\,.\,J^2(J+1)^2 - \ldots \qquad \ldots\ldots (3\,\text{b})$$

The $\bar{\nu}_0$ values were then plotted against $J(J+1)$: the intercept gave ν_0, and the slope at low values of $J(J+1)$ the correction $-\Delta(B'-B'')$. New values of $\bar{\nu}_0$ were then calculated, with the corrected $(B'-B'')$ terms, but with the same $\overline{(D'-D'')}$ terms. Plots of $\Delta\nu_0$ from these $\bar{\nu}_0$ values against $J^2(J+1)^2$ enabled $\Delta(D'-D'')$ to be evaluated.

Table 2. Some values of $\Delta_1 F_0'(J)$

J	$R(J)-Q(J)$				$Q(J+1)-P(J+1)$				Mean obs.	Calc.
	0,1	0,2	0,3	0,4	0,1	0,2	0,3	0,4		
40	21·48*	21·56*	21·77*	21·46*	21·58*	21·57*	21·35*	21·80*	21·57	21·68
41	1·97*	2·05*	2·45*	1·96*	1·98*	2·35*	2·00*	2·33*	2·14	2·21
42	2·57*	2·42*	2·91*	2·58*	2·61*	2·75*	2·57*	2·81*	2·65	2·73
43	3·20*	2·87*	3·47*	3·14*	3·14*	3·47*	3·27	3·31*	3·24	3·25
44	3·95*	3·40*	3·98*	3·75*	3·68*	3·93*	3·61	3·80*	3·75	3·78
45	4·44*	4·05*	4·64*	4·54*	4·16*	4·86*	4·04	4·24*	4·33	4·30
65	34·62	34·65*	34·71	34·74	34·61	34·68*	34·58	34·50*	34·64	34·69
66	5·30	5·28*	5·40	5·17	5·33	5·26*	5·16	5·08*	5·26	5·21
67	5·66	5·74*	5·82	5·63	5·67	5·82*	5·74	5·65*	5·71	5·72
68	6·38	6·31*	6·22	6·18	6·29	6·38*	6·18	6·27*	6·27	6·25
69	6·76	6·90*	6·84	6·66	6·52*	6·87*	6·77	6·78*	6·76	6·76
70	7·33	7·46*	7·30	7·21	6·99*	7·40*	7·38	7·21*	7·29	7·27
90	47·48*	47·20*	—	—	47·41	47·83*	—	—	47·47	47·42
91	8·09*	7·61*	—	—	7·94	8·26*	—	—	7·97	7·92
92	8·60*	8·21*	—	—	8·41	8·65	—	—	8·49	8·42
93	9·11*	8·97	—	—	8·88	9·05	—	—	8·99	8·92
94	9·67*	9·33	—	—	9·81	9·25	—	—	9·49	9·42
95	50·04*	9·96	—	—	50·00	9·90	—	—	9·97	9·92

* Asterisks indicate values involving the wave-numbers of unresolved lines.

When this had been done, it was found that the values of ν_0 calculated from (3) with the now corrected values of $(B'-B'')$ and of $(D'-D'')$ still showed some systematic departure from constancy in the region of the highest J values (90–110). The magnitude of terms in $(F'-F'')\,.\,J^3(J+1)^3$ was therefore considered. F' and F'' were calculated from the relation

$$F = \frac{2D^2}{B} + \frac{\alpha_1 \omega D^2}{6B^3}$$

(see, for example, Jevons, 1932). The results were

$$F' = -1{\cdot}7 \times 10^{-13}\,\text{cm}^{-1},$$
$$F'' < 10^{-14}\ \text{cm}^{-1},$$

so that, approximately,

$$(F' - F'') = -1{\cdot}7 \times 10^{-13}.$$

The addition of the terms $-1{\cdot}7 \times 10^{-13} \,.\, J^3(J+1)^3$ to (3) was found to lead to values of ν_0 which were then sensibly constant over the whole range of J values for all these four bands.

The constants derived in this way were finally checked by calculating the wave numbers of all the measured lines of the four bands, by first evaluating the Q branches and then using the calculated $\Delta_1 F_0'(J)$ values to get the P- and R-branch lines.

The lines of the 1,5 band were so often superimposed on other lines of the same band that accurate evaluation of the rotational constants from either $\Delta_1 F(J)$ or $\Delta_2 F(J)$ differences was found to be impossible. Accordingly, values of B_5'' and of D_5'' were obtained by linear extrapolation, and the quantities $(B_1' - B_5'')$ and $(D_1' - D_5'')$ determined from the Q-branch lines in the way described above.

§4. RESULTS AND DISCUSSION

The vibrational and rotational constants are collected together in tables 3 and 4: some comments follow.

(i) The structure of the bands makes it quite certain that the electronic transition is of the type ${}^1\Pi - {}^1\Sigma$. The ground state of SiS is most probably ${}^1\Sigma^+$ (see, for example, Herzberg, 1939). The system is therefore exactly analogous to the "4th Positive" A ${}^1\Pi$ – X ${}^1\Sigma^+$ system of carbon monoxide, and to the similar system of SiO, as was, indeed, suspected before the rotational analysis.

(ii) The energies and products of dissociation of SiS in these two states will be considered in a later paper on another ultra-violet system of SiS (see also Vago and Barrow, 1946). However, it may be noted that the fact that the D ${}^1\Pi$ state is a singlet makes it most probable that it, like the ground state, dissociates into the ground state atoms, Si(${}^3P$) + S(${}^3P$).

(iii) The new values of ω_e'' and of $x_e''\omega_e''$, determined from the band-origins, are very close to the values obtained from the original band-head measurements. As the analysis shows, this agreement arises from the circumstances that the band-heads are not very far from the origins ($\sim$2 cm.$^{-1}$), and that the separation, head-origin, changes only rather slowly from band to band.

(iv) It is to be expected that SiS should have a similar electronic configuration in its ground state to the isosteric molecule P_2, which also has 30 extra-nuclear electrons. As with other sets of such molecules, this may account for the rather striking similarity in the ground-state constants (table 5). However, no upper state of P_2 corresponding to the D ${}^1\Pi$ level of SiS is known.

(v) The bond distance in the ground state of SiS, about 1·93 A., is some 0·22 A. shorter than the uni-covalent distance (Schomaker and Stevenson, 1940). The bond in SiS is, of course, expected to be stronger, and thus shorter, than a single covalent bond, and the observed degree of shortening is in reasonable accord with the figures of 0·25 and 0·15 A. for the ground states of the similar molecules SiO and GeO.

Table 3. Constants of the D $^1\Pi$ and X $^1\Sigma^+$ states of SiS

State :	X $^1\Sigma^+$		D $^1\Pi$	
ν_e	0 cm.$^{-1}$		35028·8 cm.$^{-1}$	H
ω_e	749·65			
	(749·5)	H	512·0	H
$x_e\omega_e$	−2·575			
	(−2·56)	H	−2·38	H
$y_e\omega_e$	—		−0·045	H
B_4	0·2969$_3$		—	
B_3	0·2984$_1$		—	
B_2	0·2999$_3$		—	
B_1	0·3014$_0$		0·2632$_8$	
B_0	0·3028$_9$		0·2653$_3$	
B_e	0·3036$_3$		0·2663$_6$	
α_1	−0·0014$_9$		−0·0020$_5$	
D_4	$-1{\cdot}9_7\times10^{-7}$		—	
D_3	$-1{\cdot}9_8\times10^{-7}$		—	
D_2	$-1{\cdot}9_9\times10^{-7}$		—	
D_1	$-2{\cdot}0_0\times10^{-7}$		$-2{\cdot}95\times10^{-7}$	
D_0	—		$-2{\cdot}85\times10^{-7}$	
F	—		$-1{\cdot}7\times10^{-13}$	
r_0	1·931$_4$ A.		2·063$_6$ A.	
r_e	1·929$_0$ A.		2·059$_5$ A.	

Notes : (1) The values of r were obtained from $r=\dfrac{4{\cdot}1065}{\sqrt{\mu B}}$ A., where μ is the reduced mass in physical atomic weight units. μ was calculated for ^{28}Si ^{32}S, with Si=27·987 and S=31·982.

(2) H signifies a constant derived from band-head data.

Table 4. Positions of band-origins

Band	Origin
0,1	34163·8$_8$ cm.$^{-1}$
0,2	3424·5$_4$
0.3	2690·3$_1$
0,4	1961·2$_7$
1,5	1744·6$_1$

Table 5. Comparisons of the constants of SiS with those of the isosteric molecule P_2*

	State	ω_e	Force constant	Dissociation energy	B_e	r_e
SiS	X $^1\Sigma^+$	749·65	$4{\cdot}94\times10^5$ dyne/cm.	6·6 ev.	0·3036	1·929 A.
P_2	X $^1\Sigma_g^+$	780·43	5·56	5·03	0·3031	1·895

* Herzberg, Herzberg and Milne (1940).

§ 5. ACKNOWLEDGMENTS

It gives me great pleasure to record my thanks to Professor Herzberg, Mr. Olson and Mr. Wilson for their generosity in putting their results at my disposal and to Professor H. Dingle for facilities in the spectroscopic laboratories of the Department of Physics, Imperial College, London.

REFERENCES

Barrow, R. F., 1944. *Nature, Lond.*, **154**, 364.
Barrow, R. F. and Jevons, W., 1938. *Proc. Roy. Soc.*, A, **169**, 45.
Bowen, E. J., 1942. *Chemical Aspects of Light* (Oxford University Press), p. 179.
Herzberg, G., 1939. *Molecular Spectra and Molecular Structure : I. Diatomic Molecules.* (New York : Prentice Hall), p. 368.
Herzberg, G., Herzberg, L. and Milne, G. G., 1940. *Canad. J. Res.*, A, **18**, 139.
Jevons, W., 1932. *Report on Band Spectra of Diatomic Molecules* (Physical Society), p. 28.
Saper, P. G., 1932. *Phys. Rev.*, **42**, 498.
Schomaker, V. and Stevenson, D. P., 1941. *J. Amer. Chem. Soc.*, **63**, 37.
Vago, E. E. and Barrow, R. F., 1946 a. *Nature, Lond.*, **157**, 77.
Vago, E. E. and Barrow, R. F., 1946 b. *Proc. Phys. Soc.*, **58**, 538.

VELOCITY OF SOUND IN MIXTURES OF ARGON, HELIUM AND HYDROGEN AT LOW TEMPERATURES

By A. VAN ITTERBEEK and W. VAN DONINCK,
Physical Laboratory, University of Louvain, Belgium

Communicated by Dr. E. G. Richardson, 26 March 1946

ABSTRACT. Measurements are described of the velocity of ultrasonics in mixtures of argon, helium and hydrogen at a frequency of 524 kc./sec. as a function of pressure and at fixed temperatures near 90° and 20° absolute. From these data, information about the interaction between the gases in the mixtures is deduced, using the equation of state of Kamerlingh Onnes.

§ 1. INTRODUCTION

Some years ago one of us, with W. H. Keesom, developed an indirect method of determining the second virial coefficient of gases at low temperatures (v. Itterbeek and Keesom, 1930). This method is based on measurements of the velocity of sound as a function of pressure at different fixed temperatures. Since then this method has been employed in our laboratory using ultrasonics, and has been applied to the following gases: A, O_2, H_2, D_2, CO (v. Itterbeek *et al.*, 1938, 1943, 1944). In the last research we extended this method to gas mixtures. In this paper we report on measurements carried out on A–He, A–H_2 and H_2–He respectively at liquid-oxygen and liquid-hydrogen temperatures. From these measurements it is possible to obtain some information about the interaction between the gases concerned.

§ 2. METHOD

The velocity of sound W can be expressed by means of the equation

$$W^2 = -\frac{c_p}{c_v} \cdot \left(\frac{\partial p}{\partial v}\right)_T \cdot \frac{v^2}{M}. \qquad \text{......(1)}$$

Taking into account the equation of state of Kamerlingh Onnes,

$$pv = \boldsymbol{R}T\left(1+\frac{B}{v}\right), \qquad \ldots\ldots(2)$$

equation (1) can be transformed into

$$W = W_0\left(1+\frac{S}{\boldsymbol{R}\,.\,T}\cdot p\right), \qquad \ldots\ldots(3)$$

W_0 being the velocity of sound in the gas mixture in the ideal state ($p=0$).

$$W_0 = \frac{c_p\,.\,x + c_p'(1-x)}{c_v\,.\,x + c_v'(1-x)}\cdot\frac{\boldsymbol{R}\,.\,T}{M_1\,.\,x + M_2(1-x)} \qquad \ldots\ldots(4)$$

(M_1, M_2 are the molecular masses, $\boldsymbol{R}$ the gas constant, c_p, c_p', c_v and c_v' the specific heats for the ideal state).

Further,

$$S = B + \frac{T}{\lambda}\cdot\frac{dB}{dT} + \frac{T^2}{2\lambda(\lambda+1)}\cdot\frac{d^2B}{dT^2}\,. \qquad \ldots\ldots(5)$$

λ is a numerical factor given by

$$\lambda = \frac{x\,.\,c_v + (1-x)\,.\,c_v'}{M_1\,.\,x + (1-x)\,.\,M_2}\,. \qquad \ldots\ldots(6)$$

For the case of He–A and He–H$_2$ respectively at liquid-oxygen and liquid-hydrogen temperatures, we have $\lambda = 3/2$.

Writing

$$B = B_1\,.\,x^2 + \beta x\,.\,(1-x) + B_2\,.\,(1-x)^2 \qquad \ldots\ldots(7)$$

together with equation (5), we obtain

$$S = S_1\,.\,x^2 + \alpha x\,.\,(1-x) + S_2\,.\,(1-x)^2 \qquad \ldots\ldots(8)$$

with

$$\alpha = \beta + \frac{T}{\lambda}\cdot\frac{d\beta}{dT} + \frac{T^2}{2\lambda(\lambda+1)}\cdot\frac{d^2\beta}{dT^2}\,. \qquad \ldots\ldots(9)$$

For the case where the two components do not possess the same specific heats (A–H$_2$), λ depends on concentration (6). Equation (8) must be changed because the factors S_1 and S_2 are no longer independent of concentration. In that case S_1 and S_2 will be indicated in what follows by the notations S_1' and S_2' and computed by means of equation (5). Discussing our measurements we could, however, observe that $[S - S_1'\,.\,x^2 - S_2'\,.\,(1-x)^2]/x\,.\,(1-x)$ does not depend on concentration, which proves that the expression

$$\frac{I}{\lambda}\cdot\frac{d\beta}{dI} + \frac{I^2}{2\lambda(\lambda+1)}\cdot\frac{d^2\beta}{dT^2}$$

is small.* Thus we can put $\alpha = \beta$ approximately, and obtain in this manner some indication of the interaction between the components at low temperatures.

---

* Admitting for β the following expression: $\beta = a + \frac{b}{T^2} + \frac{c}{T^4}$, we can observe that

$$\frac{I}{\lambda}\cdot\frac{d\beta}{dT} + \frac{T^2}{2\lambda(\lambda+1)}\cdot\frac{d^2\beta}{dT^2}$$

becomes small when λ is approximately equal to 3/2.

We proceed in the following way:—We measure the velocity of sound in the gas mixture as a function of pressure at different fixed temperatures. From these measurements, we compute by the method of least squares the different values of S corresponding to the different concentrations. S_1 and S_2 are in most cases known from previous measurements carried out on the components, or $S_1(S_1')$ and $S_2(S_2')$ are computed from the temperature-variation of B given by measurements on isotherms.

The gas mixtures are prepared within a large vessel of capacity 4 or 10 l. respectively for the measurements at liquid-oxygen or liquid-hydrogen temperatures. The concentration is at first determined by means of the partial pressures. The mixture remains in this vessel for several hours. After this the gas is let into the acoustic interferometer represented in figure 1. The velocity of sound is measured in the mixture at room temperature and from these measurements the concentration is finally computed from equation (4). At low temperatures the concentration is checked again by using the value of W_0 obtained from the measurements represented by equation (3). The values of x found at room temperature and low temperatures agreed generally very well.

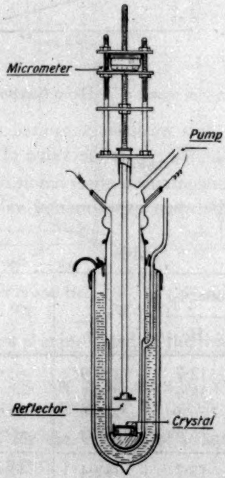

Figure 1. Acoustic interferometer.

For the measurements on the pressure dependency of the velocity of sound, the pressure is lowered in the interferometer by letting the gas stream into an evacuated vessel of capacity 5 l. The gas pressure within the interferometer is read on a closed mercury manometer by means of a cathetometer.

The frequency of the piezo-quartz used is 523·78 kc./sec. For the details of the electrical system, we refer to our previous publications.

§3. MEASUREMENTS ON THE GAS MIXTURES A–He

The values obtained for the velocity of sound as a function of pressure, temperature and concentration are given graphically in figure 2.

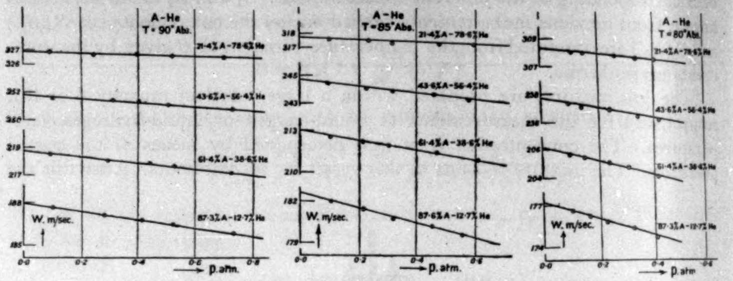

a *b* *c*

Figure 2. Velocity of sound in A–He as function of pressure.

Using these experimental data we have computed the factor S and also W_0 corresponding to equation (3). $W_{0\,\mathrm{theor.}}$ is the value of W_0 computed by means of equation (4), x being the concentration observed at room temperature. It will be seen that the agreement between experimental values and theoretical ones is very good.

Table 1

T (° K.)	Concentration (%)		$W_{0\,\mathrm{exp.}}$	$10^3 . S$	$W_{0\,\mathrm{theor.}}$
	A	He			
90	87·3	12·7	187·9	−5·24	187·8
	61·4	38·6	218·7	−3·25	218·8
	43·6	56·4	251·8	−1·85	251·8
	21·4	78·6	326·9	−0·53	326·7
85	87·3	12·7	182·4	−8·44	182·5
	61·4	38·6	212·9	−4·64	212·6
	43·6	56·4	244·6	−2·75	244·7
	21·4	78·6	317·7	−0·84	317·5
80	87·3	12·7	177·2	−0·28	177·1
	61·4	38·6	206·1	−6·49	206·3
	43·6	56·4	237·6	−4·01	237·4
	21·4	78·6	308·2	−1·69	308·0

The values S_1–A and S_2–He are taken respectively from the measurements of van Itterbeek and van Paemel (1938) on the velocity of sound in pure argon and from the measurements of Nijhoff (1928) on the isotherms of helium gas. These values are indicated in table 2.

The values of S of table 1 are drawn graphically in figure 3, the full line corresponding with the theoretical curves computed by means of the equation

$$S = S_1 . x^2 + \beta x . (1-x) + S_2 . (1-x)^2.$$

Table 2

T (° K.)	$S_1 . 10^3$ A	$S_2 . 10^3$ He	$\beta . 10^3$
90	− 6·60	0·50	−3·4
85	−10·3	0·38	−4·3
80	−12·6	0·28	−7·0

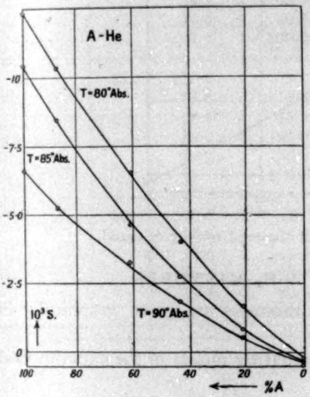

Figure 3. *S* in mixtures of A and He.

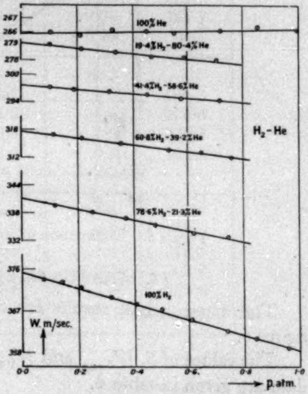

Figure 4. Velocity of sound as function of pressure at 20° K.

The interaction coefficient β is indicated in the third column of table 2.

§4. MEASUREMENTS ON THE GAS MIXTURES He–H$_2$ AT THE BOILING POINT OF LIQUID HYDROGEN

The values obtained for the velocity of sound as a function of pressure at 20°·0 K. are indicated in figure 4.

In table 3 (figure 5) we give the values of S and W_0 computed by means of the experimental values of figure 4. We see again that there is a good agreement between the values of $W_{0\ \text{theor.}}$ and $W_{0_{\text{exp.}}}$.

Table 3

T (° K.)	Concentration (%)		$W_{0\ \text{exp.}}$	$10^3 . S$	$W_{0\ \text{theor.}}$
	H_2	He			
20·3	0·0	100	375·5	−3·39	375·8
	78·6	21·4	341·1	−2·44	341·0
	60·8	39·2	317·7	−1·65	317·9
	41·4	58·6	297·6	−1·06	297·9
	19·4	80·4	279·2	−0·43	279·5
	100	0	265·9	+0·14	265·4

We found again that S as a function of the concentration satisfies equation (8), with $\beta = -2{\cdot}11 \,.\, 10^{-3}$.

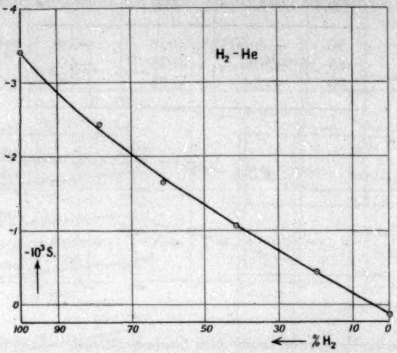

Figure 5. Comparison of theoretical and observed velocity of sound.

§ 5. MEASUREMENTS ON A–H_2 MIXTURES

The experimental results for the A–H_2 mixtures are given graphically in figure 6.

The values of S, $W_{0\,\text{exp.}}$ and $W_{0\,\text{theor.}}$ computed by means of the experimental data are given in table 4.

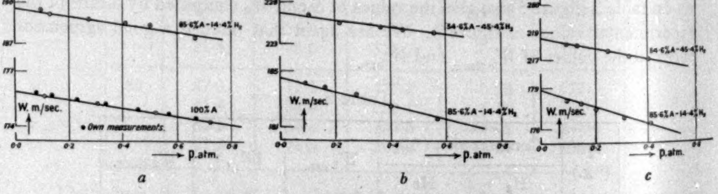

Figure 6. Velocity of sound in A–H_2 mixtures.

The values of S_2' are computed by means of the formula

$$10^3 \,.\, B = 0{\cdot}8742 - \frac{55{\cdot}818}{T} - \frac{5{\cdot}1515 \times 10^3}{T^2} + \frac{1{\cdot}0099 \times 10^5}{T^3} \qquad \ldots\ldots(10)$$

published by Keesom and van Lammeren (1932).

Table 4

T (° K.)	Concentration (%)		W_0 exp. (m./sec.)	$10^3 . S$	W_0 theor. (m./sec.)
	A	H_2			
90	100·0	0	—	−6·6	—
	85·6	14·4	189·7	−5·21	189·7
	54·6	45·4	232·0	−2·38	232·0
	36·1	63·9	278·5	−1·36	278·2
	19·5	80·5	358·5	−0·36	385·2
	0	100·0	—	+0·29	—
85	100·0	0	—	−10·3	—
	85·6	14·4	184·5	− 8·02	184·3
	54·6	45·4	225·2	− 3·62	224·4
	36·1	63·9	270·4	− 1·98	270·2
	19·5	80·5	348·0	− 0·62	348·2
	0	100·0	—	+ 0·24	—
80	100·0	0	—	−12·6	—
	85·6	14·4	178·8	− 9·85	178·9
	54·6	45·4	218·6	− 5·17	218·8
	36·1	63·9	262·3	− 3·36	262·2
	19·5	80·5	337·6	− 1·47	337·8
	0	100·0	—	+ 0·17	—

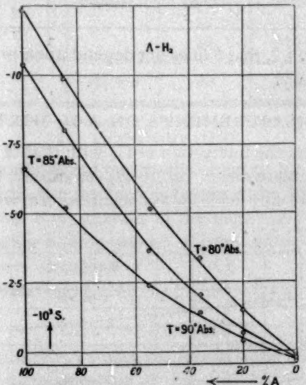

Figure 7. Velocity of sound in A–H_2 mixtures as functions of temperature.

We computed β by means of equation (8), replacing S_1, S_2 by S_1' and S_2'. The values of S_1' are calculated by means of the equation

$$10^3 . B_A = 0{\cdot}129 + 0{\cdot}5923\frac{10^3}{T} - 3{\cdot}5923\frac{10^5}{T^2} + 3{\cdot}7269\frac{10^7}{T^3} - 1{\cdot}40030\frac{10^9}{T^4} \quad \ldots\ldots (11)$$

published by van Itterbeek and van Paemel (1938). The values of S_2' are computed by formula (10), the specific heats for hydrogen being taken from the book of Farkas (1935).

The values obtained for β for the different concentrations are given in table 5.

Table 5

T (° K.)	x (%)	$10^3 . \beta$	$10^3 . \beta$ average
90	80	−1·7	
	70	−1·8	
	60	−1·7	−1·8
	50	−1·8	
	40	−1·8	
	30	−1·8	
85	80	−4·8	
	70	−4·7	
	60	−4·5	−4·5
	50	−4·3	
	40	−4·3	
	30	−4·2	
80	80	−8·5	
	70	−8·2	
	60	−7·7	−8·4
	50	−8·3	
	40	−8·4	
	30	−7·9	

We see, as remarked in § 2, that β does not depend upon pressure within the limits of experimental accuracy.

§ 6. MEASUREMENTS ON A–D_2 MIXTURES

In order to compare the interaction of H_2 with that of its isotope D_2, we have also made some measurements on A–D_2 mixtures. These measurements, indicated in figure 8, are only made for a concentration at which the influence of the interaction is largest.

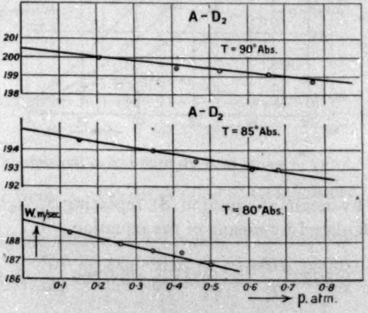

Figure 8. Results for A–D_2 mixtures.

From the experimental data of figure 8, we have computed the values of S and $W_{0\ \mathrm{exp.}}$ (see table 6). $W_{0\ \mathrm{theor.}}$ was calculated by means of the values of the specific heats of D_2 taken from Farkas.

Table 6

T (° K.)	Concentration (%)		$W_{0\ \mathrm{exp.}}$	$10^3 . S$	$W_{0\ \mathrm{theor.}}$
	A	D_2			
90	68·4	31·6	200·5	−3·64	200·7
85	68·4	31·6	195·1	−5·34	195·0
80	68·4	31·6	189·2	−7·34	189·3

In table 7 we compared the values of S obtained for A–D_2 mixtures with those of A–H_2 mixtures. It will be seen that there is no difference within the limits of experimental error.

Table 7

T (° K.)	$10^3 . S$ A–D_2	$10^3 . S$ A–H_2
90	−3·64	−3·55
85	−5·44	−5·45
80	−7·34	−7·40

Table 8

Mixture	T (° K.)	$10^3 . B_1$	$10^3 . B_2$	$10^3 . \beta$
A–H_2	90	− 8·0	−0·2	−1·8
	85	− 9·0	−0·3	−4·5
	80	−10·0	−0·6	−8·4
A–He	90	− 8·0	0·5	−3·5
	85	− 9·0	0·38	−4·3
	80	−10·0	0·28	−7·5
H_2–He	20	− 6·56	0·10	−2·11

§ 7. CONCLUSIONS

In table 8 we have summarized our results obtained for the interaction terms and compared them with the interaction between the individual components. Thus we can observe that β is generally of the same order as the B-value of the component with the higher boiling point. Furthermore, when the temperature decreases, β increases very strongly.

Further work is in hand on H_2–N_2, H_2–He, H_2–O_2 and He–O_2 mixtures.

ACKNOWLEDGMENT

We take this opportunity to express out thanks to the Belgian Foundation for Scientific Research for its financial aid of this work.

REFERENCES

Farkas, A., 1935. *Light and Heavy Hydrogen* (Cambridge).
Keesom, W. H. and van Lammeren, J. A., 1932. *Comm. Leiden*, **221** *c*.
Nijhoff, G. P., 1928 *Comm. Leiden*, Suppl., **64** *c*.
van Itterbeek, A. and Keesom, W. H., 1930. *Comm. Leiden*, **209** *a*.
van Itterbeek, A. and van Doninck, W., 1943. *Physica*, **10**, 481 ; 1944. *Ann. Phys. (Chim.)*, **19**, 88.
van Itterbeek, A. and van Paemel, O., 1938. *Physica*, **5**, 593, and 848.

REVIEWS OF BOOKS

Optique Physiologique : La Dioptrique de L'Œil et sa Correction, by Y. LE GRAND. Pp. 356 and 105 diagrams. (Paris: Revue d'Optique, 1946.)

The book under review represents Part I of a treatise by M. Le Grand on Physiological Optics. He is here dealing more particularly with the optical system of the eye on Gaussian principles, and with the method of testing and correction of refractive errors. The main contents of the book will be generally familiar to those who have studied visual optics, but the material is presented in a very clear and orderly manner. A necessary amount of algebra is included, but the text is not overburdened with it, neither is the clarity of the diagrams obscured by too many rays of light or too many details of the optical systems.

Since M. Le Grand has for many years been engaged in teaching physiological optics, it is not surprising to find a list of exercises given at the end of the book. As the solutions of the problems, and not merely the answers, are also included, it is possible for the conscientious student both to test and teach himself by this means.

A more unusual, but none the less welcome, feature in a book of this type is the inclusion of two appendices dealing respectively with elementary statistics and with the calculation of matrices in optical work. Whether the average optician will consider that he has any need to venture into these fields is perhaps a matter of doubt, but at least the material is provided in a readily assimilable form for those who have the inclination to attack it.

It is interesting to note that in the list of original papers quoted in the bibliography at the end of the book, half of them appeared in the *Transactions of the Optical Society*—a small matter, perhaps, but significant that the Society in its time performed a useful function and might have continued to do so if sufficient support had been forthcoming to keep the Society alive. Readers in this country will also be interested to see that Fincham's theory of accommodation is described as one of the most satisfactory.

Quite obviously M. Le Grand regards his subject as one worthy of very serious study by optical designers. As he remarks on p. 345, the modern correcting lens is a complicated optical instrument and the last word has not yet been said about the best design of spectacle lenses. M. Le Grand can at least claim to have given a clear account of the basic principles which must govern any future developments in such lens design.

W. D. WRIGHT.

A Survey of General and Applied Rheology, by G. W. SCOTT BLAIR. Pp. 196. (London: Sir Isaac Pitman and Sons, Ltd., 1946.) 18*s*. 6*d*.

Rheology is defined as the study of the deformation and flow of matter. Thus defined it should obviously cover a large proportion of the field of physics. In practice the subject is concerned almost exclusively with those types of matter which do not obey the simple laws of deformation or flow to be found in the elementary textbooks of physics.

Dr. Scott Blair's book is written primarily for the scientist in industry, who has to deal with matter as it is rather than with matter as the physicist would like it to be. The first part of the book gives an account of the wide variety of rheological phenomena encountered in industrially important materials, and discusses the various types of apparatus by which these phenomena may be investigated. Those wishing to pursue the subject in greater detail will find the annotated bibliography particularly helpful.

The second, and more controversial, part of the book deals with the interpretation of rheological data. The central question here discussed may be stated in the following way: What physical factors are responsible for the formation of a subjective judgment of a given rheological property on the basis of sensory impressions? Dr. Scott Blair has made extensive investigations into this question, and his discussion of this and related problems makes interesting reading.

L. R. G. TRELOAR.